Rafael Halb, BSc.

Development of a spray nozzle test bench and investigation of suspension spray drying for pharmaceutical API's and excipients

MASTER'S THESIS

to achieve the university degree of

Diplom-Ingenieur

Master's degree programme: Chemical and Process Engineering

submitted to

Graz University of Technology

Supervisor

Univ.-Prof. Dipl.-Ing. Dr.techn. Johannes Khinast

Institute of Process and Particle Engineering

Second Supervisor
Dipl.-Ing. Manuel Kreimer

Graz, June 2018

AFFIDAVIT

I declare that I have authored this thesis independently, that I have not used other than the declared sources/resources, and that I have explicitly indicated all material which has been quoted either literally or by content from the sources used. The text document uploaded to TUGRAZonline is identical to the present master‘s thesis.

21.06.18

Date

Signature

Preamble

I thank Mr Univ.-Prof. Dipl.-Ing. Dr. Johannes Khinast of the Technical University of Graz, Institute of Process and Particle Technology for the provision of the topic as well as the thereby provided technical equipment for the experimental procedure by the RCPE.

I would like to thank Dipl.-Ing. Manuel Kreimer, RCPE Graz for the technical support and his assistance in carrying out the experiment throughout the entire time. I would also like to thank him for his support in preparing for presentations and meetings.

I would like to thank Dipl.- Ing. Dr. Isabella Aigner, RCPE Graz for promoting this work through many professional discussions and suggestions.

I would like to thank all technical staff of the RCPE Graz for their helpfulness in the operation and cleaning of equipment as well as the provision of the necessary material.

I thank my family and my girlfriend as well as all friends for the support in all circumstances.

Kurzfassung

Sprühtrocknen wird häufig als Verfahrensschritt in der pharmazeutischen Industrie eingesetzt. Dabei wird ein flüssiger Feedstrom in ein heißes Trocknungsmedium eingebracht. Die versprühte Flüssigkeit ist entweder eine Lösung, oder eine Emulsion oder Suspension mit verschiedenen Flüssigkeitskomponenten, Ölen oder Feststoffen. Insbesondere die Sprühtrocknung von Suspensionen ist auf Grund der geringeren Flüssigkeitsmengen und dem damit verbundenen geringeren Energiebedarf für die Verdampfung interessant. In der Suspension wurden Partikelgröße und Form in vorgeschalteten Prozessen wie zum Beispiel der Kristallisation gezielt beeinflusst. Diese muss in nachfolgenden Prozessen wie der Trocknung unverändert bleiben. Die Suspensionen werden üblicherweise vor dem Sprühtrocknen aufkonzentriert, um die Menge an Wärmeenergie für die Flüssigkeitsverdampfung zu reduzieren. Aus diesem Grund wird im Rahmen dieser Arbeit die Sprühtrocknung beziehungsweise das Versprühen von konzentrierten Suspensionen in Hinblick auf Veränderungen der Partikelgröße, Form und Morphologie untersucht.

Im ersten Teil sollen die Eigenschaften des getrockneten Pulvers durch eine Variation der Zusammensetzung der zu versprühenden Suspension und der Temperatur des Trocknungsmediums untersucht werden. Der zu versprühende Feedstrom besteht jeweils aus unterschiedlichen Zusammensetzungen von Wasser, Isopropanol und Lactose. Die Analyse der Partikeleigenschaften und der Nachweis von Änderungen durch Variation von Prozessparametern erfolgt mittels Partikelmessung und einer dynamischen Differenzkalorimetrie-Messung. Die Restfeuchte im sprühgetrockneten Produkt wird gravimetrisch bestimmt. Von einigen Proben wurden Bildaufnahmen mit einem Elektronenmikroskop aufgenommen. Die Partikelmessung mittels Laserbeugung zeigte, dass bei einer Flüssigkeitszusammensetzung von 100% Isopropanol keine signifikanten Veränderungen der charakteristischen Partikelgrößen im Vergleich zum Ausgangsmaterial stattfanden. Je höher der Anteil an Wasser in der flüssigen Phase der Suspension ist, desto mehr Lactose wird gelöst, das in weiterer Folge zur Bildung von größeren Partikeln beim Sprühtrocknungsprozess führt. Mit steigendem Wassergehalt stieg auch der Anteil an β - Lactose im Produkt. Sprühtrocknen von Lactose erzeugte amorphes Material, das mit Hilfe der DSC-Messung durch die Existenz einer Glasübergangsregion bestätigt wurde. Durch die Elektronenmikroskop- Bilder konnte die Partikelform des getrockneten Pulvers und die zunehmende Agglomeration mit steigendem Anteil an gelöster Lactose in der Suspension gezeigt werden.

Der zweite Teil dieser Arbeit beinhaltet den Umbau eines Sprühtrockners zu einem Sprühdüsenteststand. Nach dem Umbau wurden unterschiedliche pneumatische Sprühdüsen getestet und deren Verhalten beim Sprühvorgang beobachtet. Da die Suspensionen Lösungsmittel beinhalten, musste der Sprühdüsenteststand unter Berücksichtigung eines Explosionsschutzkonzeptes ausgelegt werden. Getestet wurden eine Düse der Firma Schlick mit einem Düsendurchmesser von 800 µm und eine Düse der Firma Bete mit einem Düsendurchmesser von 400 µm. Mit der Schlick-Düse konnten Lactose Suspensionen bis zu einem Feststoffgehalt von 35 Massenprozent versprüht werden. Der maximal mögliche Feststoffgehalt beim Sprühvorgang mit der Bete-Düse lag bei 10 Massenprozent. Die Probennahme der Suspension erfolgte an verschiedenen Messpunkten, um Änderungen der

Partikelgröße während der Förderung durch die Pumpe und den Sprühvorgang aufzuzeigen. Die Vermessung der Proben wurde mittels Laserbeugung durchgeführt. Es zeigte sich, dass beim Rühr- und Sprühvorgang der Suspension eine wesentliche Änderung der Partikelgröße stattfand.

Abstract

Spray drying is widely used as a process step in pharmaceutical engineering. In spray drying, a liquid feed stream is placed in a hot drying medium. The sprayed liquid is either a solution, emulsion or suspension with various components of liquids, oils or solids. Especially spray drying of suspensions is an interesting field due to lower amounts of liquids and therefore fewer required energy consumption for the evaporation. In a suspension, the particle size and shape was specifically tailored in upstream processes as crystallization and has to be unchanged in downstream processes as drying. The suspensions are usually pre-concentrated before spray drying, to reduce the amount of thermal energy for liquid evaporation. For this reason, this thesis investigates spray drying and spraying of concentrated suspensions with regard to changes of particle size, shape and morphology.

As a first part of this thesis changes in the dried powder were investigated by a variation of the suspension composition and the temperature of the drying medium. The feed stream consists in each case of different compositions of water, isopropanol and lactose. The analysis of the particle properties or the demonstration of changes in different process parameters is carried out by means of laser diffraction and a dynamic differential calorimetry measurement. The residual moisture in the spray-dried product is determined gravimetrically. From selected spray drying samples, images were taken with an electron microscope. The particle measurement by laser diffraction showed that with a liquid composition of 100% isopropanol no significant changes of the characteristic particle sizes take place compared to the starting material. The higher the proportion of water in the liquid phase of the suspension, the more lactose is dissolved and the larger particles were formed during the spray drying process. With increasing water content, the proportion of β lactose in the product also increased. Spray drying of lactose produced amorphous material, which was confirmed by the DSC measurement by the existence of a glass transition region. The microscope images showed the particle shape of the dried powders with larger particles or agglomerate formation with increasing dissolved solids in the suspension.

The second part of this work deals with the conversion of a spray dryer to a spray nozzle test stand. After conversion, this unit was used to test various pneumatic spray nozzles and describe typical characteristics of these. Due to the handling of explosive substances, possible explosion protection measures are shown and a comprehensive explosion protection concept is created in compliance with legal regulations. A nozzle from Schlick with a nozzle diameter of 800 µm and a nozzle from Bete with a nozzle diameter of 400 µm were tested. With the Schlick nozzle, lactose suspensions could be sprayed up to a solids content of 35 wt%. The maximum possible solids content when spraying with the Bete nozzle was 10 wt%. Samples of the suspension were taken at different measurement points in order to determine changes in the particle size during the promotion through the pump and the spraying process. It was found that even when stirring and spraying the suspension a substantial change in the particle size took place.

Table of contents

List of figures

List of tables

Formula symbols

a	(m)	Distance from the nozzle to the spray area
A_P	(m²)	Projection surface of the particle
C	(1/h)	Number of air changes
c	(-)	Oxygen volume fraction
D	(m)	Droplet size
$\frac{dG}{dt_{max}}$	(kg/s)	Leakage flow
$dV/_{dt_{min}}$	(m³/s)	Minimal flow of fresh air
d_{32}	(m)	Sauter diameter
d_P	(m)	Diameter of the projection-surface equal circle
d_{PE}	(m)	Diameter of the circumferential equal circle of a particle image
d_S	(m)	Diameter of the surface equal sphere
d_v	(m)	Diameter of the volumetric equal sphere
f	(-)	Heywood factor
f_c	(-)	Correction factor
k	(-)	Safety factor
LEL	(%)	Lower explosive limit
LOC	(%)	Limiting oxygen concentration
M	(g/mol)	Molecular weight
m	(kg)	Mass
n	(-)	Number of cycles
p	(Pa)	Pressure
P_e	(-)	Probability of occurrence of an explosive mixture
P_i	(-)	Probability of occurrence of an effective ignition source
Q	(-)	Distribution sum
q	(-)	Density distribution
R_{ex}	(-)	Risk of an explosion
R_g	(-)	Limit risk of an explosion
S	(m²)	Surface of the particle
$S_{L,s}$	(g/g)	Solubility of lactose in solution
S_m	(m²)	Mass related specific surface
ΔS	(-)	Safety factor

S_{Pro}	(-)	Primary, secondary, tertiary explosion protection
S_V	(m^2)	Volume related specific surface
T	(K)	Temperature
T	(s)	Persistence time
U	(m)	Circumference of the particle
UEL	(%)	Upper explosive limit
V	(m^3)	Volume of the particle
wt	(%)	Mass fraction
V_Z	(m^3)	Hypothetical volume explosive atmosphere
X_0	(-)	Initial concentration
x	(m)	Diameter of particle

Greek formula symbols

α	(°)	Spray angel
Ψ	(-)	Form factor
K	(-)	Adiabatic exponent
ρ_P	(kg/m^3)	Mass of particle
φ_{O2}	(%)	Maximum permissible oxygen concentration
μ	(Pa*s)	Viscosity

Indices

0	Initial State
0	Number based
1	length based
1	State 1
2	Area based
2	State 2
3	Mass/ volume based
a	Quantity a
b	Quantity b
H_2O	Water
IPA	Isopropanol

L	Liquid
P	Particle
r	Type of quantity
s	Saturated
sol	Solid

1. Introduction

Spray drying offers the great advantage that it is a very product-friendly and fast drying process, generating fine droplets with a large surface area and therefore minimal required energy input for drying. This also allows the drying of highly heat-sensitive materials, such as proteins, lipids, vitamins, hormones or volatile oils. Relatively narrow particle size distributions can be achieved by spray drying and it is therefore commonly used in the pharmaceutical industry. Special attention must be given to explosion protection when working with spray dryers due to fine atomization of solvent droplets. In order to avoid explosions that could cause serious personal injury or property damage, appropriate security concepts must be developed and implemented.

In this work a possible change of particle properties by variation of process parameters during the spraying process is demonstrated. The model suspension composition consisted of α lactose monohydrate in various water-isopropanol mixtures. For the spray drying investigations, a laboratory spray dryer was used, operated in open or closed loop. The particle evaluation was carried out by particle size measurements and by thermal analysis (melting and glass transition temperatures, phase transitions, degree of crystallization). Another parameter which was determined was the moisture content of the final product (gravimetric determination).

The second part of the work was to investigate the agglomeration behavior and the abrasion by spraying with different nozzles. For this purpose a spray dryer was converted into a spray nozzle test stand. With this spray nozzle test stand two spray nozzles of different types were tested. The liquid to be sprayed was also a suspension of solid lactose particles and a liquid mixture of water and isopropanol. The evaluation was done by particle size measurements to detect possible particle abrasion or agglomeration during spraying. For this spray nozzle test stand, a complete explosion protection concept was created and implemented. Part of this work deals therefore with the basics of explosion protection and development of an explosion protection concept. Finally, the results of both parts are discussed and a possible outlook for subsequent work based on these results is given.

2. Fundamentals

In the following, different terminology of particle technology and basics of spray drying as well as measures of explosion protection will be defined. These basics form the theoretical background for all considerations and decisions that follow in the context of this work.

2.1. Particle Technology

Particle technology deals with particulate materials and describes industrial processes with gaseous, liquid or solid particles, which are contained in a continuous phase.[1] That means, the substances and material systems consist of a collection (collective) of many particles, which are referred to as mixed components, clusters, bulk materials, dust clouds, suspension, sludge, etc. depending on the context. In general one speaks of disperse materials or disperse material systems. The word disperse can be translated as meaning finely distributed and the term "particle" can also be used as a generic term for grains, drops, bubbles or microorganisms[1].

2.1.1. Particle size dependent properties

The purpose of labelling individual particles is to be able to make an orderly distinction between them. Characteristics such as size and their distribution as well as the shape of the particles are important distinguishing features[1]. But also material properties such as density, chemical composition, colour, solubility etc. are important criteria for the characterization of particles. For the particle description it is necessary to specify for each of the characteristics "size" and "shape" at least one measure or parameter (particle size and form factor)[1]. The diameter or length of a regularly shaped particle can be used as a unique geometric measure as the main dimensions for characterizing a particle. The diameter of a spherical particle can also be used for this purpose. Other geometrical information about particle size, such as volume or surface area, may be used by appropriate conversion to equivalent diameter for determination of geometric dimensions.

Equivalent diameter:

Considering an irregularly shaped particle, the equivalent diameter is the diameter of a sphere or circle with the same properties[1]. Volume, surface, projection area and projection size of the particles are the geometrical properties to which sphere or circle diameters are assigned. The most important are shown in Table 2-1.

Table 2-1: Equivalent diameters

Definition	***Symbol***	***Equation***
Diameter of the volumetric equal sphere	d_v	$d_V = \sqrt[3]{\frac{6 * V}{\pi}}$
Diameter of the surface equal sphere	d_s	$d_S = \sqrt{\frac{S}{\pi}}$
Diameter of the projection-surface equal circle	d_p	$d_P = \sqrt{\frac{4 * A_P}{\pi}}$
Diameter of the circumferential equal circle of a particle image	d_{pe}	$d_{Pe} = \frac{U}{\pi}$

Also, any physical property related to the diameter of a particle can be used to form an equivalent diameter. The most important of these are[1]:

- Diameter of the sphere with the same rate of descent
- Rate of descent equivalent diameter = " Stokes diameter"
- Aerodynamic diameter
- Diameter of the sphere with the same scattered light intensity

Specific surface

The specific surface area is another important feature for the characterization of particles. The volume-related specific surface S_V is calculated from particle surface S and particle volume V and is described by Equation 2-1.

$$S_V = \frac{S}{V} \qquad \textit{Equation 2-1}$$

The mass-related specific surface S_m is calculated from particle surface S and particle mass m and is provided by Equation 2-2.

$$S_m = \frac{S}{m} \qquad \textit{Equation 2-2}$$

A relationship between volume specific surface area S_v and mass specific surface area S_m can be established by the density of the particles ρ_p and is shown by Equation 2-3.

$$S_V = \rho_P * S_m \qquad \textit{Equation 2-3}$$

Particle shape, form factor

In most particle collectives, each particle has a different shape. It is often sufficient in practice to describe particles with globular, round, cubic, angular, flat, needle-shaped, fibrous, etc. For the form factor $\psi_{a,b}$, two independently measured quantities x_a and x_b of a particle are set in relation[1]. The mathematical description is given by Equation 2-4.

$$\psi_{a,b} = \frac{x_a}{x_b} \qquad \textit{Equation 2-4}$$

The description of the particle shape is not very accurate with the help of the shape factor, since only proportions are compared with each other. As proportions, for example, lengths or diameters are used. Form factors have been measured many times. The numerical values can only be regarded as reference values since they are valid only for the particle forms on which the measurement is based. A special often used form factor is the Heywood factor f, which compares the real particle to a bullet. The Heywood factor is defined by the comparison of specific surfaces[1]. This relationship is described by Equation 2-5 and Equation 2-6.

$$f = \frac{measured\ specific\ surface\ area}{specific\ surface\ of\ a\ sphere\ with\ diameter\ x} \qquad \textit{Equation 2-5}$$

$$f = \frac{S_V}{\frac{6}{x}} = \frac{6 * d_s^2}{d_V^3} * \frac{x}{6} \qquad \textit{Equation 2-6}$$

x is according to Heywood the diameter of a particle in its stable position (for example on an object slide)

Particle size distribution

In the particle size distribution there is a total amount of particles, which should be sorted according to the occurring sizes and characterized by the associated proportions. For representation, the particle size x, which is a measure of length, is plotted on the abscissa of a diagram. (e.g., the mesh size of a sieve or an equivalent diameter). The particle size distribution can now be displayed discretely (class wise) in diagrams or tables. On the ordinate the quantities are plotted. There are two different ways to represent the quantity. If the proportion of the total amount which lies below a certain particle size x to the total quantity is plotted, it is called a distribution sum.

The index i is a run variable and numbers the particle class, also called fraction, and the corresponding value range. The method of measuring the amount of particles in a size interval determines the quantity type. It is between 0 and 3 and indicates the exponent of the x that describes the basis of the distribution. It displays a number- (r = 0), a length- (r = 1), an area- (r = 2) and a volume- or mass based (r = 3) distribution and is shown at Equation 2-7.

$$Q_{r,i} = Q_r(x_i) = \frac{subset\ x_{min} \dots x_{max}}{total\ quantity\ x_{min} \dots x_{max}}$$ *Equation 2-7*

Figure 2-1 shows an example of a continuous representation of the distribution sum of a particle size distribution.

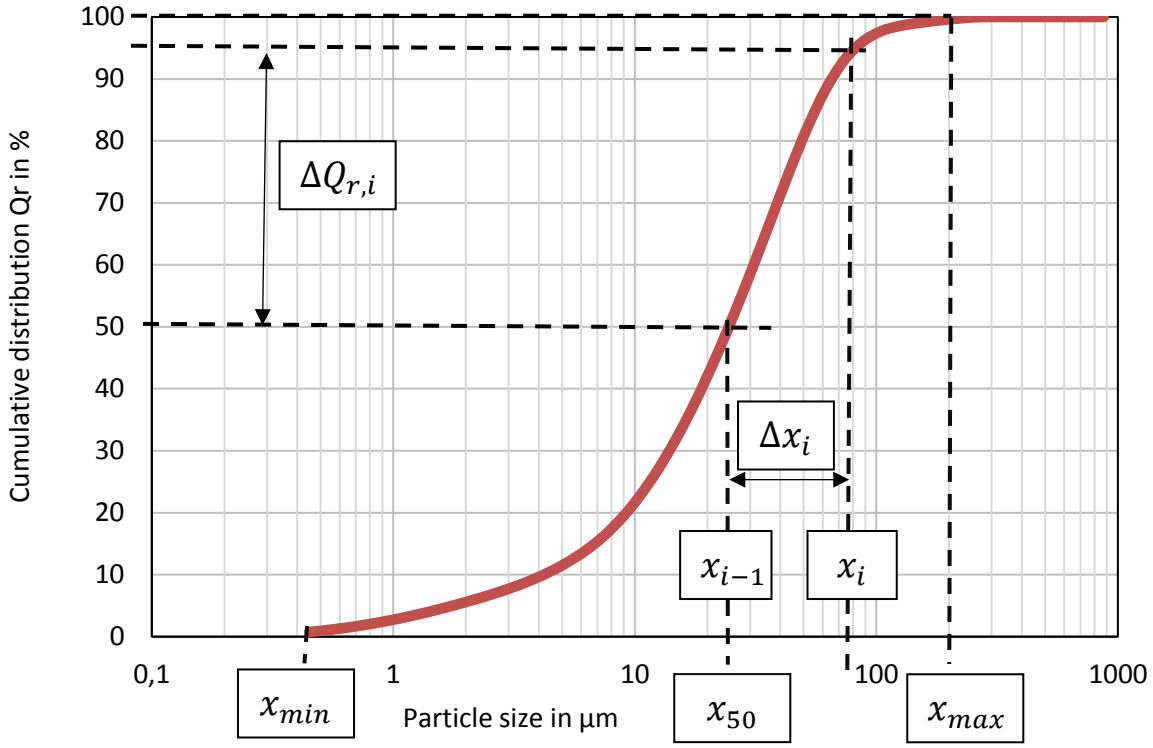

Figure 2-1: Cumulative distribution sum

The distribution density is the proportion of the total quantity in a certain size interval with respect to the interval width. Here at Equation 2-8 the index i is also the run variable and numbers the particle class, also called fraction, and the corresponding value range and r is the type of quantity with the number 0 -3.

$$q_{r,i} = \frac{Quantity\ of\ the\ fraction}{interval\ width\ \Delta x_i}$$ *Equation 2-8*

Figure 2-2 shows an example of a continuous representation of the distribution density of a particle size distribution.

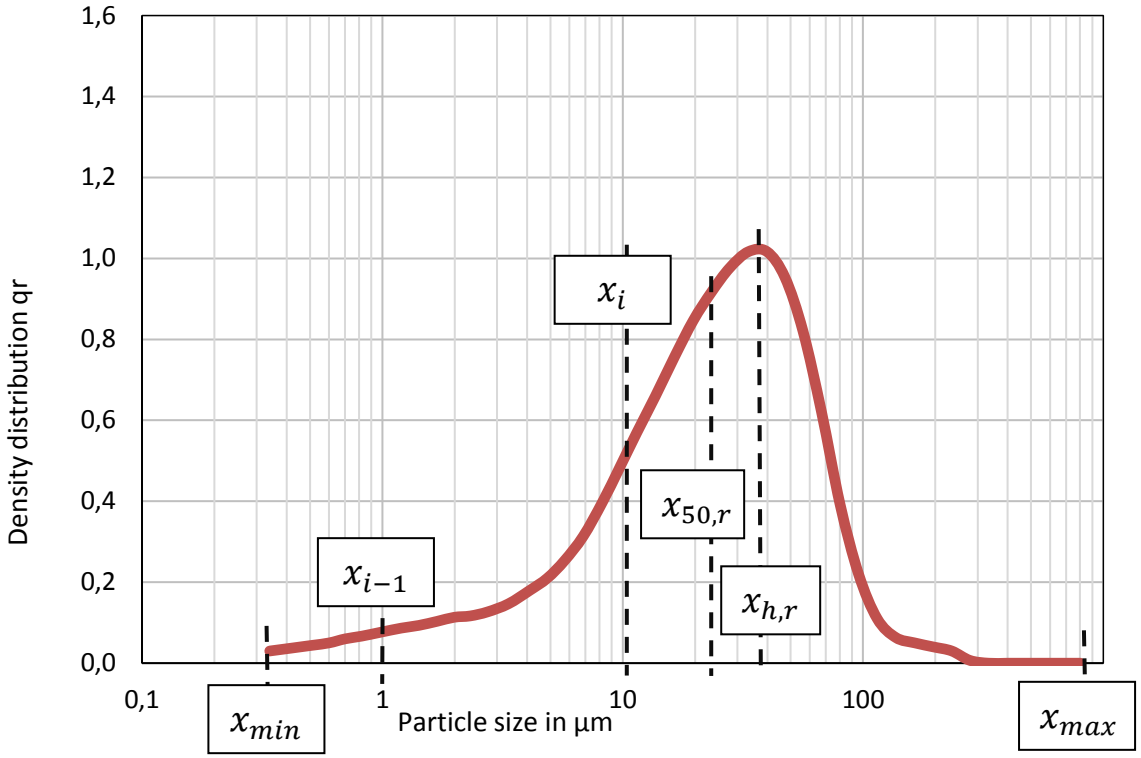

Figure 2-2: Density distribution

The median value $x_{50,r}$ is defined as the particle size, where 50% of the particles are below this value. Therefore, the quantity type must also be specified with "r". It is obtained from the intersection of the distribution sum curve Qr (x) with the 50% horizontal.

The mode value $x_{h,r}$ is the particle size with the highest amount and can be read at the maximum of the density distribution curve or at the highest column of the histogram.

x_{min} is the smallest particle size in the collective, x_{max} is the biggest particle size.

The number distribution (r = 0) counts the particles in each fraction. All counting methods of particle size analysis therefore have the quantity type "number" and provide number distributions. In the area distribution, the projection surface or surface is determined by image recording methods and classified into grain classes. The subsets in the size classes are determined by weighing. This results in the quantity type "mass". If the density of the particles is independent of their size, the masses also correspond to the volume fractions, so that mass and volume distribution are the same.

In the following, the relationship between number q_0- and volume density q_3 distribution is represented by Equation 2-9 without derivation[1].

$$q_3(x) = \frac{x^3 * q_0(x)}{\int_{x_{min}}^{x_{max}} x^3 * q_0(x) * dx}$$ *Equation 2-9*

The one for the distribution sum Q_3 is given by Equation 2-10 without derivation[1].

$$Q_3(x^*) = \frac{\int_{x_{min}}^{x^*} x^3 * q_0(x)}{\int_{x_{min}}^{x_{max}} x^3 * q_0(x) * dx} \qquad \textit{Equation 2-10}$$

with $x^* \leq x_{max}$

Specific surface area

The specific surface area S_v is an important parameter for all processes that take place on the surface. Examples would be spray drying, extraction or oxygenation in fumigation. The specific surface area can be calculated from the volume distribution q_3 or from the number distribution q_0. The calculation from the volume (or mass) distribution is shown without derivation in Equation 2-11[1].

$$S_V = 6 * f * \int_{x_{min}}^{x_{max}} \frac{1}{x} * q_3(x) * dx \qquad \textit{Equation 2-11}$$

The calculation from the number distribution is shown without derivation in Equation 2-12[1].

$$S_V = 6 * f * \frac{\int_{x_{min}}^{x_{max}} x^2 * q_0(x) * dx}{\int_{x_{min}}^{x_{max}} x^3 * q_0(x) * dx} \qquad \textit{Equation 2-12}$$

Sauter diameter

The Sauter diameter represents the average spherical size corresponding to the specific surface of the entire particle collective[1]. In other words, if the volume of the substance under consideration were divided into spheres of equal size so that the surface area of the spheres would be exactly the same as that of the collective, then these spheres would have the Sauter diameter. The Sauter diameter is inversely proportional to the specific surface and is calculated according to Equation 2-13.

$$d_{32} = \frac{6}{S_V} \qquad \textit{Equation 2-13}$$

2.2. Spray drying

The development of the spray drying technique can be traced back to the year 1860. The origin of spray drying is in the United States of America - here in 1872, the first patent for the technology of spray drying was filed[2,3]. The spray drying boom took place in World War II, where technology was intensively sought to reduce the weight and volume of food to make it easier to transport. Spray drying got a monopoly position in the dairy industry in the continuous production of milk powder. The spray-drying process quickly gained a foothold in the pharmaceutical industry as well. Due to continuous development, it has become an industrial-friendly drying technology today. A definition of spray drying is: “Spray drying is the transformation of feed from a fluid state into a dried particulate form by spraying the feed into a hot drying medium.” (Masters, 1991)

A spray dryer operates on convection mode. The moisture is removed from the feed product by application of heat and controlling the humidity of the drying medium. The uniqueness of this drying process is that the evaporation of moisture is promoted by spraying the feed into a heated atmosphere, resulting in improved drying rate.

If the process of spray drying is now considered in more detail- from the liquid feed entering the spray dryer until the dried powder at the end- it can be divided into 4 stages[2,3]:

- Atomization of the feed solution.
- Contact of spray with the hot gas.
- Evaporation of moisture.
- Particle separation.

All changes in parameters of these stages also affect features and properties of the final product.

2.2.1. Atomization

Atomization means that a fluid is broken up into a large number of droplets. The dispersion is formed within a drying gas. Due to this enormous enlargement of the surface, a very good heat transfer takes place between the drops and the drying air (a cubic meter of liquid atomized forms $2*10^{12}$ droplets of 100 µm medium size gives 60000 m² of surface)[3]. As a result, the solvent evaporates within seconds and is converted into the gas phase. The drying material never reaches the inlet temperature of the drying gas. Spray drying does not offer only the advantage that heat-sensitive substances can be dried, it is also possible to form particles with the desired physicochemical and morphological properties.

There are different types of atomizers commonly used to atomize fluids with low viscosity: rotary atomizers, hydraulic (pressure) nozzles and pneumatic nozzles. For non-Newtonian fluids with high viscosity, ultrasonic nozzles or electro- hydrodynamic nozzles are mostly used. In the context of this work, only the pneumatic nozzle will be discussed, as it was also used for the experiments.

In pneumatic nozzles, the atomization of the liquid is done in a stream of compressed carrier gas. As a result, high frictional forces are generated over the liquid surface, which lead to a disintegration into spray droplets. The atomization in drops depends on the properties of the feed (surface tension, density and viscosity) and also on the properties of the carrier gas (velocity and density). There are also nozzles, with three or more connections. If it is for the atomization of one feed it is called bi fluidic nozzle. If it is possible to atomize two different feeds, the nozzle is called a four fluid nozzle. In the pharmaceutical industry two fluid nozzles are the most frequently used nozzles, where a feed stream is atomized through a gas stream. The largest possible mass flow rate for such nozzles is approximately 1000 kg/h[2]. In general, the size of the droplets depends on the ratio of the gas and liquid flow. To prevent clogging of the nozzle, a needle driven by compressed gas pulses is placed within the nozzle in the feed supply. Thus, periodically cleaning of the nozzle can be done by forward and backward movement in the feed channel. Two fluid nozzles are commonly used to produce self- emulsifying drug delivery systems, micro/ nano capsules, solid dispersions, particles with modified release, protein powders with good stability and respiratory powders.

Variation of parameters and influence on the spray drying process

Important parameters for the selection of the spray nozzle are the feed flow rate f, the atomization pressure p, the viscosity μ and the density ρ of the feed stream[4]. By changing one or more of these parameters, the droplet diameter can be changed after atomization.

Increasing the throughput of the feed stream produces larger droplets for atomization pressure and feed viscosity. The explanation for this is that the energy input per volume or mass feed is decreased by enhancement of the throughput.

Equation 2-14 describes the mathematical relationship between droplet size D and atomization pressure p[4].

$$\frac{D_2}{D_1} = \left(\frac{p_2}{p_1}\right)^{-0.3} \qquad \textit{Equation 2-14}$$

The index 1 is the initial state, index 2 is the final state. This relationship is valid only if the same nozzle and fluid with the same properties were used. In general, higher atomization pressure results in formation of smaller droplets. This can be explained by the fact that more energy is available for the division of the liquid flow due to the higher pressure.

As the viscosity increases the energy supplied to the nozzle must overcome larger viscous forces. The relationship between the viscosity of the feed stream and the droplet diameter D obtained after the atomization is that the droplet diameter increases with higher viscosity μ[4]. This effect is described by Equation 2-15.

$$\frac{D_2}{D_1} = \left(\frac{\mu_2}{\mu_1}\right)^{-0.2}$$ *Equation 2-15*

The actual spray angle α of a nozzle can be calculated by the diameter d of the spray surface and the distance a of the nozzle to it by using Equation 2-16[4].

$$arctan \propto = \frac{a}{\frac{d}{2}}$$ *Equation 2-16*

Spray nozzles have a spray angle of 50-90° [4]. The larger the spray angle, the smaller the droplets become, because with increasing angle the liquid tangential velocity of the nozzle increases. A further increase in the angle beyond 90° has only a negligible influence on the drop formation.

2.2.2. Drying procedure

In the spray drying column, the atomized liquid encounters the heated drying gas. The moisture evaporates very quickly from the droplet surface resulting in the formation of particles. A very important parameter for this process is the uniform distribution of the drying air in the entire drying column. In co current dryers, the liquid feed stream and the drying gas flow in the same direction. In this case, the feed stream is sprayed into the area of the drying stream where the highest temperature of the process is present. On the way to the other end of the column, the drying stream loses more and more energy due to the evaporation of the solvent. An often observed problem is that coarsely dispersed drops are not dried fast enough and therefore adhere to the chamber wall. This is an undesirable effect that occurrence strongly affects the process efficiency. Co current dryer are the most universal and the most often used type of drying chamber[3].

At counter current, the feed stream and the drying gas stream enter at the opposite end of the drying chamber. The exit temperature of the product is higher than that of the drying medium. The feed stream contacts the drying stream at the location in the spray dryer where it has the lowest temperature in the spray column. The liquid content in the drops protects the substance from a too quick drying process. Counter current spray dried powder is a frequently porous low-density powder with a tendency of agglomerate formation. Furthermore, the settings of the drying stream are important parameters for the spray drying process. Too low drying gas flow may result in a non-dry product, too high drying gas flow may result in product loss, because dried powder might be blown out with the drying air. Only about 5% of all spray drying chamber in industry are counter current spray dryer[2]. The reason for that is their unsuitability for food and pharmaceutical processes, there is a risk that the product will be parched.

Variation of parameters and influence on the spray drying process

In connection with the drying procedure, the inlet temperature is an important value for the drying process. The higher the inlet temperature, the greater the amount of evaporated surface per time and therefore higher throughputs are possible. On the other hand, lower inlet temperatures also reduce the wet bulb temperature and thus protect active substances from destruction.

The temperature of the drying air before entering the cyclone is called outlet temperature. This temperature is a result of the energy and mass balance and cannot be regulated independently. It is the temperature to which the product maximal is heated.

The amount drying gas is the mass flow (volume flow) which is fed to the spray drying column per time. The higher the drying gas flow rate, the greater the particle movement and the smaller the residence time in the spray dryer.

2.2.3. Collection of dried powders

After the drying process in the spray dryer column it follows the collection and separation of the particles. The particles fall either by gravity into a collecting tank connected to the lower side of the column or are transported with the gas flow. Separation of the particles from the gas flow is usually done via a cyclone or bag filter.

In the event that larger particles are not carried along with the gas stream, there are so-called riser pipes, which supply an additional hot gas stream laterally at the lower end of the spray-drying column. This method is relatively common in spray dryers at the laboratory scale[3]. In a cyclone, the particles of the drying gas are separated by centrifugal force which is created by setting air in a fast rotational motion. There are laboratory scale spray dryer cyclones with a special coating on the inside of the cyclone to prevent powder agglomeration by electrostatic forces. The exhaust air passes through fabric in bag filters and the movement of the product particles stops. With such filters, particles smaller than 1µm in diameter can be separated[2].

2.3. Particle size measurement techniques

The particle measurement technique is essential for the description of disperse substances. The task of the particle measurement technique is not only to determine changes between the starting material and end material during a process step, it also can be used to search for suitable process steps with which the desired properties of a product can be achieved. In the pharmaceutical industry, particulate measurement technology is very important for quality control and the regulation and control of process engineering. The most common methods for determining the particle size distribution are[1]:

- Sieving techniques
- Microscopic techniques
- Sedimentation techniques

- Optical techniques

Sieving techniques

In the screening process, the mass fraction is determined, which remains on each sieve with different mesh size. If the particle passes through a mesh, it counts to the sieve transition. If it remains on the loop, it counts to the residue. Gravity alone is not sufficient for the screening process and additional lateral movements are necessary. Therefore, very often vibration screenings are performed. The particle size range for the application of the analysis sieving extends from approx. 5 µm in the wet sieving up to 125 mm sieve opening width with the vibration sieving[1].

Microscopic techniques

For particle analysis via microscopic techniques, light and electron microscopy are available. A shape- and size-specific image of the particles is possible with a light microscope up to about 2µm, in electron microscopy the limit is 0.1nm[1]. Microscopy is a time- consuming and cost- intensive method for particle analysis because of the elaborate preparation of the samples. The determination of physical particle properties is therefore in the foreground instead off geometric statements about particle collectives.

Sedimentation techniques

In any sedimentation method used for particle analysis, the settling velocity w_s of the particle is the reference size. Before starting the measurement, agglomerates and adhering micro particles must be separated from each other. Particle size analysis is possible with sedimentation in the gravitational field as well as in a centrifugal field. The measuring principle in sedimentation is based on the temporal change of the solids content during the settling process, measured at a certain height of the sedimentation vessel or it is scaled below (above) a measurement level the accumulating amount of solids depending on the time.

Optical techniques

Many optical methods are counting methods, that means, they have the number as quantity type. The primary result of such a counting method is the number distribution sum Q_0 or the number density function q_0. A conversion into mass proportions can be done by Equation 2-9 and Equation 2-10. In all counting methods, the problem is to count a sufficiently large number of particles, so that even for fractions that occur in the particle collective with only small proportions, a sufficient statement security is achieved.

In the imaging procedures, an image is made of the particles of the analytical sample, each individually measured and assigned to a grain class depending on the size. The acquired image is digitized by grayscale grading with high resolution and scanned line by line. A distinction is made between static and dynamic image analysis methods. In the case of the static method, the particles are fixed, for example on glass slides or as images. In dynamic image analysis methods, snapshots of moving

particles in a liquid or gas stream are evaluated. A size range of 0.03 to 30mm can be analysed with this method and in addition, information can be obtained about the shape of the particles[1].

Scattered light methods are all methods, where the scattering and absorption of light on individual particles or particle collectives are measured to determine the size and the concentration of the particles. The measuring principle in the scattered light measurement is based on deflection and thus a change in direction in the propagation of a light wave with the wavelength when it hits a particle. The physical theories underlying these calculations are the Fraunhofer diffraction for comparatively large particles and the Mie theory, which is used for large and also for small particles. In practice, instruments operating on the scattered light method are calibrated with nearly monodisperse standard powders of known particle sizes.

In an absorbance measurement, the intensity attenuation of a light beam if a fluid passes the distance between the light source and the sensor is detected. If dispersed particles are contained in the fluid, the attenuation of the light beam can be significantly influenced thereby. The mathematical description is made by Lambert's law.

2.4. Explosion protection

The use of flammable or explosive chemicals is inevitable in many industrial processes for the manufacture and further processing of products. In order to minimize the risk of damage to people and machines which have to work and operate under such circumstances, a comprehensive analysis and implementation of security measures is necessary.

2.4.1. Definition of characteristic parameters

For the assessment of the risk of explosion, the following safety data of the substance are most frequently used.

Flashpoint FP:

According to DIN V 14011, the flash point of a substance is the lowest temperature at which an ignitable vapour-air mixture can form over a liquid.

If the temperature is below the flash point, the flame cannot spread even if an ignition source is present because the heat from the oxidation is insufficient to stoke up the mixture to the temperature required for combustion. A flash point below room temperature is very dangerous because the combustible substance can be ignited at any time by a spark without any further heat input. Examples of flashpoints are listed in Table 2-2.

Table 2-2: Flashpoint of substances

Substance	***US Environmental Pollution Agency [°C]*** [5]	***Design Institute for Physical Property Data DIPPR [°C]*** [5]	***LSI Sicherheitsdatenbank der Schering AG [°C]*** [5]
Acetone	-24	-18	-19
Ethanol	13	13	12
Ethylenglycol	111	111	110
Isopropanol	12	12	12
Methanol	11	11	11
Toluol	-	4	6

Lower flammable limit LFL:

Flammable substances have a limit concentration below a mixture of substance and air is not ignitable. There is a lack of fuel or excess air. This point is also called the lower explosion limit.

Upper flammable limit UFL:

The limit concentration above a mixture of combustible substance and air which is not ignitable is called upper explosion limit. There is too much fuel or too less air available. Figure 2-3 shows the lower and upper explosion concentration.

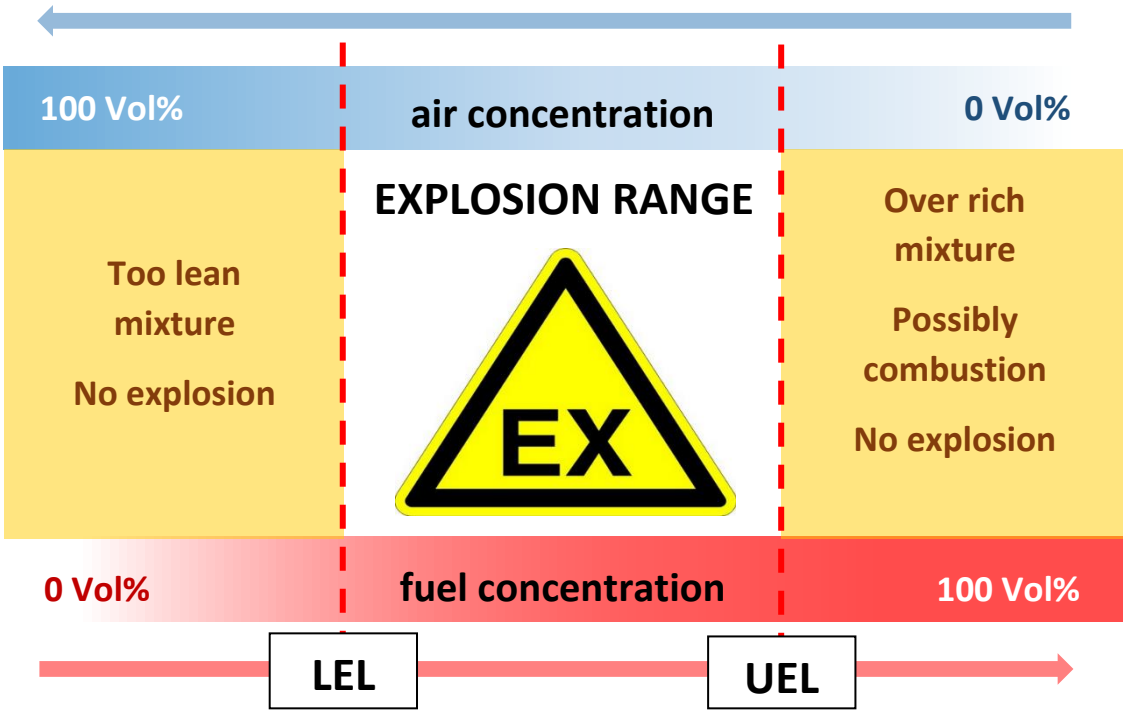

Figure 2-3: Lower and upper explosion limit

The lower and upper explosion limits depend on both pressure and temperature. They are an unpredictable empirical property of combustible substances and are determined according to given standards.

Limiting oxygen concentration LOC:

An inert gas is added to an explosive mixture until flame propagation is no longer possible. The oxygen limit concentration is thus the maximum concentration of oxygen in a fuel / air / inert gas mixture in which an explosion does not occur[6]. In closed systems this is easy to realize by monitoring the oxygen content with an oxygen sensor. The limiting oxygen concentration does not say anything about the inertisation. Even if the LOC is adhered to, an explosive atmosphere can occur if enough oxygen is added. This case can occur for example if there is a leakage. The limit oxygen concentration is also an explosive limit.

Ignition temperature IGT:

The ignition temperature is the temperature to which a flammable substance must be heated so that a combustion reaction with atmospheric oxygen starts automatically. It is not a substance constant. This safety index is dependent on many external parameters such as the shape of the hot surface, the volume and the material of the ignition container, the state of motion of the mixture and the concentration of the fuel / air mixtures[6].

Minimum ignition energy (MZE)

The minimum ignition energy (MZE) is the lowest capacitive stored energy determined under prescribed experimental conditions, which is sufficient to barely ignite the mixture of an explosive atmosphere[6].

Maximum explosion pressure p_{max}:

The maximum explosion pressure is the highest pressure level in a closed vessel that occurs if an optimal fuel gas / air mixture explodes. The maximum explosion pressure is usually not volume-dependent. For most organic gases and vapours mixed with air at initial atmospheric conditions it is about 8 to 10 bar; it increases proportionally with the absolute initial pressure and is inversely proportional to the absolute initial temperature. The maximum increase in pressure over time is volume-dependent. If the maximum increase in pressure is multiplied by the third root of the relevant volume, it obtains a constant value. This KG value is the maximum increase in pressure over a volume of 1 m³ [6,7].

2.4.2. Probability of an explosion

The basis in determining the explosion risk of disperse systems of combustible substances with air or other gaseous oxidants is the probability principle.

When determining the risk of explosion of disperse systems of combustible substances with air or other gaseous oxidants, the basis of the probability principle applies. The risk of an explosion can be represented by a combination of several probability components and must not exceed a certain limit risk.[6] This relationship can be expressed by Equation 2-17.

$$R_{ex} = P_e * P_i * S_{pro} \leq R_g \qquad \textit{Equation 2-17}$$

P_e is the location-dependent probability of occurrence of an explosive mixture. P_i the probability of the occurrence of an effective ignition source in the local area of the explosive mixture. S is the expected extent of damage if the explosive mixture is ignited. The task of the explosion protection is to reduce one or more of these risk components in such a way that the limit risk R_g is never exceeded. P_e, P_i and S_{pro} are also called primary, secondary and tertiary explosion protection.

2.4.3. Primary explosion protection

A mixture forms an explosive atmosphere when the content of the composite of combustible components with the oxidizing components is within the explosive limits. The primary explosion protection measures are to reduce the content of combustible or oxidizing substances or to ensure that a certain ratio is maintained.

Replacement of dangerous explosive substances

If possible, flammable substances should be replaced with non-flammable (e.g. water) for the process. The same applies to the cleaning agents. Hydrocarbons with low flashpoints may be replaced by hydrocarbons with higher flashpoints. Even if combustible fillers are used, the possibility should be investigated of whether they can be replaced by non- flammable fillers.

Prevention of the formation of explosive atmospheres inside the equipment

The formation of an explosive atmosphere can be prevented by keeping the temperature of the liquid constantly at least 5 Kelvin below the flash point[5]. If the liquid is a mixture of several components, a temperature difference of 15 Kelvin should be aimed for[5].

The risk of explosion can also be reduced by performing the process under vacuum or low pressure. The explosion parameters p_{max} (maximum explosion pressure) and K value (maximum pressure increase) are influenced by the outlet pressure for an explosion. By applying vacuum it can be achieved that no explosion can take place below 20 mbar[8], or the maximum explosion pressure remains below atmospheric pressure. For most flammable substances the outlet pressure is below 100mbar[5].

Prevention of the formation of explosive atmospheres in the surrounding of equipment

If there is a concentration of combustible material in the tank above the upper explosion limit, it can lead to the formation of an explosive atmosphere in the case of leakage.

Constructive measures can help to ensure explosion protection and thus ensure safety for workers and employers. Particular attention should be paid to the design and construction of all apparatus and fasteners. Technically sealed devices are a prerequisite for a smooth process flow. A leak test before commissioning of the system contributes to explosion protection. When using explosive substances, it is reasonable to limit the operational release. By blowing in inerting agents, the explosion can be suppressed. Another measure to protect workers is compliance with the maximum escape route length.

The emergence of an explosive atmosphere can also be prevented by ventilation. In the open air or rooms with sufficient natural ventilation, no further protective measures may be necessary. Alternatively, a suction unit can be installed in the process room to achieve a sufficiently high air circulation.

Degree of ventilation

The degree of ventilation has to be equated with the power of the exhaust system. The minimum volume flow of fresh air dV/dt_{min} is calculated, which is needed for dilution in case of leakage to prevent

the formation of an explosive atmosphere. This value is compared with the volume flow of the exhaust fan at maximum power. For safe operation of the system, the calculated value must be less than the specified value according to the planning protocol of the process room 2.

Important for the minimum volume flow of fresh air dV/dt_{min} are the maximum leakage flow dG/dt_{max}, a safety factor k applied to the lower explosive limit, the LEL and the ambient temperature T. Equation 2-18 shows the mathematical relationship[5].

$$dV/dt_{min} = \frac{\frac{dG}{dt}_{max}}{k * LEL} * \frac{T}{293} \qquad \textit{Equation 2-18}$$

To determine the safety factor k, the source and degree of release of the leakage must be considered more closely.

The source of leakage is a point or a location from which gas, vapour, mist or liquid may be released into the surrounding to form an explosive atmosphere. The degree of release is divided into 3 groups- continuous, primary and secondary. In continuous release, it is a constant or at least very frequent escape of explosive substances from the apparatus or the system into the environment expected. This normally leads to zone 0[9]. If the malfunction of an explosive substance occurs periodically or occasionally during normal operations, it is called a primary release. This normally leads to zone 1 [9]. A secondary release is not expected to occur in normal operation- if it does occur it is only infrequently and for short periods. This normally leads to zone 2 [9]. The safety factor k is shown in Table 2-3.

Table 2-3: Safety factor k

Safety factor k according to LEL[5]	
Continuous and primary release	0.25
Secondary release	0.5

An example for a continuous type of release is a surface of a flammable liquid open to the atmosphere. There is always the danger that an explosive atmosphere will be formed. In case of activation of the safety valve or leakage through a corrosion hole, a secondary type of release is present. Any events that are rarely or not expected to occur are assigned to the secondary type of release. For the following calculation, it is assumed that during the opening for regular charging procedures or sampling and venting during the charging process, a release of the solvent occurs in the surrounding atmosphere. This is assigned to the primary release.

The lower explosion limit must be used as concentration in kg / m³ for the calculation of the minimum volume flow of fresh air. A conversion from the often used representation in volume percent to a concentration specification in kg / m³ can be carried out at atmospheric conditions with Equation 2-19[5].

$$LEL\left[\frac{kg}{m^3}\right] = 0.416 * 10^{-3} * M * LEL[vol\%] \qquad \textit{Equation 2-19}$$

Here, M is the molecular weight of the substance in kg/kmol.

Hypothetical volume Vz

The hypothetical volume Vz is the volume of potentially explosive atmosphere around the source of release. Depending on the volume of the room, it can be determined with the hypothetical volume whether the potentially explosive area has to be defined for the entire room or for partial areas. The hypothetical volume is calculated with the minimum volume flow of fresh air and the number of air changes C[5]. This is shown in Equation 2-20.

$$V_Z = \frac{\left(\frac{dV}{dt}\right)_{min}}{C} * f_c \qquad \textit{Equation 2-20}$$

The air exchange rate c is a measure of the supply air volume flow of the room based on the total volume of the room. This parameter with the unit [1 / h] indicates the exchangeable volume of the room per time.

In practice, the real number of air changes is always less than given by C. The equation for the hypothetical volume Vz can be extended with a correction factor f_c. This factor takes into account non-idealities in the extraction. The value range goes from 1 (ideal case) to 5 (impeded air flow).

Estimation of persistence time

The time until the concentration of an explosive substance in the surrounding atmosphere in the event of a leak has dropped so far that no more explosion can take place is called persistence time. The persistence time is calculated according to Equation 2-21[5].

$$t = -\frac{f_c}{c} * ln\left(\frac{LEL * k}{X_0}\right) \qquad \textit{Equation 2-21}$$

For this formula, the lower explosion limit must be in the unit volume percent [vol%]. X_0 is the initial concentration of the combustible substance if there is a leakage. Assuming that near a leakage the largest possible amount of the explosive solvent is evaporated, X_0 is the ratio of vapour pressure and total pressure.

From the hypothetical volume and the persistence time, a possible classification in zones can be made together with the degree of ventilation. According to the standard EN 60079-10, the degree of ventilation is divided into 3 subgroups. These are shown in Table 2-4.

Table 2-4: Degree of ventilation

Degree	*Condition*	*Zone*
good	Concentration during release becomes immediately lower than lower explosion limit	**Zone 2 or no hazard**
fair	Stable situation below the lower explosion limit during release	**Zone 1**
poor	Concentration during release can not be kept below the lower explosion limit	**Zone 0**

In addition to technical explosion protection measures, organizational and personal activities also contribute to safety. Operating instructions as well as a sufficient qualification are among the organizational measures. A cleaning plan should be prepared for the correct execution of all cleaning work. Special care must be taken on poorly accessible surfaces and difficult-to-reach places. For dust deposits a vacuum cleaner has to be used, blowing procedures or sweeping are not permitted. Potentially explosive areas should be marked for better perception and access regulations must be set up.

Important personal measures include, for example, the wearing of conductive clothing or shoes.

Inertisation

Inerting creates an inert or nonreactive atmosphere of the plant or the entire laboratory space, so that no explosion or fire can occur. This is achieved by reducing the oxygen content. Inert gases which are most commonly used in industry are nitrogen, steam carbon dioxide and noble gases like argon or helium. The maximum permissible oxygen concentration φ_{O_2} during inertisation is given by the LOC minus a safety value ΔS and is shown in Equation 2-22[5].

$$\varphi_{O_2} = LOC - \Delta S \qquad \textit{Equation 2-22}$$

Inertisation distinguishes between partial and total inertisation.

Partial means here that the oxygen concentration is reduced below the LOC minus the safety value, but the now inertized atmosphere becomes explosive again when air is supplied. In the case of total inerting, the volume fraction of oxygen is reduced to such an extent that the LOC is not exceeded even when the air is supplied. The oxygen volume fraction must always be monitored metrological in both cases. The difference between partial and total inertisation is shown in Figure 2-4 in a triangular diagram with the components fuel, oxidizer and inert gas[10]. That means, each mixing ratio of the three components within the orange area is partial inertized. Within the green area, each mixing ratio is total inertized. The area where an explosive atmosphere can occur is located between LEL and UEL. The span narrows as the oxidizer decreases and finally disappears completely.

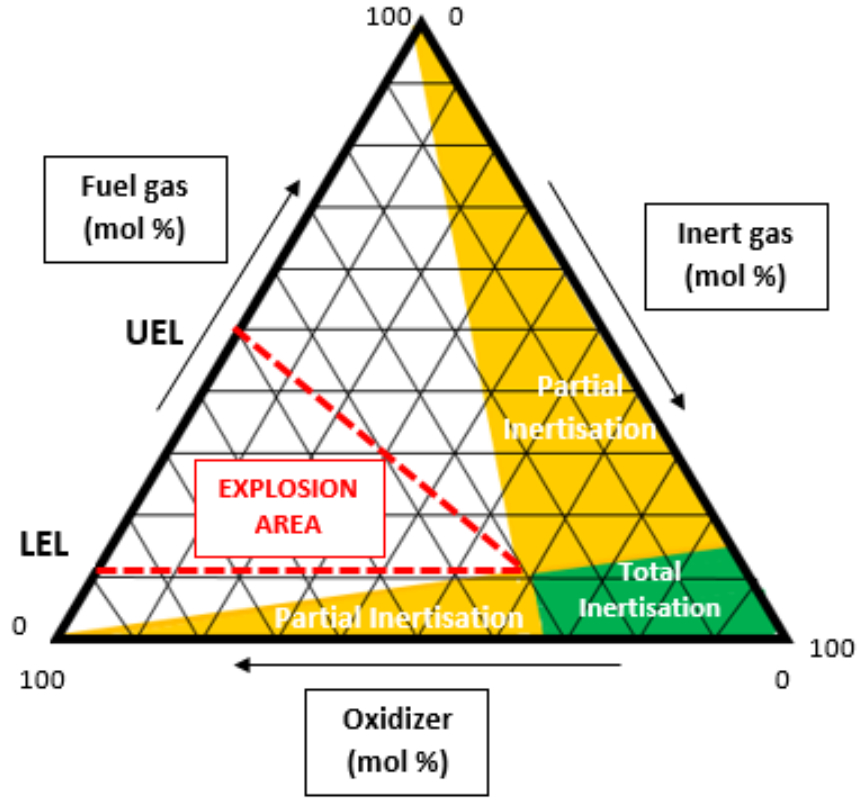

Figure 2-4: Difference between partial and total inertization

There are different methods that are used for inerting[11]:

- Pressure swing procedure
- Vacuum pressure swing method
- Partial evacuation
- Replacement
- Flushing
- Permanent inert atmosphere

At the pressure swing process, the tank is filled with inert gas up to the maximum permissible tank pressure. Then it is relaxed again to ambient pressure. These cycles are repeated until the permissible oxygen concentration is reached. Identical results are possible by evacuating and re-pressurizing with inert gas. This procedure is called vacuum pressure swing method. Both are the best method for inertization.

The volume fraction of oxygen after n cycles is calculated for isothermal pressure change as follows in Equation 2-23[11]:

$$c_n = c_i + (c_0 - c_i) * \left(\frac{p_1}{p_2}\right)^n \qquad \textit{Equation 2-23}$$

The volume fraction of oxygen after n cycles is calculated for adiabatic pressure change as follows in Equation 2-24[11]:

$$c_n = c_i + (c_0 - c_i) * \left(\frac{p_1}{p_2}\right)^{\frac{n}{\kappa}} \qquad \textit{Equation 2-24}$$

Here, c_0 is the initial oxygen volume fraction, c_i the oxygen volume fraction in the inert gas and c_n the oxygen volume fraction after n cycles. p_1 is the lower pressure limit and p_2 is the upper pressure limit. n is the number of cycles and κ is the adiabatic exponent. Due to the partial evacuation, the amount of oxygen in the container is reduced, while at the same time the minimum ignition energy increases at a lower pressure.

Inerting by displacement is an economical process because the amount of inert gas which is needed and the time required are small compared to other inertisation processes.

2.4.4. Secondary explosion protection

If explosion hazards can not be completely or only partially eliminated by primary explosion protection measures, other precautions must be taken to ensure that the risk of an explosion is minimized. The secondary explosion protection includes all measures to prevent sources of ignition, so that a detonation of an explosive atmosphere is not possible. The hazardous area is divided into several zones. Within these defined areas, there are special requirements for the equipment, which are used in the respective zone. It also defines how to demonstrate compliance with these minimum requirements.

There is a classification according to zones for mixtures of air and flammable gases, vapours or mists. Depending on the degree of danger, they are divided into zone 0, zone 1 and zone 2. Explosive atmospheres of air and dust are divided into zones 20, 21 and 22 depending on the frequency of occurrence. Table 2-5 gives an overview of the zone concept of explosive atmospheres[5].

Table 2-5: Zone concept

Zone 0 and Zone 20	***Example***
Areas in which a potentially explosive atmosphere exists permanently, over long periods of time or frequently.	The area inside of containers or equipment for dusting goods also in mills, dryers, mixers, delivery lines, silos
Zone 1 and Zone 21	***Example***
In normal operation, an occasional formation of an explosive atmosphere is possible.	The vicinity of charging openings, filling or discharge openings, the vicinity of zone 0, the nearer area at filling points in containers or areas where dust is deposited in such quantities that occasional whirling may occur during normal operation
Zone 2 and Zone 22	***Example***
Areas where during normal operation a potentially explosive atmosphere normally does not occur or if, only for a short time (for example in the case of faults)	Areas around enclosed pipelines which are technically leak-proof. Areas surrounding zone 0 or 1 or areas where dust is expected to accumulate

Depending on the probability of the occurrence of an explosive atmosphere, a selection must be made of the equipment with possible electrical or mechanical ignition sources. According to ATEX directive 94/9 / EC for electrical apparatus for hazardous areas there are 2 groups requested from devices which can be classified. Group 1 is electrical equipment for mines susceptible to fire damp. Group 2 is electrical equipment for places other than mines. Group II is subdivided into IIG for use where gases or vapour may be present and IID for use where dusts may be present. In Group 2, there are 3 subcategories, which are described in more detail.

- Category 1: for use in zone 0 or 20 (very high level of safety);equipment can be used also in zones 1, 2 or 21, 22
- Category 2: for use in zone 1 or 21 (high level of safety); equipment can be used also in zones 2 or 22
- Category 3: for use in zone 2 or 22 (normal level of safety)

2.4.5. Tertiary (constructive) explosion protection

If primary and secondary measures do not provide safe protection, constructive measures must be taken to be hit.

- Explosion-proof construction
- Explosion pressure relief
- Explosion suppression
- Prevention of flame
- Explosion transmission

2.4.6. Legal basis for explosion protection

The Ordinance on Explosive Atmospheres (VEXAT), BGBl. II No. 309/2004 as amended, came into force on August 1, 2004. VEXAT contains requirements for explosion protection in workplaces, construction sites and external workplaces within the meaning of the Employee Protection Act. This regulation transposes EU Directive 1999/92 / EC on minimum requirements for improving the safety and health protection of workers which are exposed to the risk of an explosive atmosphere. In the Vexat Ordinance are regulated the following obligations[12,13]:

- Identification, evaluation and documentation of the explosion hazards
- Information, instruction and work release
- Tests, measurements, hazard analysis and accident prevention
- Primary, secondary and tertiary explosion protection measures
- Requirements for electrical systems and objects in potentially explosive atmospheres

The legal framework of CE marks in the European Union for equipment which is used in explosive atmospheres is governed by directive 1999/92 / EC of the European Parliament and of the Council of 16 December 1999 on the minimum requirements for improving the safety and health protection of workers potentially at risk from explosive atmospheres and directive 2014/34 / EU of the European Parliament and of the Council of 26.2.2014 on the harmonization of the laws of the member states relating to equipment and protective systems intended for use[13,14].

In Austria, these guidelines are contained in the Federal Law BGBl I No. 77/2015 Machinery Marketing and Notification Act - MING last amended by Federal Law BGBl I No. 96/2016 and Federal Law BGBl. II No. 52/2016 Explosion Protection Ordinance 2015 - ExSV 2015[15–17].

The essential requirements are defined by these guidelines. The technical specification takes place in the harmonized standards. These are prepared by the European standardization organizations (CEN, CENELEC, ETSI), published in the Official Journal of the EU and transposed into national standards[18]. If the manufacturer meets the harmonized standards applicable to the product, the presumption of conformity exists. This means that the product can be expected to meet these requirements. It is recommended to use standards, but in principle it is optional whether they are used.

3. Material and Methods

3.1. Materials

For all tests carried out, both the ProCept spray dryer and the modified spray nozzle test stand, a suspension of a saturated lactose solution with different proportions of water and isopropanol and dispersed lactose is used.

3.1.1. Lactose

Lactose or milk sugar is a carbohydrate, a disaccharide and consists of the sugar molecules D-galactose and D-glucose. Lactose occurs naturally in mammalian milk as well as in dairy products. Lactose is the most commonly used excipient for pharmaceuticals, especially as a filler for tablets and capsule production[19]. It is a white to almost white crystalline powder with a weak sweetening power. The lactose shows mutarotation, because in each case only the OH group of the anomeric carbon atom of a monosaccharide is involved in the formation of the glycoside bond[20]. Since the OH group of the other anomeric carbon atom is not blocked by a glycoside bond, both α and β and open-chain lactose forms can be build. The most stable form is α lactose monohydrate. In this form, lactose crystallizes from supersaturated aqueous solution at T <93.5 °C[19,20], depending on the conditions in prisms or pyramids. Crystallization from aqueous solution at T> 93.5 °C. leads to anhydrous β lactose[19,20]. Fast dry (for example, spray drying) gives an amorphous equilibrium mixture of α and β lactose. Differences in physical properties between α and β lactose are shown in Table 3-1[20].

Table 3-1: Difference in physical properties between α and β lactose

	α lactose	***β lactose***
Melting point (anhydrous) [°C]	223	252,2
Melting point (hydrous) [°C]	201.6	---
Solubility [g Lactose/ 100g H_20] at 0°C	5	45,1

Commercial products never contain a pure lactose form, it is usually a mixture of α lactose and β lactose. The glass transition temperature is dependent on the moisture content of the lactose, it is for lactose with 0% humidity 101°C and decreases with increasing moisture content[21].

For all experiments carried out in this work, lactose with the product name “GranuLac® 230" from the company dairy MEGGLE Wasserburg GmbH & Co. KG is used.

3.1.2. Isopropanol

2-Propanol or isopropanol is a colorless, alcoholic-smelling liquid that mixes well with water, alcohols, simple hydrocarbons, ethers, and oxygen-containing solvents. Isopropanol is highly flammable and burns with the oxygen of the air with a sooting flame. The vapors are heavier than air and can form explosive mixtures with them. 2-Propanol is produced industrially by hydration of propene on acidic ion exchange resins as a catalyst. It also can be obtained by catalytic hydrogenation of acetone. Table 3-2 lists the most important chemical and physical properties[22]. For the experiments isopropanol ≥ 99.5% from Carl Roth GmbH +Co. KG was used.

Table 3-2: Chemical and physical properties of isopropanol

Density at 20°C [g/cm³]	0.87
Initial boiling point [°C]	82
Melting point [°C]	-89
pH- value	defined according to DIN 19260 only in aqueous media
Partition coefficient n octanol / water (log KOW)	0.05

Table 3-3 lists data relevant to explosion protection[7].

Table 3-3: Relevant data for explosion protection

Vapor pressure at 20°C [hPa]	43
Lower explosive limit [vol % at 1 bar]	2
Upper explosive limit [vol % at 1 bar]	13.4
Inertisation LOC [mol %]	8.7
Flash point [K]	20
Explosion pressure [bar]	7.8
Minimum ignition energy [mJ]	0.65
Ignition temperature [K]	399

3.1.3. Spray dryer ProCept

All spray drying experiments are carried out with a lab- scale spray dryer from ProCept.(Zelzate, Belgium) The ProCept spray dryer consists of 3 main components: the glass spray columns and fixture, a computer unit for controlling and monitoring process parameters and a so-called nitrogen unit. The operation of the plant is operated with a spray drying column. To extend the residence time of the product, the operation is also possible with up to 3 columns. The feed stream is conveyed with a peristaltic pump in the spray drying column. The flow rate of the pump can be controlled by the computer unit. For a targeted adjustment of the mass flow, a calibration curve must first be created. The feed is transported with the peristaltic pump towards the pneumatic nozzle, where atomization of the liquid takes place. Afterwards the fine dispersed droplets dry along the drying column. The diameter of the spray nozzle can be varied, further it is possible by conical attachments to change the spray cone. The gas stream for the atomization process can be controlled by a setting wheel on the computer unit. Other parameters that can be set are the drying gas flow and the inlet temperature of these into when it enters the spray column. The spray drying column and the computer unit are shown in Figure 3-1.

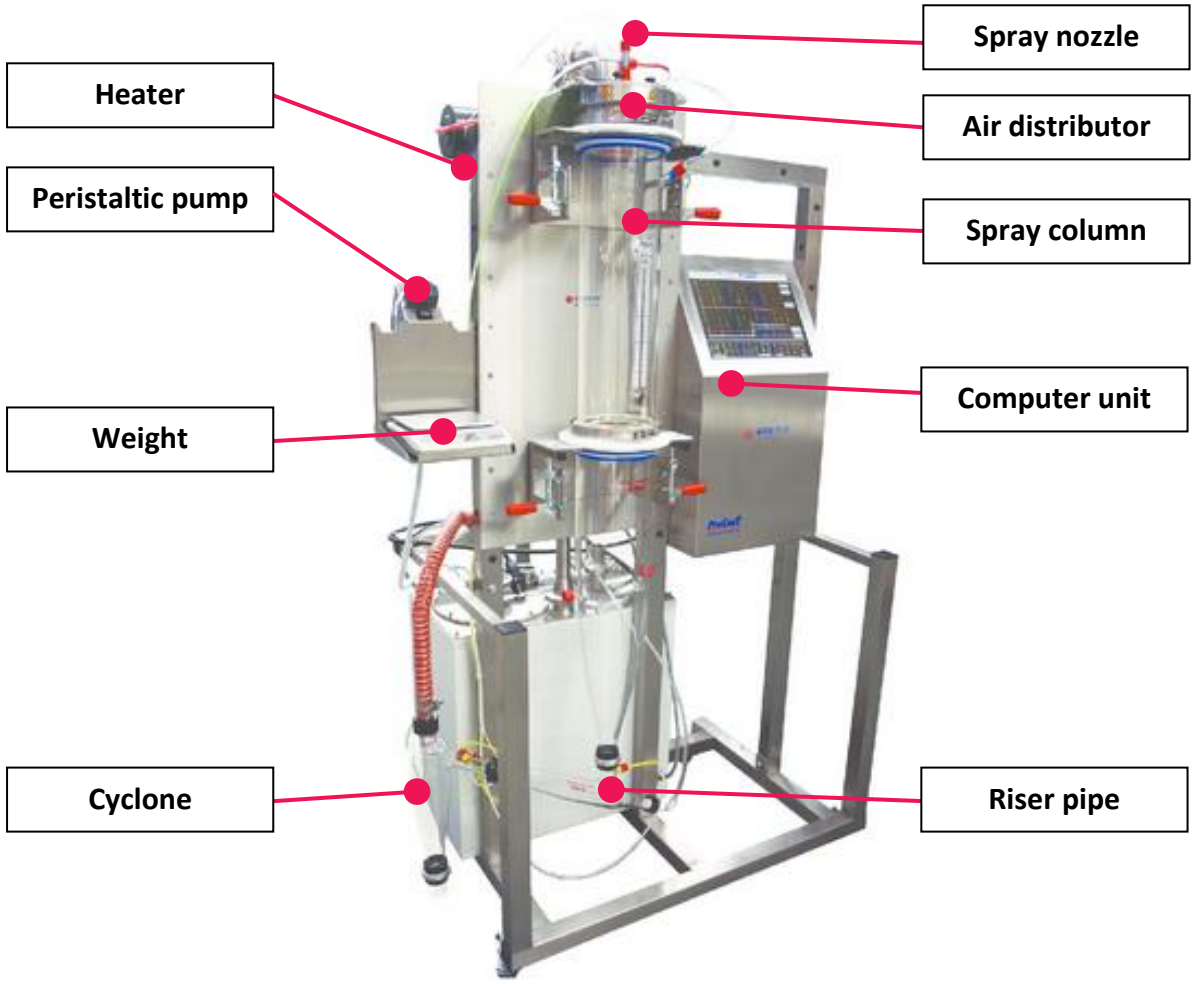

Figure 3-1: Components of the ProCept spray dryer (http://www.pro-c-ept.com/, access: 13.03.2018)

For the separation of the dried particles from the gas stream three different cyclones in different sizes are available. For the experiments the large size (separates > 5µm) glass cyclone was used. Each cyclone has a different pressure drop between entry and exit of the gas flow and thus a different particle size separation. All glass parts can be quickly and easily connected by a plastic screw and the spray drying columns are connectable by a clamp fastener.

Spray drying with the ProCept spray dryer can be carried out as an "open loop" or as a "closed loop" process. "Open loop" process means the inlet drying air is sucked out of the room by a blower, cleaned by a filter, scaled in the heater and fed to the spray drying column. In contrast, in the closed-loop process, nitrogen from a nitrogen bottle is used as the drying medium. The nitrogen is recycled. In this case, the nitrogen gas is passed after the drying step in the so-called "nitrogen unit". This unit controls the nitrogen consumption, if necessary, fresh nitrogen from the gas bottle is supplied. The solvent-loaded nitrogen is passed through a filter and then a condenser, thereby entrained particles and the solvent is separated. Before the gas is returned to the heater and subsequently to the drying column, it flows through a filter again. The "closed loop" process is used, when working with explosive solvents. Figure 3-2 shows the nitrogen unit.

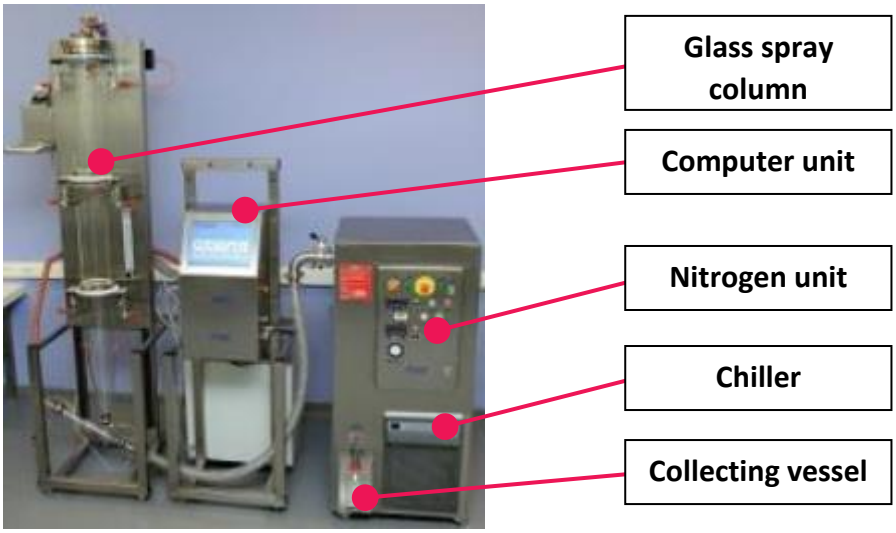

Figure 3-2: Nitrogen unit (http://www.pro-c-ept.com/, access: 13.03.2018)

3.1.4. Spray nozzle test stand

The spray nozzle test stand is a converted spray dryer with the purpose to test different spray nozzles. The main focus of the system is to assess particle size changes from the spraying process and to evaluate stability of the spraying process (nozzle clogging). To ensure the safety of man and material, an explosion protection concept was developed for the spraying of explosive substances.

Explosion protection

It must be expected in the event of leakage of the spray nozzle test stand that isopropanol exits and forms an explosive atmosphere with the ambient air. Therefore, a precise analysis with regard to the danger of explosion was carried out.

According to the experimental protocol, the maximum mass flow of isopropanol is settled to 2 kg / h. For the design of the explosion protection, isopropanol, a flammable solvent to be sprayed is decisive. Process room 2 has an estimated volume of 100 m³, an air exchange number of 20 / h and the exhaust fan volume is 500 m³ / h.

The explosion protection measures for the spray nozzle test stand is the use of a suction fan and the creation of a zone concept. In addition, a partial inertization of the suspension to be sprayed is carried out. For this purpose, nitrogen is used as sputtering gas. For a correct interpretation of the explosion protection, the degree of ventilation is evaluated and the hypothetical volume and the persistence time are calculated as it is shown in Chapter 2.4.3. For the calculation it is further assumed that the room temperature is 25°C and the room has a volume of 100m³. Equation 2-18 provides the minimum volume flow of fresh air. The conversion of the lower explosion limit from the unit volumetric percentage into kg / m³ is carried out with Equation 2-19. The k- value is set to 0.25.

$$dV/dt_{min} = \frac{\frac{2}{3600} * (273.15 + 20)}{0.25 * 0.0500} * \frac{1}{293} * \frac{\frac{\frac{kg}{h}}{\frac{s}{h}} * K}{\frac{kg}{m^3} * K} = 0.0445 \frac{m^3}{s} = 160.2 \frac{m^3}{h}$$

The minimum volume flow of fresh air which is explained in Chapter 2.4.3 can be used to calculate the volume of the explosive atmosphere created in the event of a leak around the spray nozzle test stand.

$$V_Z = \frac{0.0445}{\frac{20}{3600}} * 3 * \frac{\frac{m^3}{s}}{\frac{s}{h} * h} = 24.2727 m^3$$

In order to ensure a sufficient certainty of the calculation, the factor f is determined with the value 3. The persistence time is calculated using Equation 2-21. The vapour pressure of isopropanol at atmospheric pressure and 25 °C is 42.6 hPa[22].

$$t = \frac{-3}{0{,}0055} * \ln \frac{2 * 0{,}25}{\frac{42{,}6 * 100}{1013{,}25}} = 769{,}60 s$$

The exhaust fan power in process room 2 is with a maximum volume flow of 500 m³ / h sufficient for the spray nozzle test stand. Even with a leakage flow of 100% of the feed stream, the blower output is adequate. The hypothetical volume is important for the division into zones of the process room. If a spherical expansion of the explosive solvent is assumed in the case of a leakage it can be determined a radius by using the volume formula of a sphere. This results in a radius of about 2 m around the spray

nozzle test stand within which only ATEX-certified devices are to be used. It must also be considered that isopropanol vapours are heavier than air and thus sink to the bottom. This results in a zone concept, which is shown in Figure 3-3.

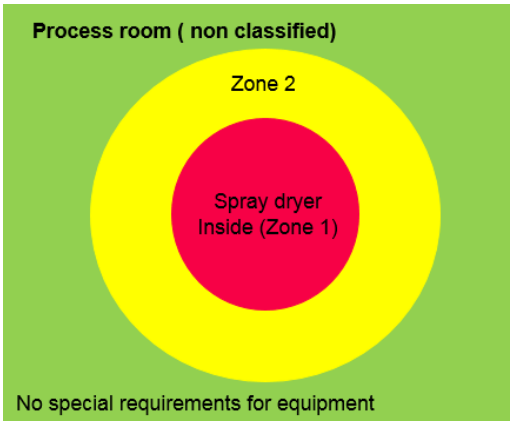

Figure 3-3: Zone concept of the process room

The interior of the spray room is declared zone 1. Within a range of 2 meters, only devices approved for operation in zones 0, 1 or 2 may be used. For the rest of the process area, no special requirements with regard to explosion protection for appliances are necessary.

Modification of the spray dryer

For operation as a spray nozzle test stand, a spray dryer from the company GEA Niro GEA Process Engineering A / S called Niro Atomizer was modified. The spray dryer has a stainless steel chamber with approximate 800mm diameter x 620mm straight side x 700mm cone bottom. The lid can be raised and lowered by a pneumatic system. Figure 3-4, Figure 3-5 and Figure 3-6 show the spray dryer before the necessary construction measures.

Figure 3-4 Spray dryer front

Figure 3-5: Spray dryer side 1

Figure 3-6: Spray dryer side 2

The control panel of the spray dryer has been removed and replaced by a new one with all the control elements which are needed for operating the spray nozzle test bench. All pipe connections have been

replaced by pipes with inch dimensions or standard hose connections. As collecting container and at the same separator for the sprayed suspension and gas flow a converted pressure cooker is used. To monitor the oxygen content in the atomizing air, an oxygen sensor Crowcon XgardIQ with ATEX certification for Zone 1 and Zone 2 from PCE instruments is installed. A cooled scrubber is used to remove the solvent from the exhaust air. The attachment of the spray nozzles is effected by a bracket with an adjustable linkage, which is fastened by means of a flange on the spray cover Figure 3-7 shows a flow chart of the spray nozzle test stand.

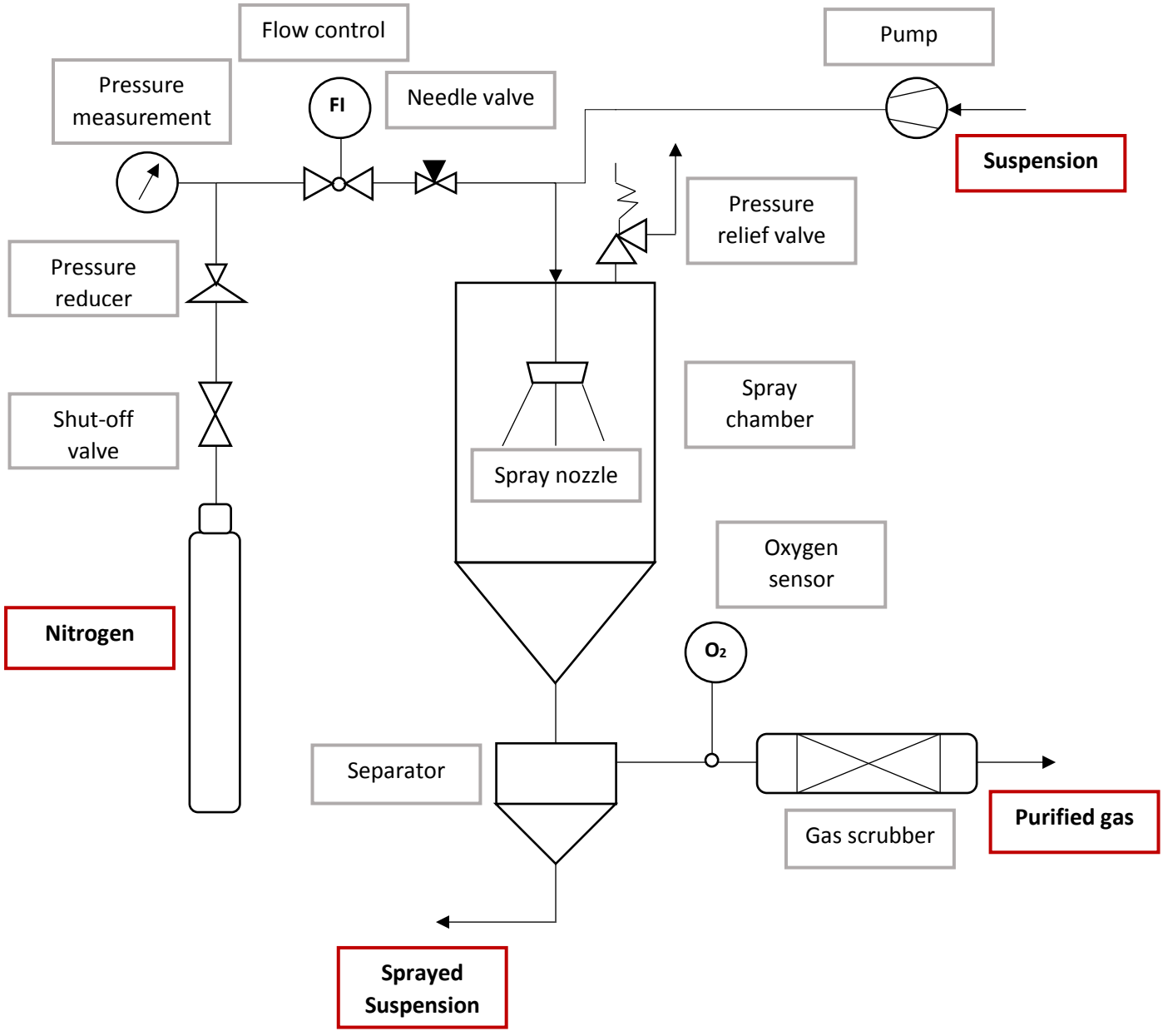

Figure 3-7: Flowsheet of the spray nozzle test stand

The nitrogen is provided by a nitrogen bottle. A shut-off valve and a pressure reducer control the nitrogen inlet. The fine control of the nitrogen flow is carried out by a needle valve and the measured volume flow can be read from a flow meter. With this value and the measured pressure, the actual

nitrogen flow can be calculated. Thereafter, the nitrogen continues to the spray nozzle inside the spray nozzle test stand. The suspension is feed from the container to the spray nozzle by an eccentric screw pump MX 10-s from the company Knoll. After spraying, the sprayed suspension is collected in a separator. The gas stream continues to a gas scrubber. Between separator and scrubber, the oxygen sensor is installed. This serves to monitor the partial inertization. The cleaned gas from the scrubber is fed to the suction system installed in the process room.

Figure 3-8 and Figure 3-9 show the spray nozzle test stand with accessories.

Figure 3-8: Spray nozzle test stand side 1

Figure 3-9: Spray nozzle test stand side 2

3.2. Methods

This chapter explains the experimental preparation and the test procedure with the ProCept spray dryer and the spray nozzle test stand.

3.2.1. Spray drying experiments

The activities of the spray drying tests with the ProCept spray dryer contain the preparation of the suspensions, the spray drying and the evaluation and interpretation of the spray dried lactose powder by using scattering light method for particle size measurements, differential scanning calorimetry and scanning electron microscope images for structure analysis of lactose.

Preparation of the suspensions

Suspensions with a mass fraction of 10% solids and 90% solution content were sprayed. The solution fraction consisted of a saturated solution of lactose (GranuLac® 230) and a mixture of different

proportions of isopropanol and water. The experiments were carried out with isopropanol and isopropanol / water mixtures with a mass fraction of isopropanol of 100%, 75%, 50%, 25% and 0%. An overview of the individual compositions of the saturated solutions used for experiments is presented in Table 3-4. The first two columns are the mass fraction of isopropanol w_{IPA} or of water w_{H20}. $X_{L,s}$ describes the solubility of lactose in the liquid mixture with the respective composition. ρ_{sat} is the density of the lactose-saturated solution. The $X_{L,s}$ value for a blend composition of 25 wt% isopropanol is an interpolated value. The other experimental data were used from Kreimer at al.[23].

Table 3-4: Liquid composition (w_{IPA}, w_{H2O}), solubility of lactose ($X_{L,s}$), ratio of dissolved solids to total solids ($S_{L,s}$) and density of the saturated solutions (ρ_{sat}) for spray drying experiments

w_{IPA}/ wt%	w_{H2O}/ wt%	$X_{L,s}$/ %	$S_{L,s}$/g/g	ρ_{sat}/g/cm³
0	100	23.29	18.90	1.068
25	75	12.60	7.90	0.944
50	50	1.90	2.06	0.899
75	25	0.67	0.32	0.865
100	0	0.008	0.008	0.774

In order to ensure that a saturated state was reached, an excess of lactose was weighed in for the first time. The reference solubility was $X_{L,s}$ from Table 3-4. In order to allow a sufficiently large mass transfer between the three components, the mixture remained for at least 12 hours at room temperature with constant mixing on a magnetic stirrer.

After that, the excess lactose was filtered off and the density was measured and compared with the saturated state. A filter of the type MN 618 from Macherey-Nagel was used. Then 10 wt% of lactose was weighed in from the saturated solution and added. The density was determined with the density meter DSA 5000M from Anton Paar.

Table 3-5 shows the measured densities for the respective solutions. X_d is the dissolved mass loading and is defined by Equation 3-1.

$$X_d = \frac{m_d}{m_{sol}} \qquad \textit{Equation 3-1}$$

m_d is the dissolved mass of lactose and m_{sol} is the mass of dissolved and suspended solids.

Table 3-5: Measured density and literature values of saturated lactose solution[23]

Xd	w_{IPA}***/ wt%***	w_{H2O}***/ wt%***	$\rho_{measured}$***/g/cm³***	ρ_{sat}***/g/cm³***
$7.2*10^{-4}$	*0*	*100*	*1.066*	*1.068*
$2.2* 10^{-2}$	*25*	*75*	*0.979*	*0.944*
$1.5* 10^{-1}$	*50*	*50*	*0.909*	*0.899*
$4.0*10^{-1}$	*75*	*25*	*0.848*	*0.865*
$5.9* 10^{-1}$	*100*	*0*	*0.783*	*0.774*

$\rho_{measured}$ is an average of 3 measurements. By comparison with ρ_{sat} the saturated state was controlled.

Spray drying

All experiments on the ProCept spray dryer were carried out on the basis of the highly flammable isopropanol with nitrogen as an atomizing and drying medium. Experiments with different spray nozzle diameters showed that lactose agglomerates easily. To prevent clogging, the largest possible nozzle diameter of 1.2 mm was chosen. In addition, a spray cone attachment was used to reduce the spray radius and thus reduce lactose deposits on the wall of the spray column. Parameters that can be varied on the spray dryer are listed in chapter 3.1.3. With a sputtering medium flow of 12 liters per minute, a fine, homogeneous division of the suspension drops could be achieved. Subsequently, this setting was kept constant for all experiments. The inflow of the drying medium was set at 0.6 m³ per minute. For the determination of the mass flow, a calibration straight line was created for the different concentrations. After this, the mass flow was set at 7.4 g / min. For the 100 wt% isopropanol suspension in the saturated solution this corresponds to 100% pump performance for those with 75 wt% 96%, 50 wt% 91%, 25 wt% 85% and 0 wt% mass isopropanol 80% pump performance. Each suspension was sprayed at 4 different temperatures - at 80 °C, at 110 °C, at 140 °C and at 170 °C. The suspension was kept well mixed by using a magnetic stirrer. The test duration was determined by the sprayed amount of suspension, but never lasted longer than 45 minutes. The amount of lactose obtained was weighed.

Evaluation and interpretation of the collected samples

Before the samples were examined for changes in the particle size distribution, they were dried in a drying cabinet. A drying cabinet of the model series VD from Binder was used. It is shown in Figure 3-10.

Figure 3-10: Drying cabinet

Inside the drying cabinet, a vacuum can be generated by a pump. This offers the advantage that the drying process can be carried out at a lower temperature and thus also the samples are kept from possible destruction or chemical conversion by heat. From each spray drying test, 3 samples were prepared for the drying cabinet. In the course of drying, the residual moisture content of the spray-dried samples was also determined. This was done gravimetrically, which means that the samples were weighed before and after drying. After a sufficiently long drying time, it could be assumed that the samples contain virtually no residual moisture. The gravimetric determination of the residual moisture was carried out by an analytical balance called SI 234 A from Denver Instruments. The error range of this balance is d = 0.1 milligrams. The used analytical balance is shown in Figure 3-11.

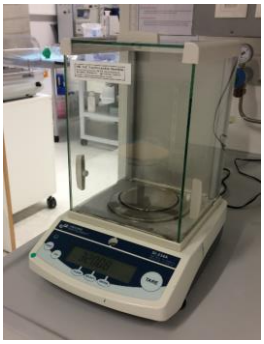

Figure 3-11: Analytical scale

The sample weights were between 1.30 and 1.50 g. It was dried with a pressure of 100 mbar at a temperature of 80 ° C. Equation 3-2 was used to calculate the residual moisture RM of the samples.[%]

$$RM = \frac{m_{wet} - m_{dry}}{m_{wet}} * 100\ [\%] \qquad \textit{Equation 3-2}$$

m_{wet} is the weight mass of sample before the drying and m_{dry} is the mass after drying.

The particle size analysis was carried out by a scattered light method. The scattering and absorption of light on individual particles were measured. Physical theories are the Fraunhofer and Mie theory. The particle size analysis was carried out by Helos of the company Sympathec. The measurement of the samples were done in wet-dispersed mode, which means that a few particles were given into a cuvette which was filled with liquid. A magnetic stirrer kept the particles in the liquid in motion during the measurement. Lactose particles were dispersed in isopropanol - suspensions in their saturated solution. For the measurement, it was important to perform a reference measurement before starting.

Practical experience in the particle measurement showed that an optical concentration of 15-25% is ideal for the laser diffraction measurement. This can be displayed by the evaluation software. The lactose particles or suspension were added with a spatula of the liquid. Various pretreatment methods, mixing ultrasound and suspension, were tried. This is shown in Figure 3-12.

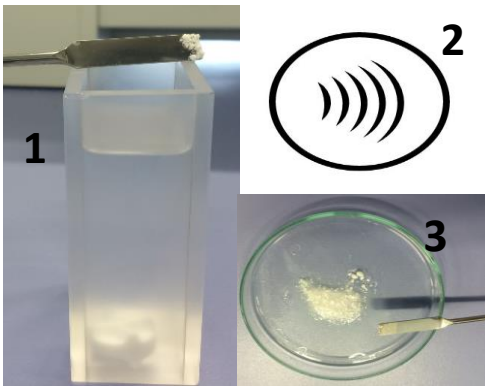

Figure 3-12: (1) Adding with spatula; (2) Acoustic irradiation with ultrasonic; (3) Making suspension

In pretreatment with ultrasound, a significant difference in the particle size distribution was observed. As a test, the sample with an isopropanol content of the saturated solution of 0% was selected which had been sprayed at a temperature of 80 °C. Agglomerates formed during spray-drying were broken up. This is shown in Figure 3-13.

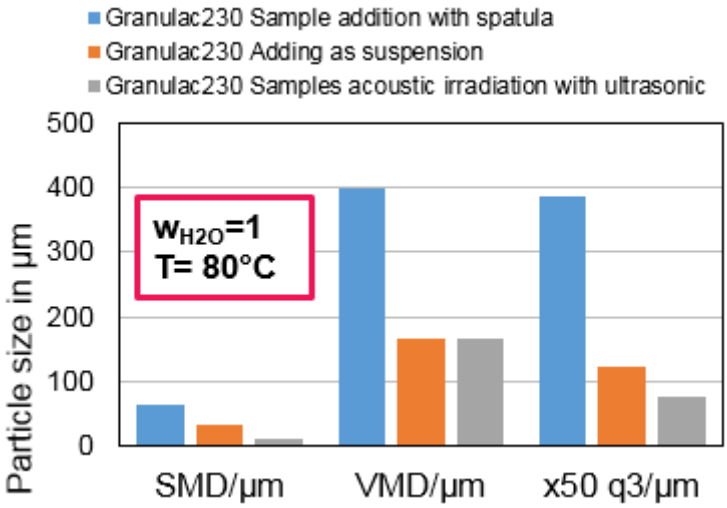

Figure 3-13: Influence of different sample preparation on the particle size

All results were evaluated by adding the lactose powder with a spatula, as this reflected the true particle state after spray drying. Subsequently, DSC measurements of the spray dried lactose powder were carried out. This measurement was intended to show possible changes in the structure of lactose. The temperature range of the DSC measurement was -25 °C to 270 °C. The heating rate was 5 °C / min. No special preparations had to be made for this, the laboratory team was given a few grams of the samples to be examined and a sample plan. Furthermore, the FELMI Laboratory of the Graz University

of Technology was commissioned to take pictures with the scanning electron microscope of the spray dried lactose.

3.2.2. Spray nozzle test stand

The preparations for the test procedure at the spray nozzle test stand were the production of the saturated lactose solution and the suspension to be sprayed. Subsequently, the particle size distribution of the lactose suspension was determined.

Preparation of the suspensions

Tests on the spray nozzle test stand were carried out with suspensions of a saturated lactose solution with 80 wt% of isopropanol and 20 wt% of water and suspended lactose in different concentrations. In order to reach the saturation state, the same procedure was adopted as in the preparation of the saturated solutions for the ProCept spray dryer in Table 3-4. The compositions of the suspensions used for the spray nozzle test are shown in Table 3-6.

Table 3-6: Composition of suspension

Solid content suspension / wt%	***Solution content with dissolved solid / wt%***	***Isopropanol content in liquid mixture /wt%***	***Water content in liquid mixture /wt%***
5	*95*	*80*	*20*
10	*90*	*80*	*20*
15	*85*	*80*	*20*
25	*75*	*80*	*20*
30	*70*	*80*	*20*
35	*65*	*80*	*20*

A check of the saturation state by a density measurement of the saturated solutions was not carried out.

Spray nozzle test

Two spray nozzles from different manufacturers were tested in this work. The first nozzle tested was from the module system series 970 from Schlick with a nozzle diameter of 800 µm[24]. The maximum flow rate is 0.25 l / min with an atomizing air of 5.08 m_n^3 / h[24].

The second nozzle tested was from the company Bete from the XA er series. The diameter of the nozzle is 400 µm[25]. The maximum flow rate depends on the fluid pressure and is between 0.32 l / min and 1.2 l / min. The required amount of atomizing air varies from 5.5 m_n^3 / h to 25.1 m_n^3 / h[25]. Figure 3-14 and Figure 3-15 show the Schlick nozzle and the Bete nozzle.

Figure 3-14: Schlick nozzle

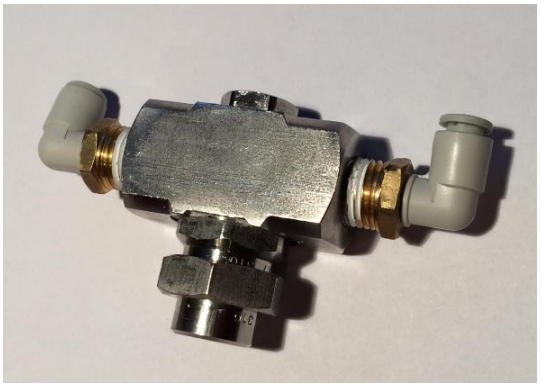

Figure 3-15: Bete nozzle

For the different solids concentrations, calibration curves were created by feeding through the nozzle without connecting the sputtering system. Table 3-7 shows the experimental plan of the spray nozzle test stand and the exact description of the used nozzle.

Table 3-7: Experimental plan

No.	***Solid content of suspension / wt%***	***Nozzle***	***Total mass flow /kg/h***	***Mass flow dry substance /kg/h***
1	*35*	Schlick 970/3 D 4.484/3	*2.91*	*1*
2	*30*	Schlick 970/3 D 4.484/3	*3.32*	*1*
3	*25*	Schlick 970/3 D 4.484/3	*4*	*1*
4	*15*	Schlick 970/3 D 4.484/3	*5.66*	*1*
5	*10*	Bete nozzle 1/4Xa00-7 FC7-7	*1.50*	*0.15*
6	*5*	Bete nozzle 1/4Xa00-7 FC7-7	*3.32*	*0.15*

The aim was a spraying time of 30 minutes. The pump performance depended on the throughput of dry substance lactose. The term "dry substance lactose" includes the suspended lactose as well as the dissolved lactose in the saturated liquid. For all experiments with the Schlick nozzle, a throughput of dry substance of 1 kg / h was desired. For the Bete nozzle, a throughput of dry substance lactose of 0.15 kg / h was desired

As atomizing air, nitrogen from a gas bottle was used. The amount of nitrogen used for atomization had been determined by visual observation of the atomization pattern of the nozzle. For each experiment, the atomization air was adjusted to enable visually fine atomized droplets. To measure the amount of nitrogen consumed, a flow meter and a pressure gauge from Krohne were used. The Krohne flow meter indicated the volume flow in l / h. With the measured pressure and by using the ideal gas equation, this could be converted into the actually volume flow in Nl / h. The Krohne flowmeter was also for air, the measurement error in nitrogen was neglected due to the small difference in molecular weights. Table 3-8 shows the measured pressure and volume flow as well as the calculated volume flow of experiments 1 to 6.

Table 3-8: Volumetric flow

No.	***Solid content of suspension / wt%***	***Nozzle***	***Measured Pressure /bar***	***Measured flow/ l/h***	***Calculated volume flow/ l/h***
1	*35*	Schlick nozzle	*3.19*	*1000*	*3149.00*
2	*30*	Schlick nozzle	*5*	*1000*	*4935.80*
3	*25*	Schlick nozzle	*5*	*1000*	*4935.80*
4	*15*	Schlick nozzle	*5.03*	*1000*	*4965.50*
5	*10*	Bete nozzle	*5.31*	*2000*	*10483.72*
6	*5*	Bete nozzle	*5.31*	*2000*	*10483.72*

Samples were taken from the starting suspension, after the pump, after the nozzle without atomizing air and after spraying with atomizing air.

Particle size measurements method

The collected samples were analyzed for particle size changes with the Helos from Sympathec in wet-dispersed mode. The measurements were done in the saturated solution of the related sample. Therefore, enough sample was collected from each processed material, where a large amount was filtered and used as measurement solution. A small amount of material was used for the particle size measurements.

4. Results

4.1. Spray drying experiments

This part presents the test results of the spray drying experiments. By means of a DSC measurement, changes in the crystal structure of lactose during the spray-drying process were detected. The particle size was analyzed with the Helos Particle Sizer and scanning electron microscope pictures were taken. The residual moisture was determined gravimetrically.

4.1.1. Raw material lactose

DSC measurement

By means of the DSC measurement, the melting point, crystallization and the amorphous or crystalline state of lactose were determined by changes in enthalpy flows. Figure 4-1 shows a DSC curve of the raw material. (GranuLac® 230 from the company Meggle).

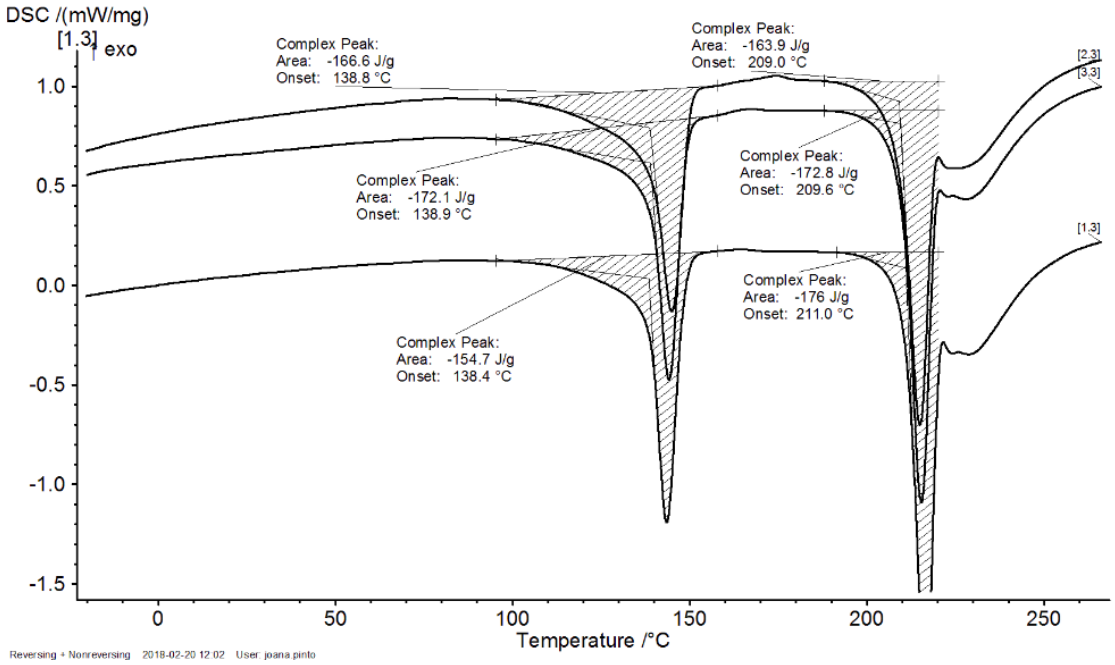

Figure 4-1: DSC curve GranuLac® 230

In this diagram, the raw material lactose was analyzed three times by DSC measurement. In DSC curves, the heat flux determines if a reaction is exothermic or endothermic. For example, melting of a solid requires input of heat and is therefore an endothermic process, which is represented through a peak in negative vertical direction. In the case of GranuLac® 230, this results in 2 characteristic peaks. The 1st peak is at 140 °C and indicates the endothermic dehydration of α lactose monohydrate with an enthalpy between 154.7 and 172.1 J/g. (3 different measurements). The 2nd peak shows the endothermic melting point of lactose near 210°C (literature: 201.6°C) [20] and an enthalpy of 163.9 to 176 J/g. GranuLac® 230 from Meggle consists of α lactose monohydrate only and therefore no peak occurred for β lactose.

Particle size analysis by Helos

The raw material GranuLac® 230 from Meggle has a Sauter diameter (SMD) of 8.17 µm and a volume-median diameter (VMD) of 31.40 µm. The x_{50} is 26.60 µm and the mode diameter $x_{h,r}$ is 39.85 µm. The density distribution of GranuLac® 230 is shown in Figure 4-2.

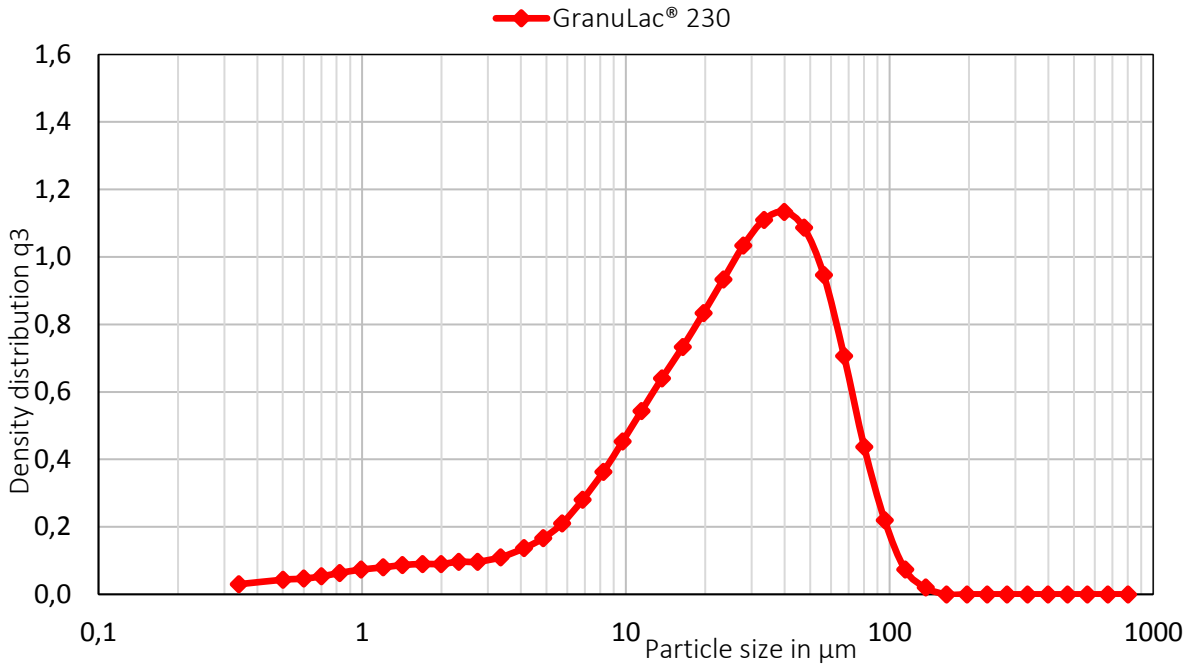

Figure 4-2: Density distribution of GranuLac® 230

Scanning electron microscopy image (SEM)

SEM images of the particles enabled information about the size, shape and structure of the raw material and the spray dried powders. Figure 4-3 shows an electron micrograph of the raw material GranuLac® 230. Typical are the sharp edges of bigger particles and very fine material created by the grinding process.

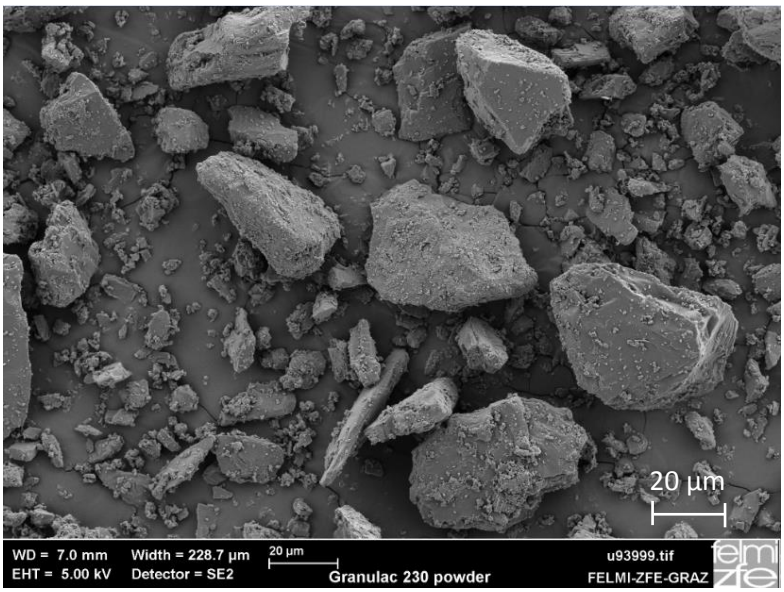

Figure 4-3: Scanning electron microscopy image of GranuLac® 230

4.1.2. Spray dried lactose at different temperatures and a liquid composition of w_{IPA}= 1

DSC measurement

The DSC curve of spray dried lactose at a drying temperature of 80°C and an isopropanol mass content of w_{IPA} = 1 is shown in Figure 4-4. A glass transition region at 69.7 °C marks the transition from amorphous to crystalline α lactose[19]. Another glass transition region at 82.1 °C and a heat capacity of 0.028J / (g * K) could indicate that a small portion of the suspended lactose particles were dissolved in the liquid due to an experimental error prior to the spray drying process. The resulting amorphous spheres and the amorphous particles that agglomerate on primary particles have different thermodynamic stabilities. The SEM image (see Figure 4-8 (a)) does not show a significant number of spherical particles that would support this thesis. Thus, it could also be an artifact in the DSC curve. Furthermore there are 2 characteristic peaks for α lactose. The peaks near 140 °C characterize the endothermic dehydration, the peak at about 210 °C the endothermic melting of α lactose. At a spray drying temperature of 80 °C and a liquid composition of 100 wt% of isopropanol, the end product was α lactose in the amorphous state.

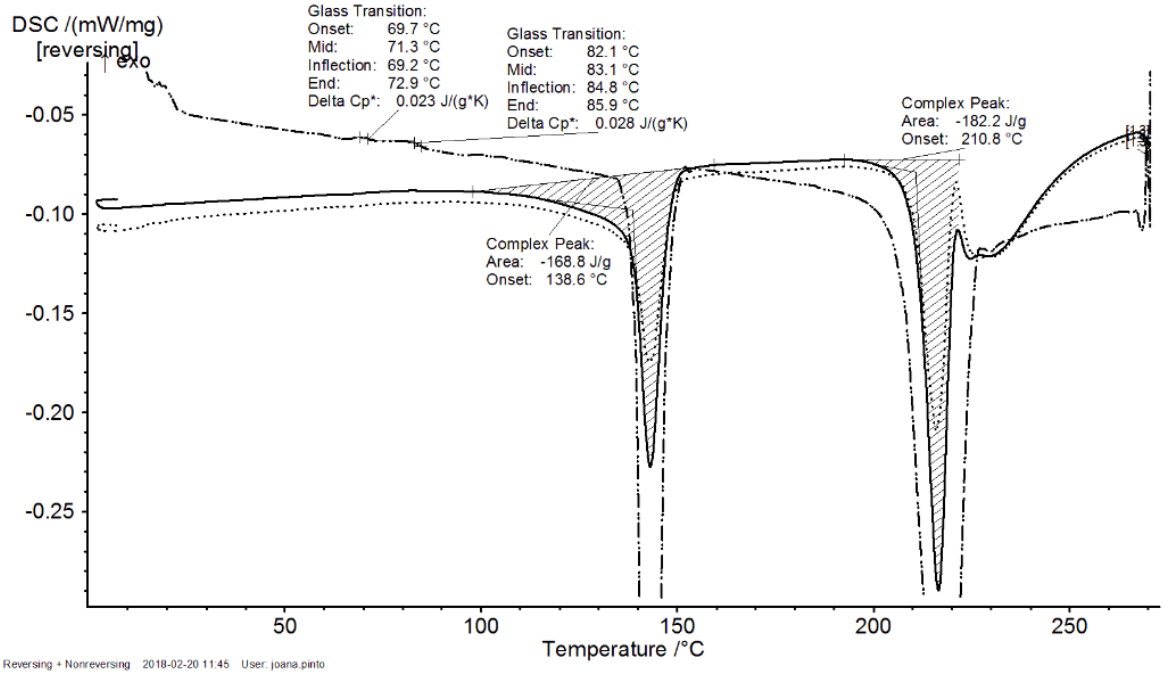

Figure 4-4: DSC curve of spray dried lactose at a drying temperature of 80°C and a liquid composition w_{IPA}=1

For the sprayed sample at a drying temperature of 170 °C, no clear glass transition area is visible in the DSC curve (Figure 4-5). This means that crystalline α lactose was formed at higher temperatures and a liquid composition of 100% isopropanol. Normally, this rapid drying would require amorphous lactose because there is no time for crystal formation. There is no peak, which indicates β lactose. A balance between α and β Lactose only occurs in an aqueous system. Since lactose is practically insoluble in isopropanol and the starting material consists exclusively of α lactose, it explains why no β lactose was formed in the spray samples with a mass fraction w_{IPA}= 1 for the liquid composition.

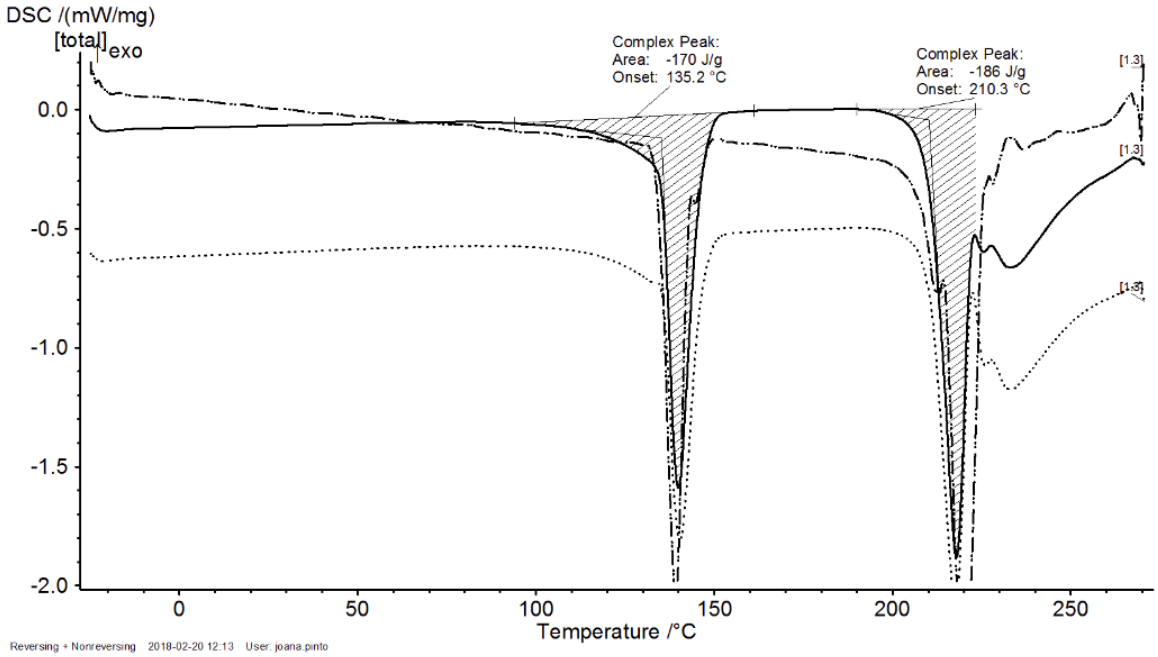

Figure 4-5: DSC curve of spray dried lactose at a drying temperature of 170°C and a liquid composition $w_{IPA}=1$

The DSC curves for 110 °C and 140 °C are similar to the curve at 80 °C and therefore are not shown in this work. Table 4-1 shows the results of the DSC measurement in tabular form for spray dried lactose for different drying temperatures with a liquid composition of isopropanol $w_{IPA}= 1$.

Table 4-1: Overview DSC measurement spray dried lactose with a liquid composition $w_{IPA}=1$

	Drying Temperature [°C]			
	80	110	140	170
Glass transition temperature [°C]	69.7	67.5	62.1	no
Glass transition heat capacity [J/(g*K)	0.023	0.018	0.062	no
Dehydration temperature [°C]	138.6	137.6	137.9	135.2
Dehydration peak specific enthalpy [J/g]	-168.8	-145.5	-160.6	-170
α lactose melting peak temperature [°C]	210.8	211.1	211.3	210.3
α lactose melting peak specific enthalpy [J/g]	-182.2	-189.5	-192.1	-186
β lactose melting peak temperature [°C]	no	no	no	no
β lactose melting peak specific enthalpy [J/g]	no	no	no	no

The different glass transition temperatures can have 2 possible causes. On the one hand, the glass transition temperature decreases with increasing moisture content of the material, this could have happened during storage between drying and DSC measurement. The storage time varied from sample to sample. The samples were not placed in a desiccator. On the other hand, the quantities of amorphous and crystalline lactose have an influence on the glass transition, at higher temperatures more amorphous material is built[19].

Particle size analysis by Helos

Figure 4-6 shows the density distribution of spray dried samples at different temperatures with a mass fraction of 100% isopropanol of the saturated solution. These are compared to the starting material GranuLac® 230 from Meggle.

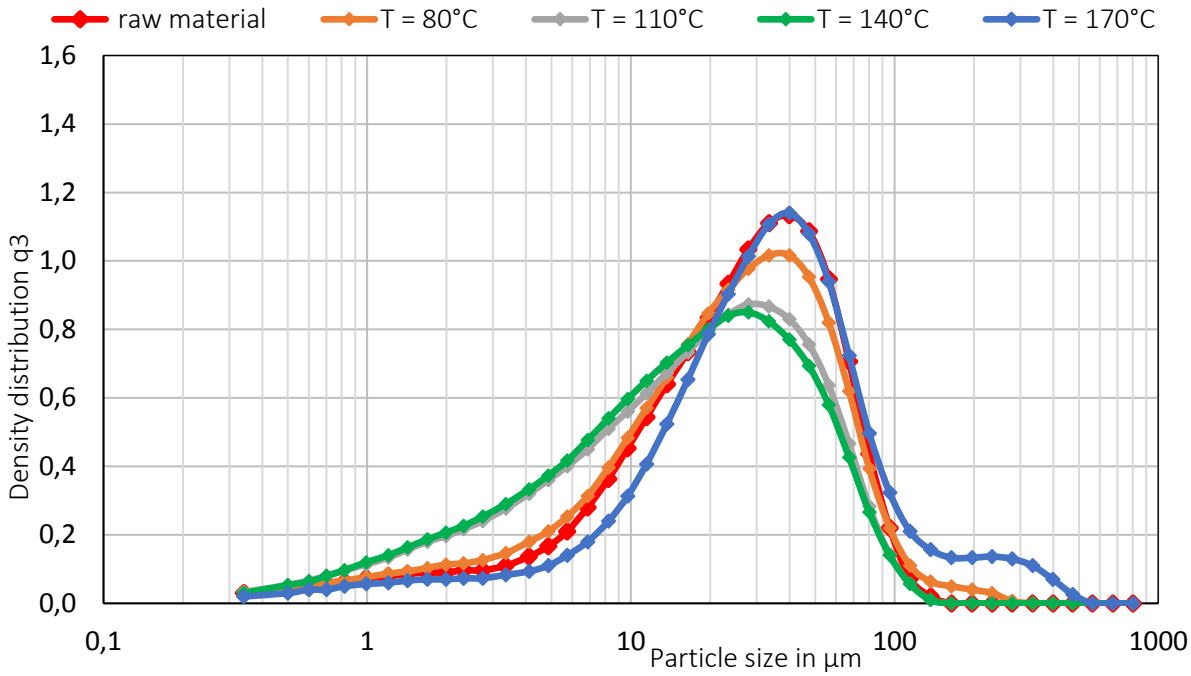

Figure 4-6 q_3 distribution of spray dried lactose at different temperatures with a liquid composition w_{IPA}= 1

The samples, which were spray dried at a temperature of 110 °C and 140 °C, had a higher fines content with respect to the raw material. For the sample that had been sprayed in a drying stream at a temperature of 80 °C, no significant change could be observed. In Figure 4-7, the associated SMD, VMD, and x_{50} to Figure 4-6 are shown.

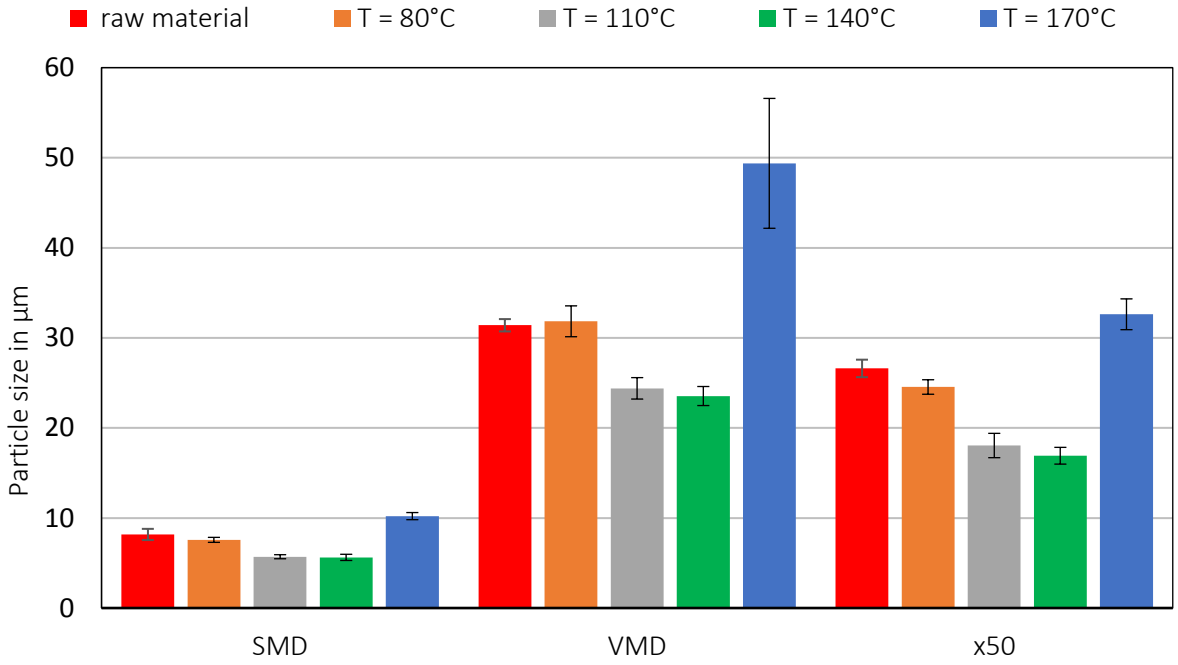

Figure 4-7: SMD, VMD and x_{50} of spray dried lactose at different temperatures with a liquid composition w_{IPA}=1

The spray dried sample at 80 °C had the least difference to the starting material. With increasing drying temperature T = 110 °C and T = 140 °C, the SMD, VMD and x_{50} were first getting smaller, at a temperature of 170 °C, a sudden increase in these values was observed. The fact that larger particles were produced at a spray drying temperature of 170 °C could be explained by the DSC measurement. For the sample which was spray dried at 170°C, no glass transition is visible. This means that the sample was already present in crystalline form during the measurement. At high spray drying temperatures, amorphous lactose should form, which is hygroscopic[19, 26] . Glassy amorphous materials can be considered as solid liquids with extremely high viscosities with $\mu > 10^{12}$ Pas[27]. When the glass transition region is exceeded, the specific free volume in the amorphous matrix increases, allowing the molecules to rotate freely. The viscosity drops and an increased agglomeration behavior is given[27]. This behavior can be observed by increasing the temperature or presence of a plasticizer[19]. These plasticizers are low molecular weight substances that increase the mobility of the molecules - in the case of lactose it is water[28]. As a result of the viscous flow, particles can adhere to one another at the contact points due to surface tension[28]. The finding of the largest particles at a spray drying temperature of 170 °C could be explained by recrystallization of the lactose due to the lack of glass transition. The glass transition temperature was exceeded, the viscosity decreased and particles agglomerated. Subsequently, a recrystallization of amorphous α lactose to α monohydrate occurred. This process could be caused by the proportion of water in the ambient air, which acted as plasticizer. Lactose can recrystallize spontaneously from a relative humidity of 45%[19].

Scanning electron microscopy image (SEM)

Figure 4-8 shows SEM images of spray dried lactose at different temperatures with an isopropanol content of the saturated solution of 100 wt%. Lactose has a very low solubility in isopropanol. (Table 3-4; $S_{L,s}$= 0.008 g lactose/g solution) The images show no significant difference between the starting material GranuLac® 230 and the sprayed samples. With different temperature of the drying stream, no significant changes were observed. Size and shape of the particles was constant before and after the spraying process.

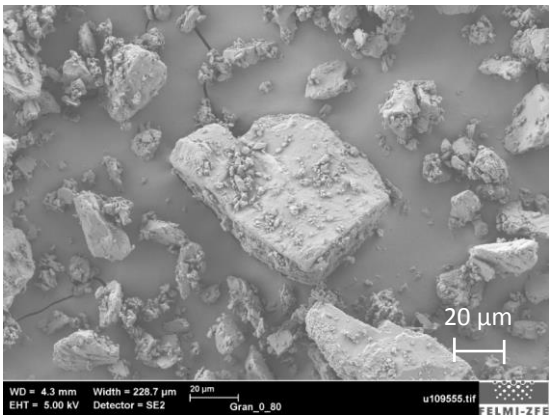

(a)

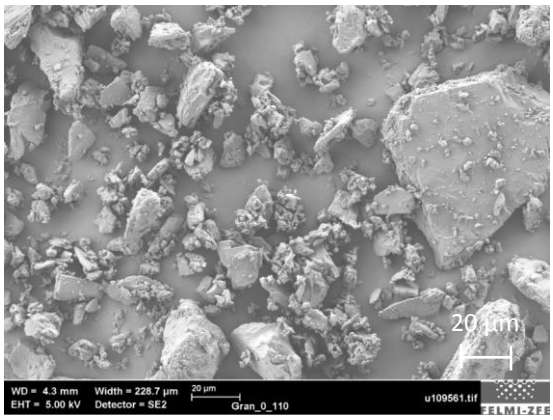

(b)

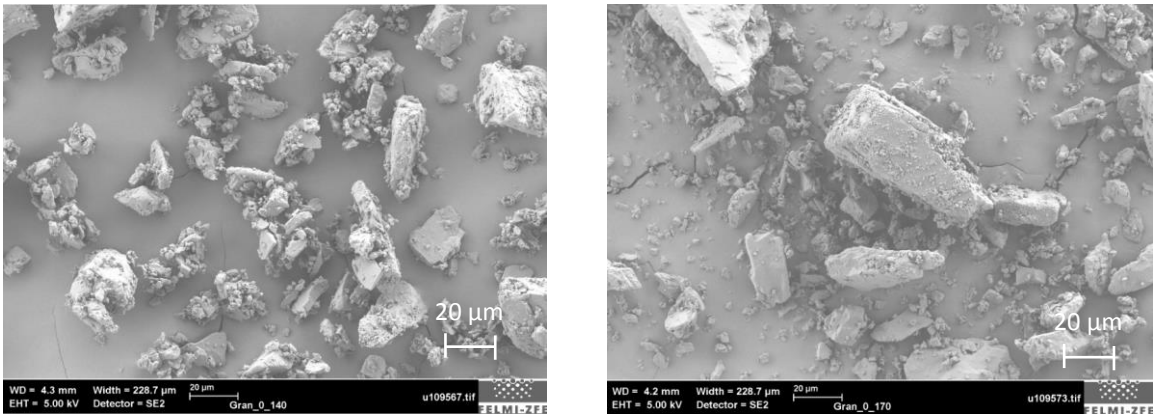

(c) **(d)**

Figure 4-8: SEM Image of spray dried lactose with a liquid composition w_{IPA}= 1; Spray drying temperature (a) 80 °C, (b) 110°C, (c) 140°C, (d) 170°C

Table 4-2 shows the moisture content of each sample in tabular form. The indication of humidity is in percent. Drying of the powder at a sufficiently high temperature and vacuum produces stable anhydrous α lactose. The transformation takes place by thermal removal of the water of crystallization from α lactose monohydrate. For the spray dried sample at 170 °C, the amorphous lactose was probably converted to crystalline α lactose monohydrate. The assumption that the amount of α lactose monohydrate and thus the amount of water increased with higher temperature could also explain the rising residual moisture with increasing temperature.

Table 4-2: Residual moisture w_{IPA}=1

			Residual moisture [wt %]			
X_d	***w_{IPA}***	***w_{H2O}***	***80°C***	***110°C***	***140°C***	***170°C***
$5.9 * 10^{-1}$	*1*	*0*	*0.116*	*0.274*	*0.318*	*0.378*

4.1.3. Spray dried lactose at different temperatures and a liquid composition of w_{IPA}= 0.75

Figure 4-9 shows the DSC curve of spray dried lactose at a drying temperature of 80°C and 75 wt% isopropanol in the liquid.

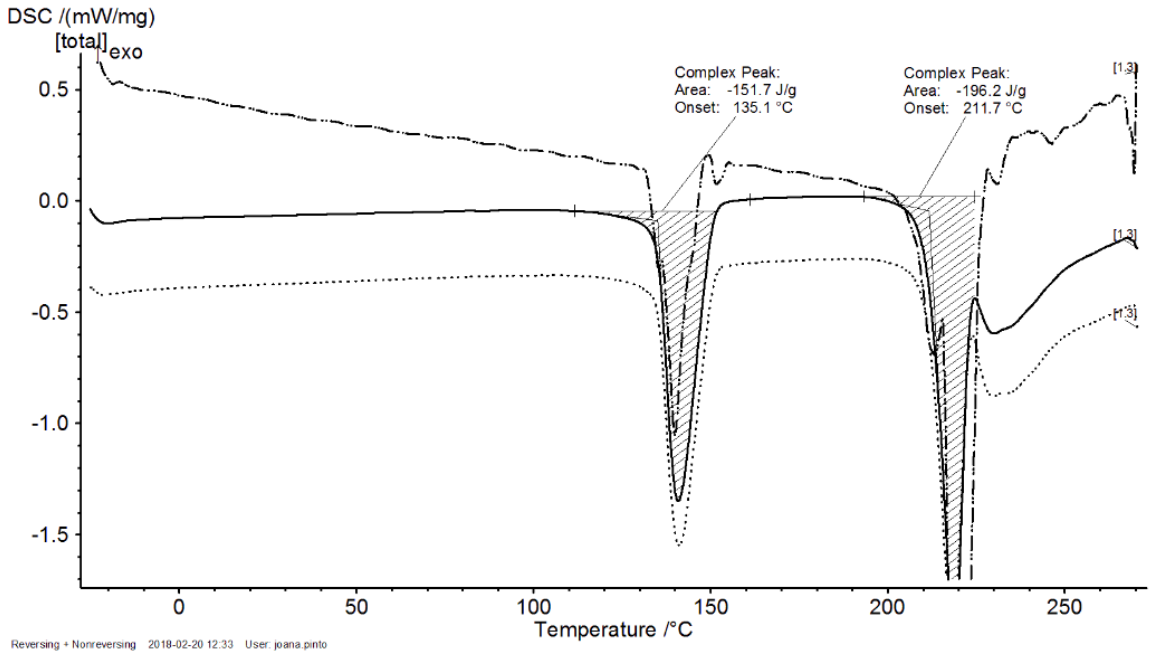

Figure 4-9: DSC curve of spray dried lactose at a drying temperature of 80°C and a liquid composition w_{IPA}=0.75

DSC curves were measured for 2 samples with an isopropanol mass content of 75 wt% and spray dried at two different drying temperatures of 80 °C and 170 °C. In both samples, no glass transition region was recognizable. Crystalline lactose had been formed in these spray drying samples. Again, the peaks indicate that these samples consist of α lactose monohydrate only. Table 4-3 shows the overview of the DSC measurement. For samples spray dried at 110 °C and 140 °C, no DSC measurement was performed.

Table 4-3: Overview DSC measurement of spray dried lactose with a liquid composition w_{IPA}=0.75

	Drying Temperature [°C]	
	80	170
Glass transition temperature [°C]	no	no
Glass transition heat capacity [J/(g*K)	no	no
Dehydration temperature [°C]	135.1	136.9
Dehydration peak specific enthalpy [J/g]	-151.7	-160.6
α lactose melting peak temperature [°C]	211.7	211
α lactose melting peak specific enthalpy [J/g]	-196.2	-194.2
β lactose melting peak temperature [°C]	no	no
β lactose melting peak specific enthalpy [J/g]	no	no

Particle size analysis by Helos

The individual density distributions of spray-dried samples at different drying temperatures and an isopropanol content of 75 wt% of the liquid are shown in Figure 4-10.

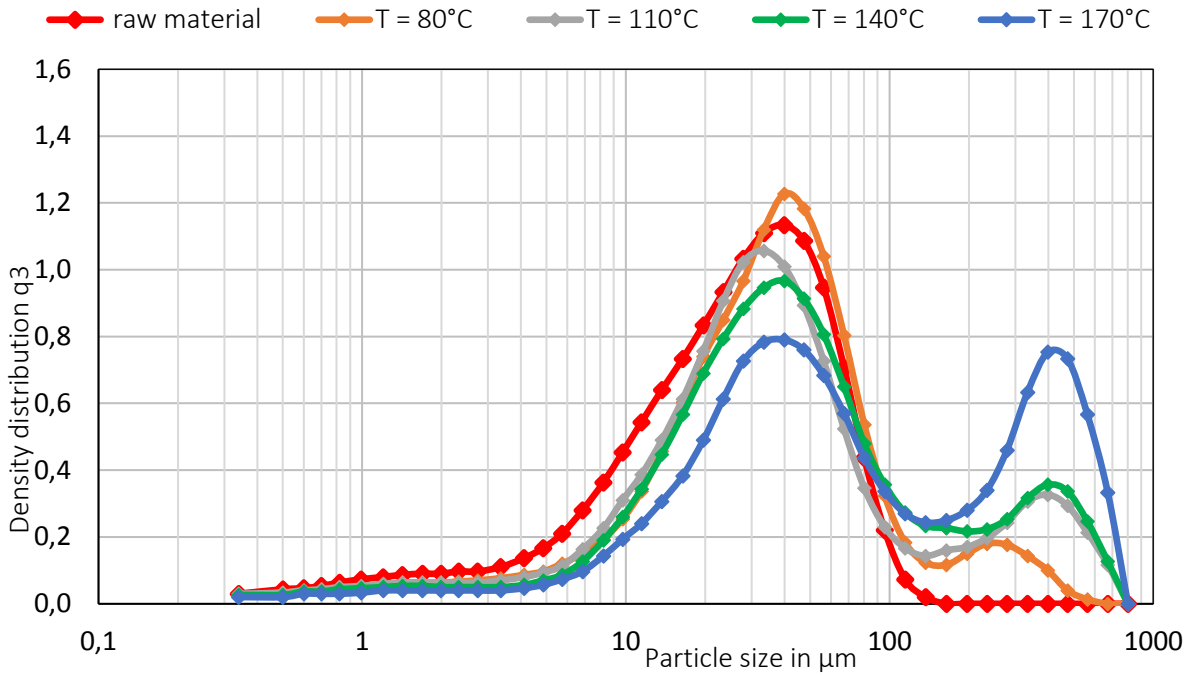

Figure 4-10: q_3 distribution of spray dried lactose at different temperatures with a liquid composition w_{IPA}=0.75

In Figure 4-11 the SMD, VMD and x_{50} of spray dried lactose at difference temperatures with a liquid mass fraction of 75% isopropanol is shown.

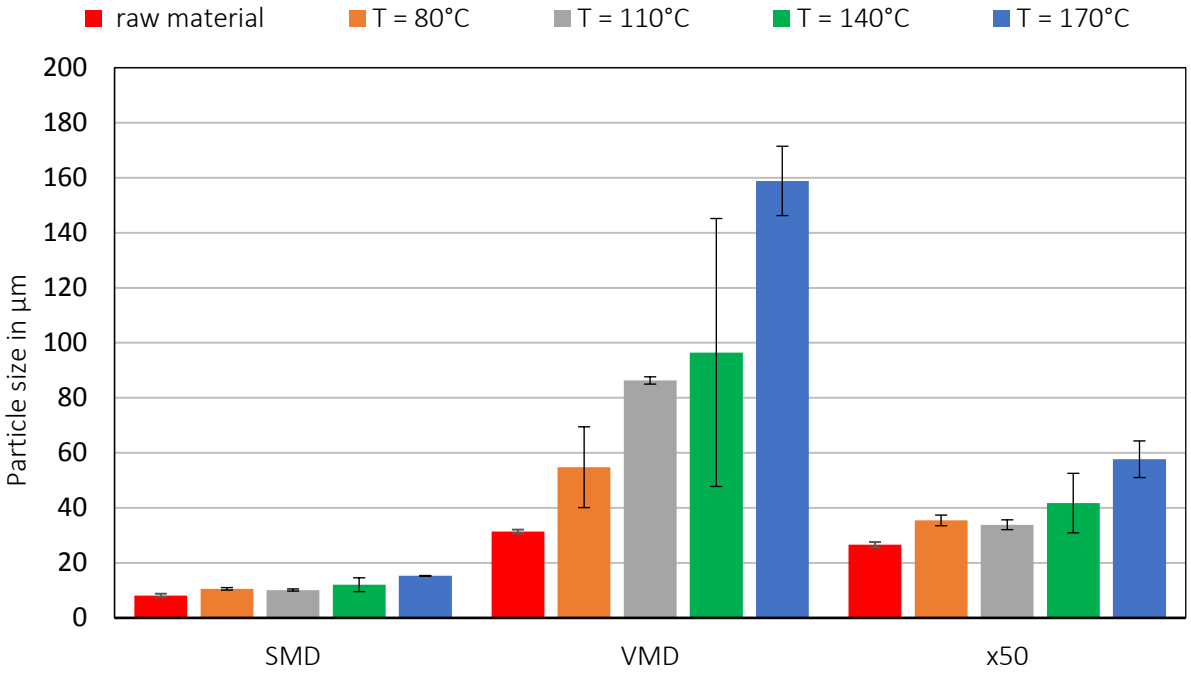

Figure 4-11: SMD, VMD and x_{50} of spray dried lactose at different temperatures with a liquid composition w_{IPA}=0.75

In general, a trend could be observed in this series of measurements that the particle sizes increased with rising temperature. The biggest difference was found here in the VMD value. In the spray dried

sample with a temperature T = 140 °C, a relatively large standard deviation occurred. Again, due to a lack of glass transition region of the sample at 80°C and 170 °C, it can be assumed that a conversion of amorphous into the crystalline state by moisture absorption from the environment had taken place before the particle size and DSC measurement. The higher the spray drying temperature, the more amorphous lactose had formed and the more water had been absorbed because of the hygroscopic effect[29]. The more water is absorbed, the more agglomerate the particles because the amorphous lactose sticks primary particles to larger particles. This resulted in the increasing size of the particles with increasing temperature.

Scanning electron microscopy image (SEM)

The electron micrographs in Figure 4-12 depicted the surface and bulk morphologies of lactose with an isopropanol content of 75 wt% of the saturated liquid and a drying temperature of 80 °C and 170 °C. At a spray drying temperature of 80°C, it can be observed that agglomeration of very fine particles took place. This could be attributed to the fact that the energy input at a drying temperature of 80 °C was not sufficient to evaporate the contained water quick enough to prevent agglomeration. As the water content rises, the amount of lactose dissolved increases due to the better solubility in water. The dissolved lactose could precipitate during the drying process. This acted as a binder and stuck the particles together. At a drying temperature of 170 °C again no significant difference to the original sample could be seen in the electron micrographs. Since only a small part of the sample was recorded by means of SEM image, it is also possible that no representative result is present here.

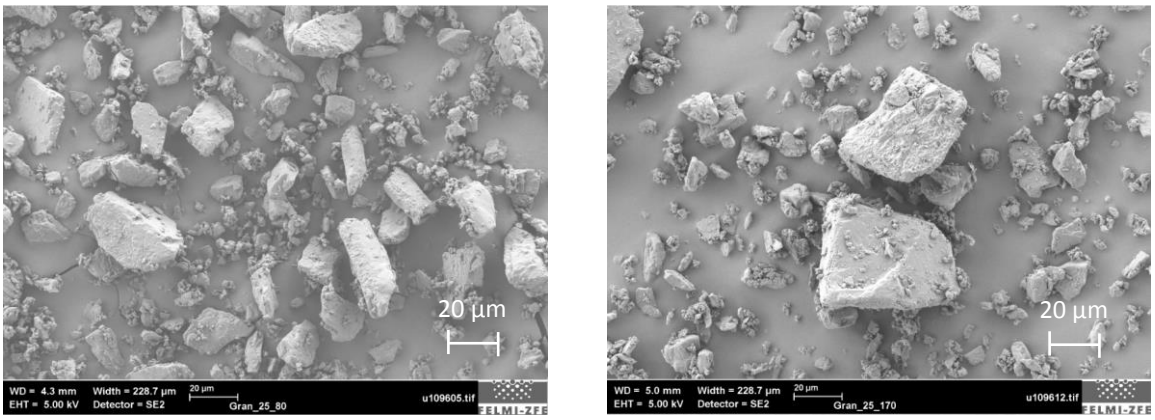

(a) **(b)**

Figure 4-12: SEM Image of spray dried lactose with a liquid composition w_{IPA}= 0.75; Spray drying temperature (a) 80°C, (b) 170°C

Table 4-4 shows the moisture content of each sample in tabular form. The indication of humidity is wt%. With all spray drying temperatures a product with very low residual moisture could be achieved. The residual moisture fluctuated between 0.50 and 0.90 percent. There is no trend recognizable, one possible reason could be that amorphous lactose had absorbed water from the air after spray drying and thus the moisture determination was falsified.

Table 4-4: Residual moisture w_{IPA}=0.75

			Residual moisture [wt %]			
X_d	w_{IPA}	w_{H2O}	80°C	110°C	140°C	170°C
$4.0*10^{-1}$	75	25	0.583	0.837	0.508	0.905

4.1.4. Spray dried lactose at different temperatures and a liquid composition of w_{IPA}= 0.5

DSC measurement

At a water content of 50 wt% in the liquid part, β lactose was found in the samples. Water is very important for the formation of β lactose. Only in aqueous solutions, a balance of α and β lactose forms. In equilibrium, an aqueous lactose solution consists of 38% α and 62% β lactose at room temperature[19]. The samples sprayed at 80 °C had a peak for β lactose in the DSC curve. The specific enthalpy, which is indicative for the amount of β lactose, was -20.68 J / g at a spray drying temperature of 80 °C and -11.99 J / g at 170 °C. Isopropanol could affect the formation of β lactose, so it already appeared at a spray drying temperature of 80 °C. Figure 4-13 shows the DSC curve of spray dried lactose at 80°C and a liquid composition of 50 wt% isopropanol. There are three characteristic peaks. At 136.1 °C dehydration takes place, at 210.7 °C the decomposition of α lactose and at 222.2 °C the decomposition of β lactose (literature melting point: 252°C)[20]. Although lactose has been described many times in the literature, deviations from the physio-chemical properties are repeatedly found. These deviations arise partly due to different manufacturing processes or the raw material used. Due to the size of the peaks, it can be concluded that more α than β lactose was formed. The existence of a glass transition region suggests that the spray dried sample was in an amorphous state.

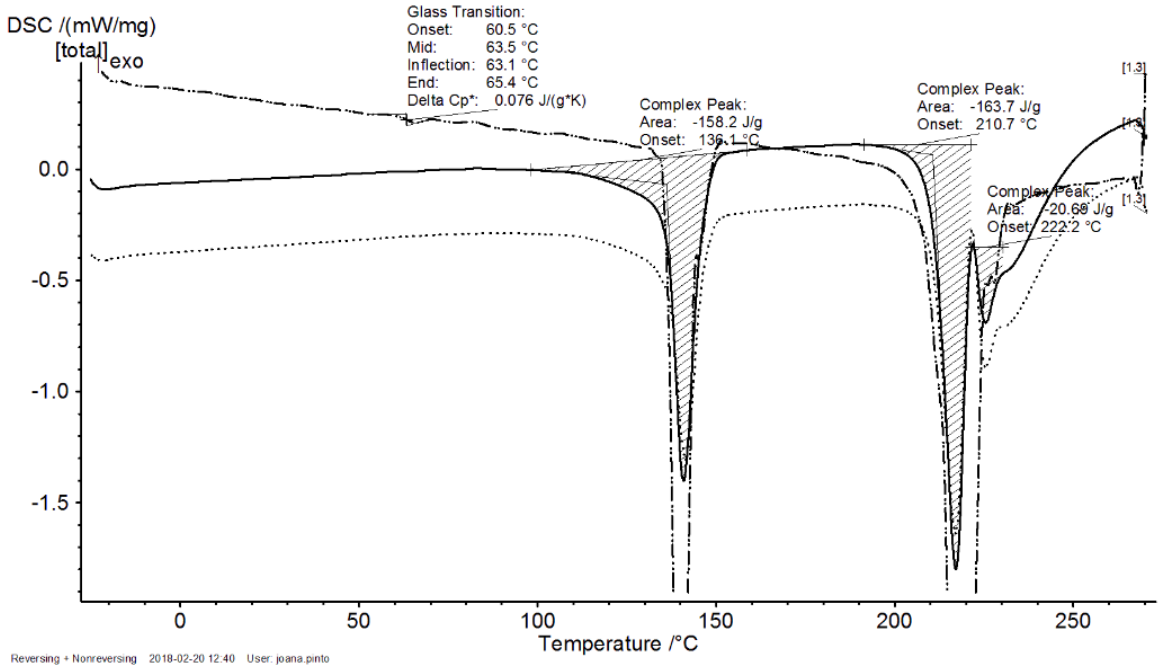

Figure 4-13: DSC curve of spray dried lactose at a drying temperature of 80°C and a liquid composition w_{IPA}=0.5

In comparison, in the DSC curve of the specimen sprayed at 170 ° C, the delta cp of the glass transition was lower. The change in the specific heat capacity at the glass transition temperature depends on the amorphous content in the sample[29]. The glass transition temperature depends on the moisture surrounding the sample. As the humidity increases, the temperature required for recrystallization decreases[29]. This is shown in Figure 4-14. The spray dried sample at 80 °C would therefore have a higher water content than the sample, which was sprayed at 170 °C. This statement also coincides with the measured moisture contents in Table 4-6. (80°C 0.98% humidity; 170°C 0.781% humidity)

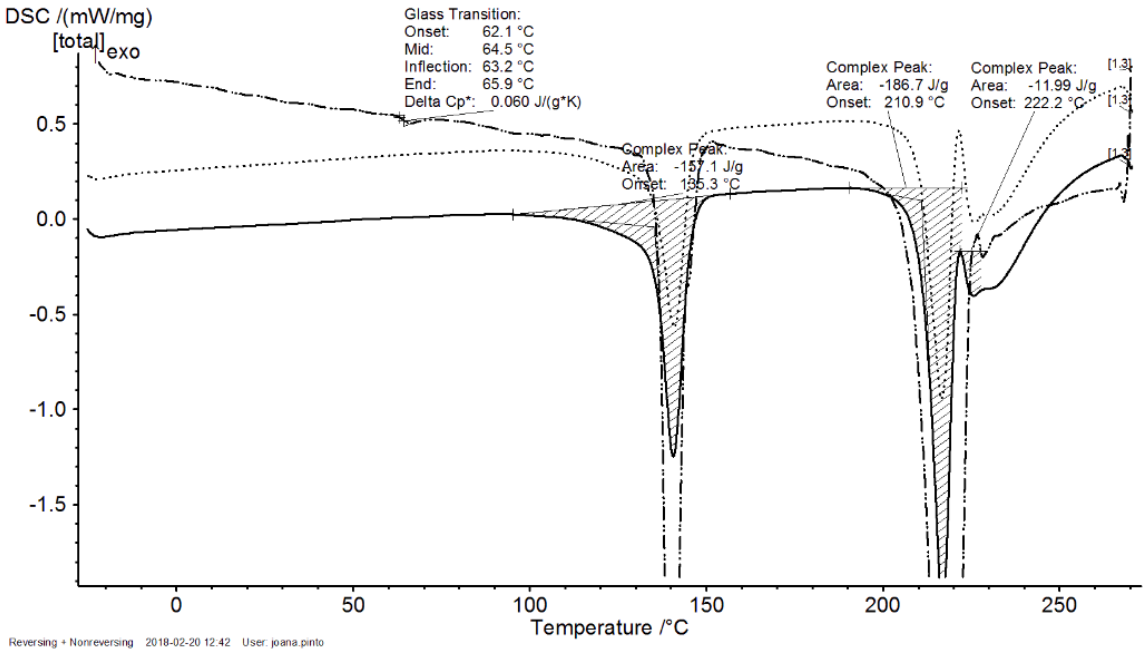

Figure 4-14: DSC curve of spray dried lactose at a drying temperature of 170°C and a liquid composition w_{IPA}=0.5

Table 4-5 shows the overview of the DSC measurement. For samples spray dried at 110 °C and 140 °C, no DSC measurement was performed.

Table 4-5: Overview DSC measurement of spray dried lactose with a liquid composition w_{IPA}=0.5

	Drying Temperature [°C]	
	80	170
Glass transition temperature [°C]	60.5	62.1
Glass transition heat capacity [J/(g*K)	0.076	0.06
Dehydration temperature [°C]	136.1	135.3
Dehydration peak specific enthalpy [J/g]	-158.2	-157.1
α lactose melting peak temperature [°C]	210.7	210.9
α lactose melting peak specific enthalpy [J/g]	-163.7	-186.7
β lactose melting peak temperature [°C]	222.2	222.2
β lactose melting peak specific enthalpy [J/g]	-20.68	-11.99

Particle size analysis by Helos

The density distribution of the spray dried samples at different drying temperatures and 50 wt% isopropanol is shown in Figure 4-15.

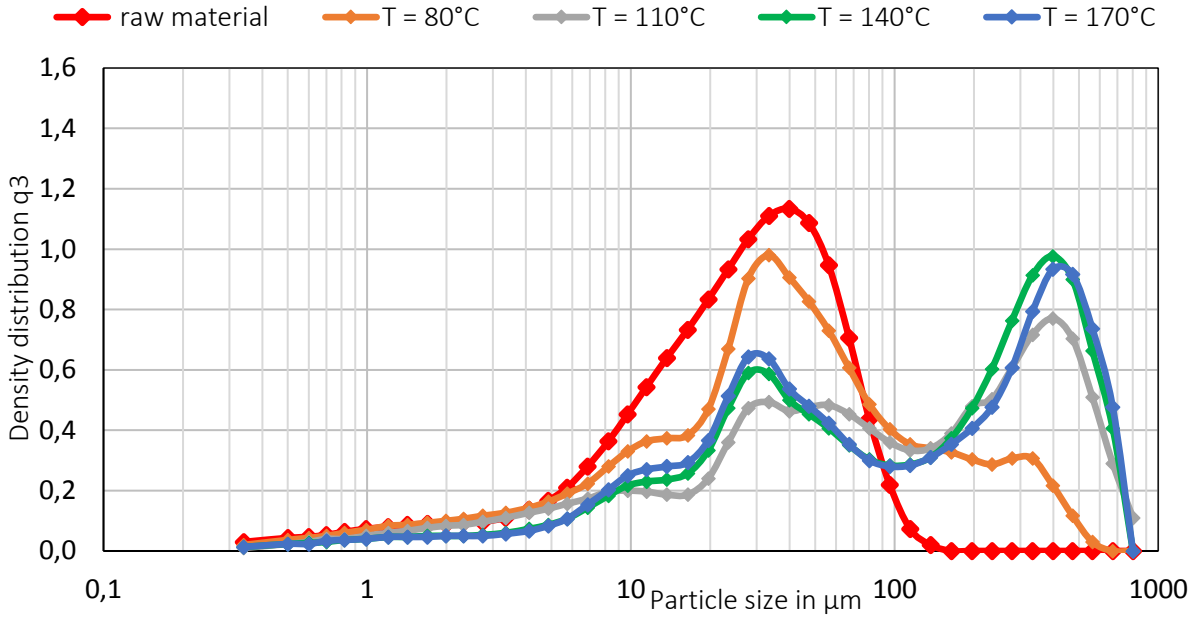

Figure 4-15: q_3 distribution of spray dried lactose at different temperatures with a liquid composition w_{IPA}=0.5

It was striking that with increasing spray drying temperature, a second peak in the density distribution occurred at about 400 µm. Figure 4-16 shows the associated SMD, VMD and x_{50}.

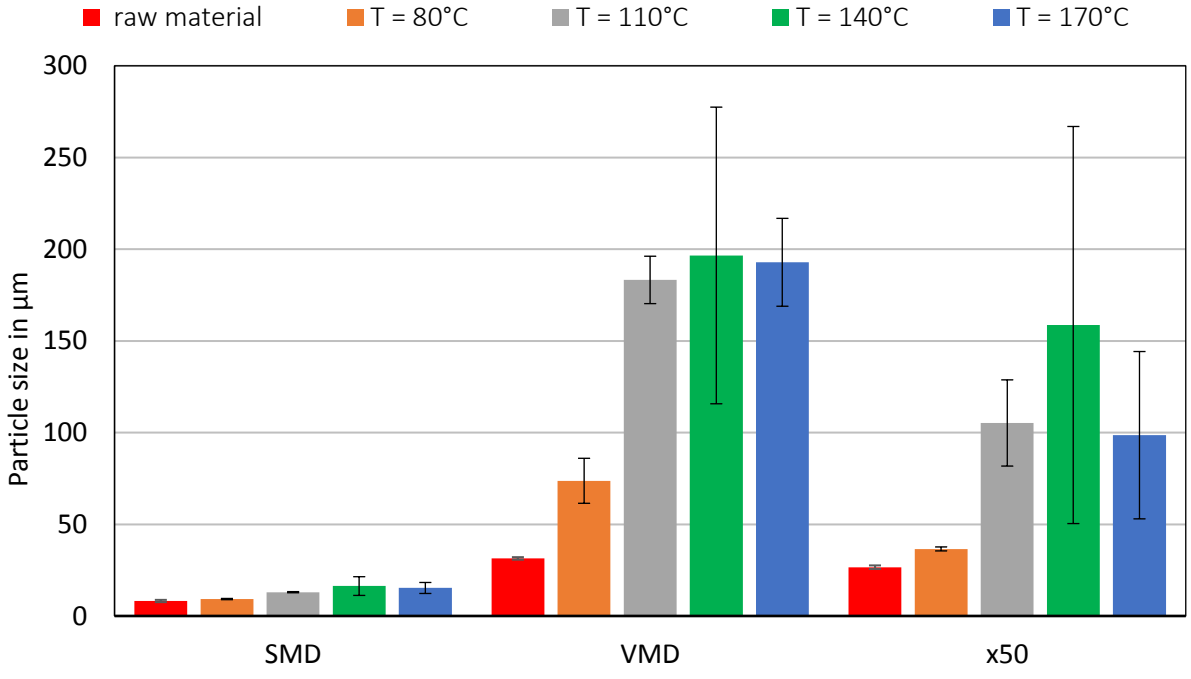

Figure 4-16: SMD, VMD, x_{50} of spray dried lactose at different temperatures with a liquid composition w_{IPA}=0.5

As the spray-drying temperature increased, the particle size also increased. This can in turn be explained with the aid of the associated DSC curves. In the fast drying process, such as in spray drying, amorphous lactose forms mainly [19]. The cp value of the sprayed sample at the glass transition at 80 °C was higher (0.076 J / (g * K)) than that of the sample sprayed at 170 °C (0.06 J / (g * K). The area marking

the melting of α lactose was lower at 80 °C (-163.7 J / g) than at 170 °C (-186.7 J / g). It is made the assumption that at higher temperatures more amorphous lactose was built. That would mean that in the sprayed sample at 170 °C, a larger proportion of amorphous lactose was converted into crystalline lactose than in the sample which was sprayed at 80 °C. In this conversion of amorphous α lactose into α lactose monohydrate, moisture was absorbed from the environment[19,29]. As a result, the particles agglomerated more and resulted in larger particles. In addition, more β lactose was also formed at a spray drying temperature of 80 °C. (see Table 4-5) β lactose is also slightly hygroscopic in the amorphous state.[19,29]

Scanning electron microscopy image (SEM)

Figure 4-17 shows SEM images of spray dried lactose at different temperatures with an isopropanol content of the saturated solution of 50 wt%. In the starting sample of lactose, very small particles were found loose, not adhered to larger particles. In the samples with a liquid composition of 50 wt% isopropanol these fine particles were completely agglomerated. At a spray drying temperature of 80 °C significantly larger agglomerates of the dissolved lactose were found in the saturated solution than in the sample which was spray dried at 170 °C emerged.

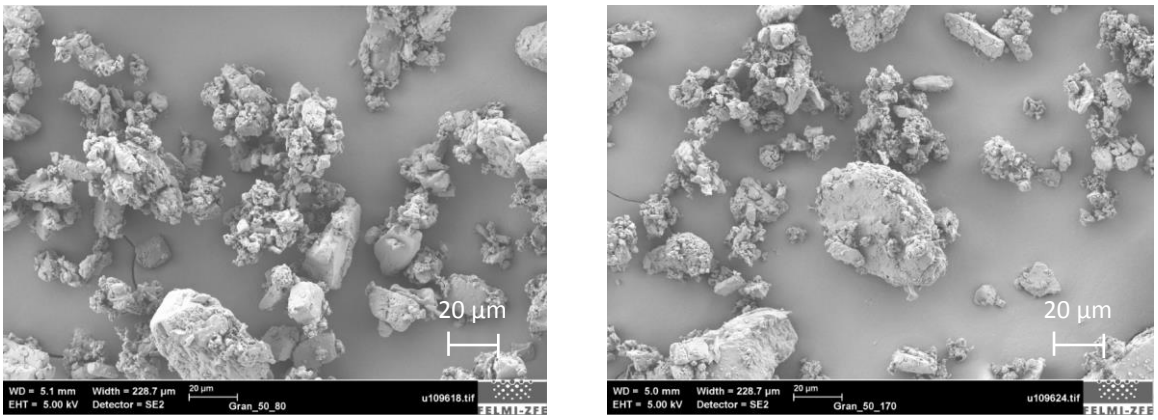

(a) **(b)**

Figure 4-17: SEM Image of spray dried lactose with a liquid composition w_{IPA}= 0.50; Spray drying temperature (a) 80°C, (b) 170°C

Table 4-6 shows the moisture content of each sample in tabular form. The indication of humidity is in wt%. Even with an isopropanol content of 50 wt% in the liquid phase of the suspension, the products were obtained with a water content below 1%.

Table 4-6: Residual moisture w_{IPA}=0.5

			Residual moisture [wt %]			
X_d	***w_{IPA}***	***w_{H2O}***	***80°C***	***110°C***	***140°C***	***170°C***
$1.5 * 10^{-1}$	*50*	*50*	*0.980*	*0.994*	*0.513*	*0.781*

4.1.5. Spray dried lactose at different temperatures and a liquid composition of w_{IPA}= 0.25

DSC measurement

Figure 4-18 shows the DSC curve of spray dried lactose at a drying temperature of 80 °C and a liquid composition of 25 wt% isopropanol. For comparison, Figure 4-19 shows spray dried lactose at a drying temperature of 170 °C and the same liquid composition.

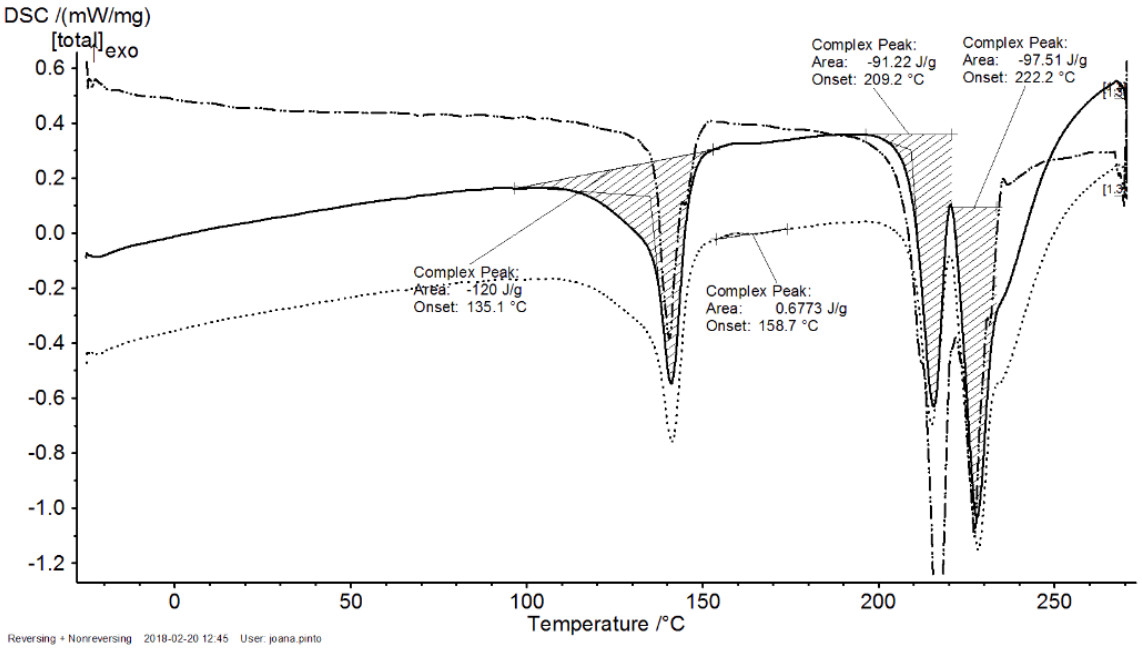

Figure 4-18: DSC curve of spray dried lactose at a drying temperature of 80°C and a liquid composition w_{IPA}=0.25

With a liquid composition of 25 wt% of isopropanol and 75 wt% of water, spray drying produced a mixture of α and β lactose. The peak at 207.9 °C indicates α lactose and the peak at 221°C β lactose[19,21].

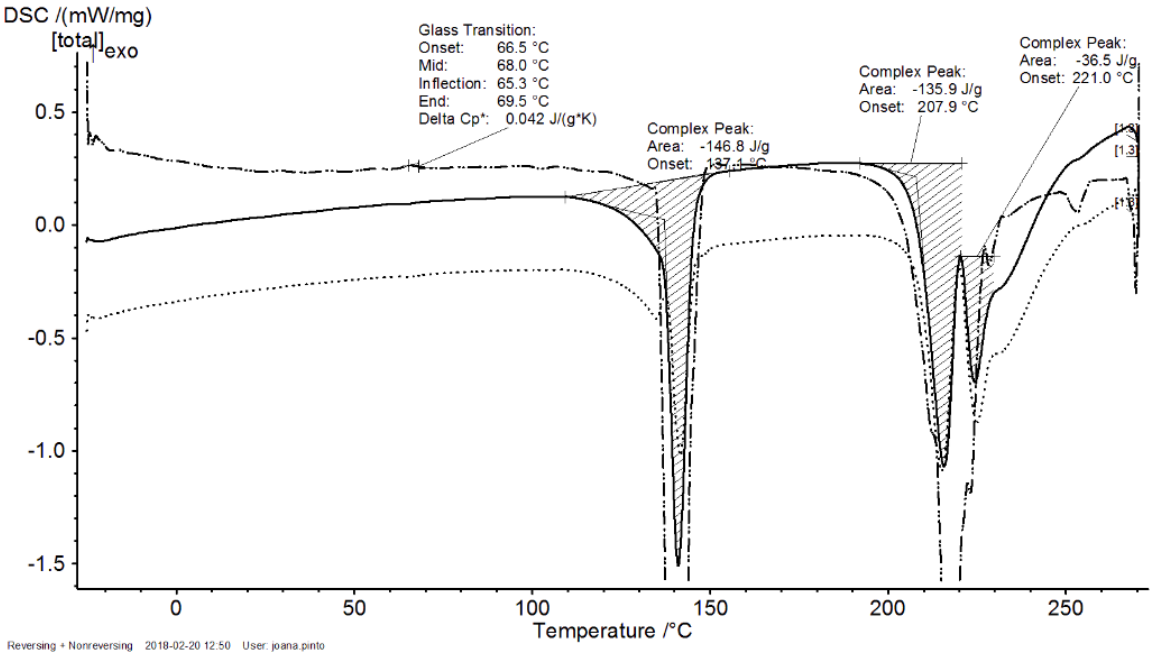

Figure 4-19: DSC curve of spray dried lactose at a drying temperature of 170°C and a liquid composition w_{IPA}=0.25

At low drying temperature, the proportion of β lactose was higher than that of α lactose. This can be seen in the DSC curves. For samples spray dried at 80 °C and 170 °C, these specific enthalpy were in absolute terms 97.51 J / g and 36.5 J / g, respectively. (Compare Figure 4-18 and Figure 4-19) The fraction of β lactose decreased at higher temperatures. At 80 °C a glass transition was lacking, which indicates that the sample was crystalline, at 170 °C amorphous lactose was present. The peak at the 80 °C sample at 158.7 °C could be explained as an artifact or a contamination. In the DSC curve of the starting material no corresponding peak was measured at this point. Table 4-7 shows the results of the DSC measurements for the spray dried lactose samples with a liquid composition w_{IPA} = 0.25 in tabular form.

Table 4-7: Overview DSC measurement of spray dried lactose with a liquid composition w_{IPA}=0.25

	Drying Temperature [°C]	
	80	170
Glass transition temperature [°C]	no	66.5
Glass transition heat capacity [J/(g*K)	no	0.042
Dehydration temperature [°C]	135.1	137.1
Dehydration peak specific enthalpy [J/g]	-120	-146.8
α lactose melting peak temperature [°C]	209.2	207.9
α lactose melting peak specific enthalpy [J/g]	-91.222	-135.9
β lactose melting peak temperature [°C]	222.2	221
β lactose melting peak specific enthalpy [J/g]	-97.51	-36.5

Particle size analysis by Helos

Figure 4-20 shows the density distribution of spray dried lactose at different temperatures with a liquid composition of 25 wt% of isopropanol.

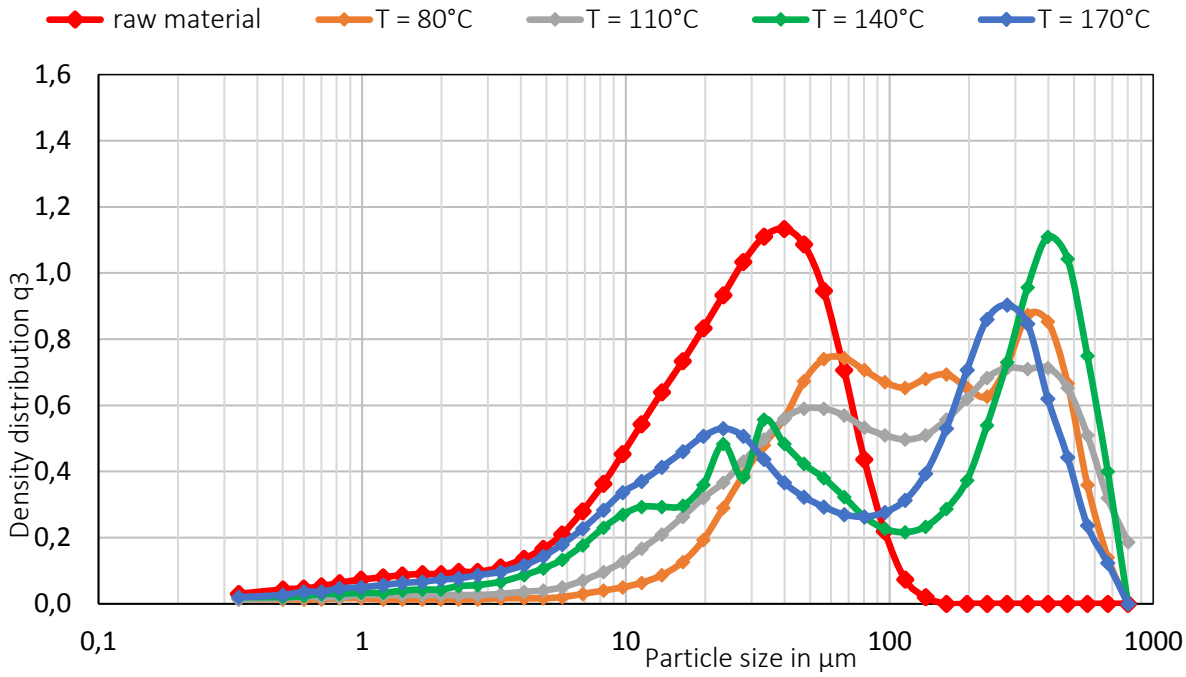

Figure 4-20: q_3 distribution of spray dried lactose at different temperatures with a liquid composition w_{IPA}=0.25

The SMD, VMD and x50 values associated with Figure 4-20 are shown in Figure 4-21.

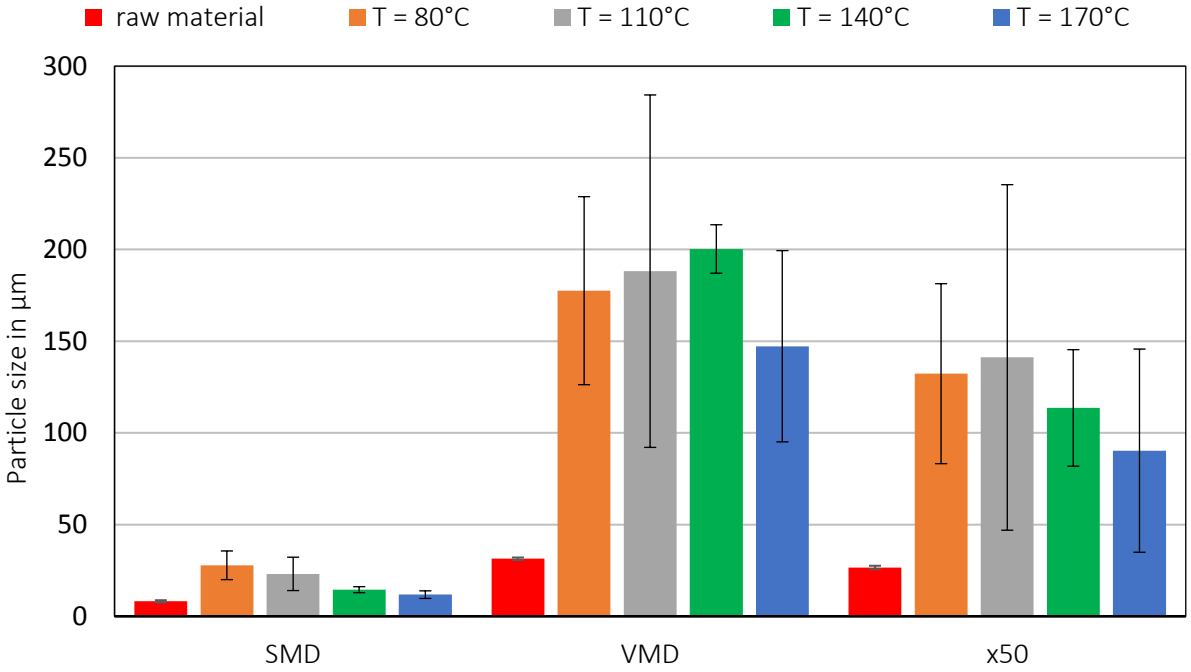

Figure 4-21: SMD, VMD, x_{50} of spray dried lactose at different temperatures with a liquid composition w_{IPA}=0.25

Also in the sample series whose liquid composition consists of 25 wt% isopropanol, a similar trend can be observed as with the samples of 50 wt% isopropanol: The density distribution developed a second peak in the coarse material region, simultaneously the 1st peak, which characterizes the starting

material, was getting continuously smaller. The SMD and VMD slightly decreased with higher temperature. And also the x_{50} showed the same trend. Comparing the DSC measurements (Table 4-7) of the spray dried sample at 80 °C with that at 170 °C, the results of particle size measurements with Helos can be explained. Again, the particle size can be described with the conversion of amorphous to crystalline lactose and the associated agglomeration. At the sample sprayed at 80 °C, no glass transition was visible in the DSC curve. That means lactose was present mainly in crystalline form. When the dissolved lactose was dried sufficiently fast, amorphous lactose is formed[19]. There was detected an amorphous fraction in the spray dried sample at 80 °C and 100 wt% water in the liquid phase of the suspension. It can be assumed if the liquid composition is 75 wt% water, also an amorphous part had been build (Figure 4-23). This in turn could mean that amorphous lactose had already been converted to crystalline lactose before the DSC measurement. Due to the absorption of water during this restructuring, stronger agglomeration occurred. This could explain why larger particles were measured at 80 °C. At 170 °C there is a glass transition region, which means that the sample still consisted in part of amorphous lactose.

Scanning electron microscopy image (SEM)

The influence of the drying temperature to the particle form of spray dried suspensions with a solution composition of 25 wt% isopropanol is shown Figure 4-22. At 80 °C, the primary particles are almost completely covered by agglomerates. The higher the proportion of water in the liquid phase of the suspension was, the greater was the amount of lactose dissolved. A higher water content resulted in more agglomeration. The agglomerates became smaller with higher drying temperature. Due to the shorter drying time, fewer particle collisions occurred between moist particles and as a result of that there was less agglomeration.

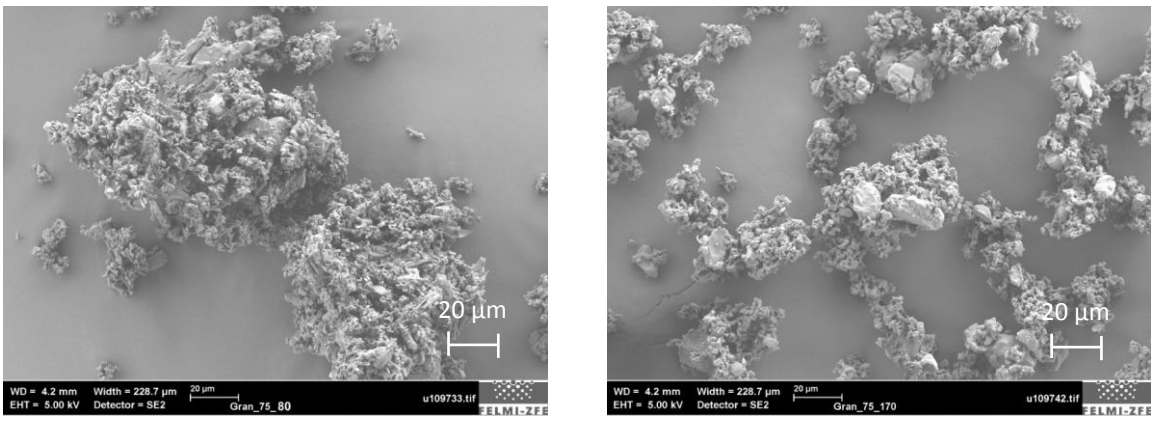

(a) **(b)**

Figure 4-22: SEM Image of spray dried lactose with a liquid composition w_{IPA}= 0.25; Spray drying temperature (a) 80°C, (b) 170°C

As the water in the solution of the suspension rose, the residual moisture of the spray dried lactose powder increased. Table 4-8 shows the moisture content of each sample in tabular form. The indication of humidity is in percent. In the spray drying samples with an isopropanol content of 25 wt% in the solution, a trend can be recognized that with increasing spray-drying temperature, the moisture

content decreased. At higher temperatures, the drying flow had a higher heat flow, which could evaporate more liquid during the residence time in the spray dryer. The moisture content at 110 °C of 0.947% could indicate a measurement error in the gravimetric moisture determination.

Table 4-8: Residual moisture w_{IPA}=0.25

			Residual moisture [wt %]			
X_d	***w_{IPA}***	***w_{H2O}***	***80°C***	***110°C***	***140°C***	***170°C***
$2.2 * 10^{-2}$	*25*	*75*	*1.730*	*0.947*	*1.332*	*1.262*

4.1.6. Spray dried lactose at different temperatures and a liquid composition of w_{IPA}= 0

DSC measurement

In Figure 4-23 the DSC curve of spray dried lactose at a drying temperature of 80°C and a water content of 100% in the liquid is shown.

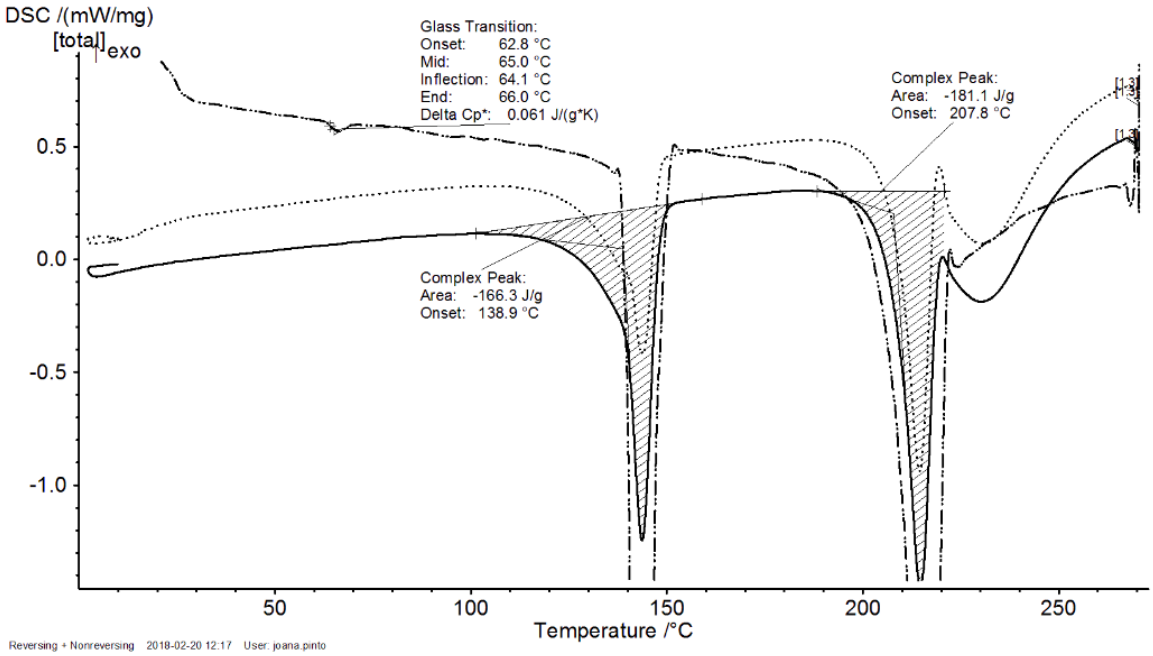

Figure 4-23: DSC curve of spray dried lactose at a drying temperature of 80°C and a liquid composition w_{IPA}=0

Here, during spray drying mostly α lactose was formed. This indicates the peak at 207.6 °C. Another non-formed peak at around 230 °C shows a small proportion of β lactose. An existing glass transition region suggests that an amorphous content of lactose had formed.

Figure 4-24 shows the DSC curve of spray dried lactose at a drying temperature of 110°C and a solution composition of 100% water.

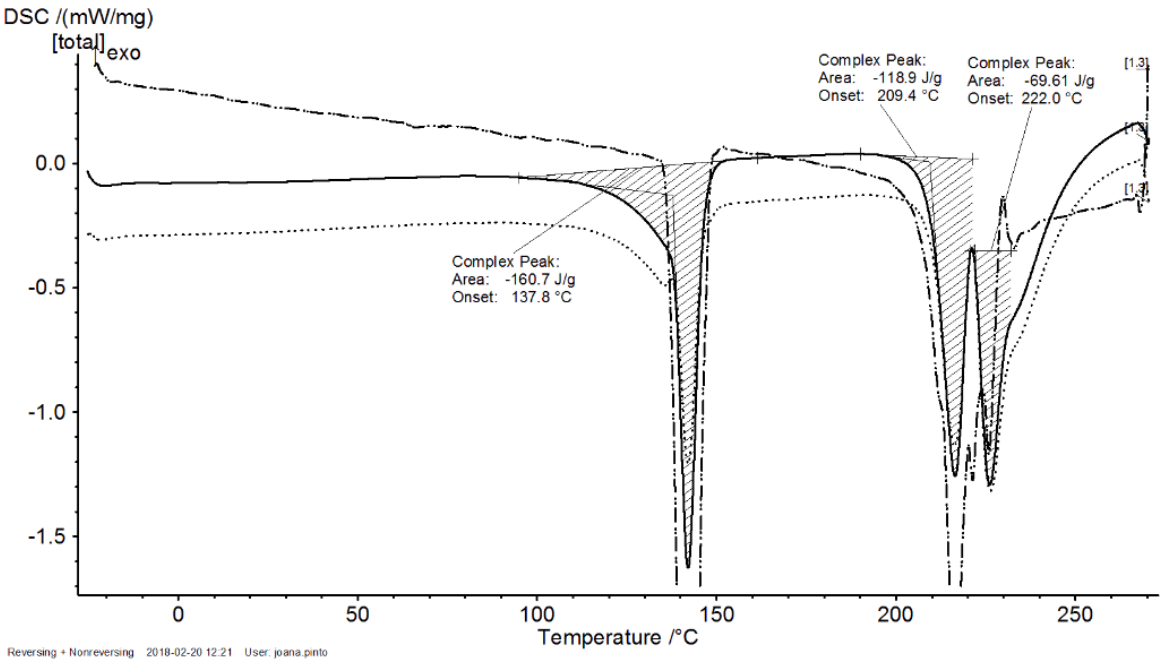

Figure 4-24: DSC curve of spray dried lactose at a drying temperature of 110°C and a liquid composition w_{IPA}=0

In contrast to the sprayed sample at 80 °C (see Figure 4-23), the lactose was in crystalline form (no glass transition region). At higher temperature, more β lactose was formed. The associated peak is at 222 °C.

Figure 4-25 shows spray dried lactose with a liquid composition of 100% water. The sample was sprayed at 140°C.

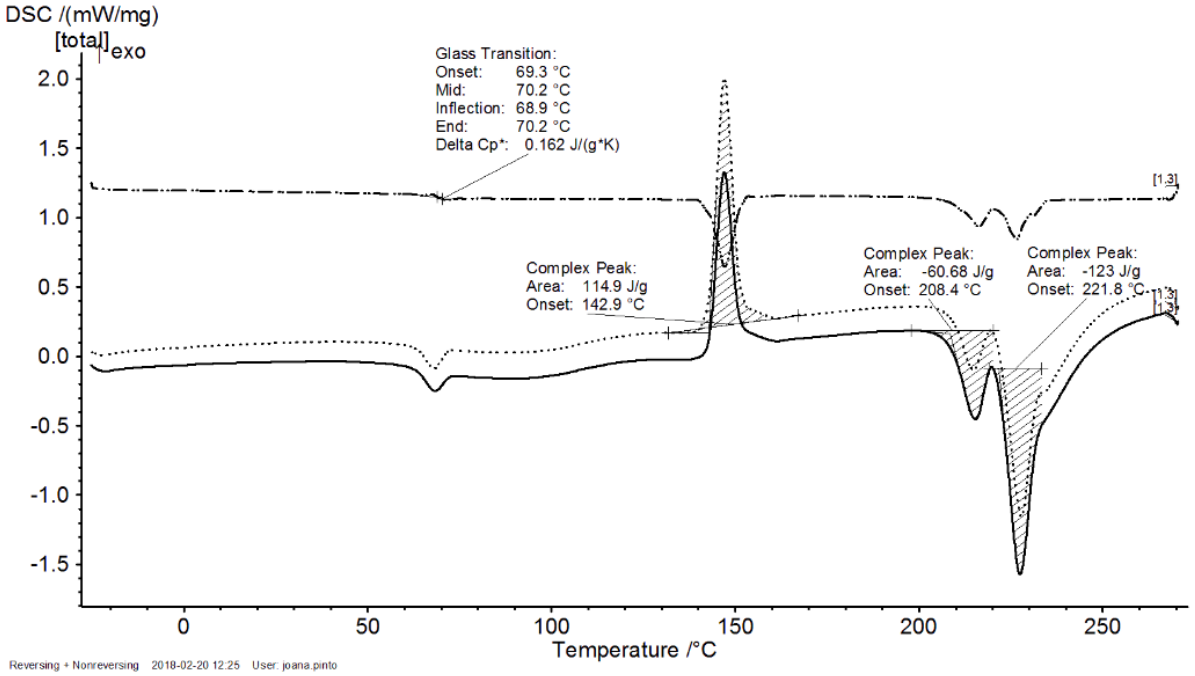

Figure 4-25: DSC curve of spray dried lactose at a drying temperature of 140°C and a liquid composition w_{IPA}= 0

Here, after the glass transition region, an exothermic peak at 142.9 °C occurred. This peak indicates a recrystallization process, which could be an experimental error during the handling of the suspension.

By heating the suspension before the spray drying process, the suspended particles went into solution because of better solubility with temperature increase and then crystallized out during the drying process. The reason for this could be the magnetic stirrer, in which the heating plate switched on due to a technical defect during the stirring process.

Lactose spray dried at 170 °C had a content of amorphous material. (Glass transition 62.2°C) The corresponding DSC curve is shown in Figure 4-26. Far more β lactose was produced than α lactose.

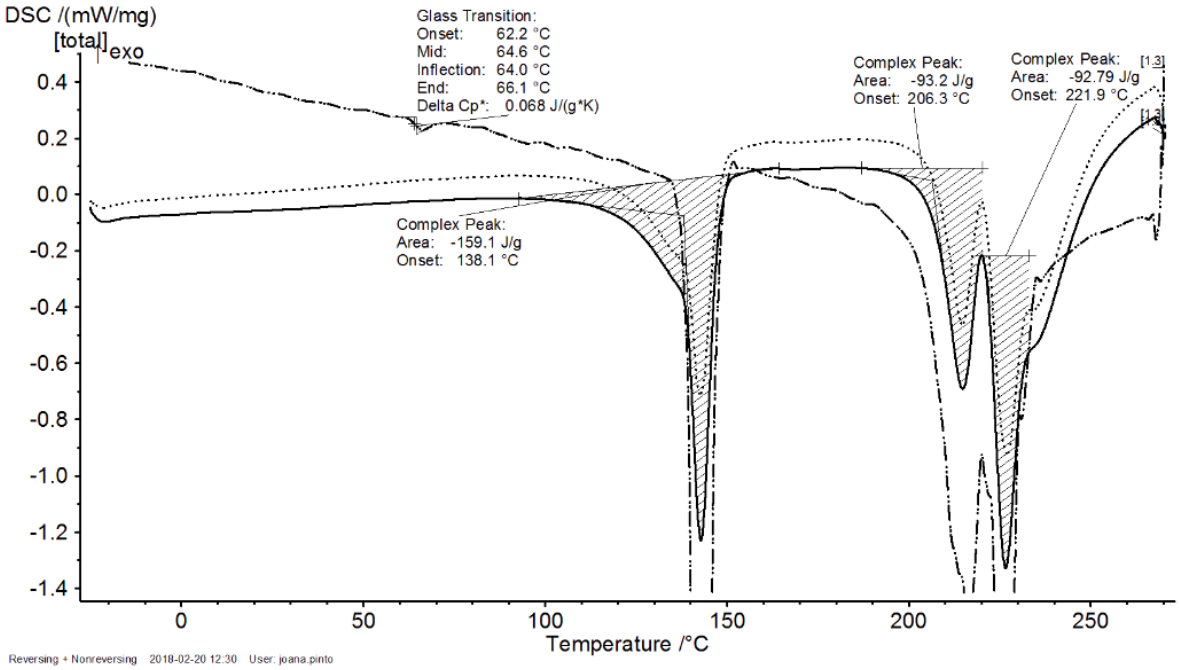

Figure 4-26: DSC curve of spray dried lactose at a drying temperature of 170°C and a liquid composition w_{IPA}=0

The anomers of lactose show mutarotation in aqueous solution with a room temperature equilibrium of 38% α and 62% β lactose[19]. In isopropanol, the equilibrium state does not take place, thus the spray drying samples with a high isopropanol content of the liquid fraction consisted largely of the starting lactose form- α lactose monohydrate. From a water content of 50 wt% of the liquid phase, the β lactose fraction increased with rising water content. In addition, more β lactose was formed at higher temperatures, which can be explained by a better solubility of β lactose in water compared to α lactose monohydrate.[19] There was no trend to detect the formation of amorphous or crystalline lactose. In principle, more amorphous lactose should be formed at high spray drying temperatures. [19] However, amorphous lactose could already undergo shifts in structure to the crystalline form during the storage of the samples. Table 4-9 lists the results of the DSC measurement of spray dried lactose with a liquid composition of 100% water.

Table 4-9: Overview DSC measurement of spray dried lactose with a liquid composition $w_{IPA}=0$

	Drying Temperature [°C]			
	80	110	140	170
Glass transition temperature [°C]	62.8	no	69.3	62.2
Glass transition heat capacity [J/(g*K)	0.061	no	0.162	0.068
Dehydration temperature [°C]	138.9	137.8	no	138.1
Dehydration peak specific enthalpy [J/g]	-166.3	-160.7	no	-159.1
α lactose melting peak temperature [°C]	207.8	209.4	208.4	206.3
α lactose melting peak specific enthalpy [J/g]	-181.1	-118.9	-60.68	-93.2
β lactose melting peak temperature [°C]	no	222	221.8	221.9
βα lactose melting peak specific enthalpy [J/g]	no	-69.61	-123	-92.79

Particle size analysis by Helos

The density distribution of spray dried lactose at different temperatures and a liquid composition of 100 wt% water is shown in Figure 4-27. In the spray drying samples, whose liquid content consists only of water, a contrary trend to the other series of samples whose liquid content is a mixture of different ratios of water and isopropanol, was observed. As the spray drying temperature increased, the particulate matter became finer. This trend can also be seen on the SMD, VMD and x_{50} of this sample series. The SMD, VMD and x_{50} are shown in Figure 4-28.

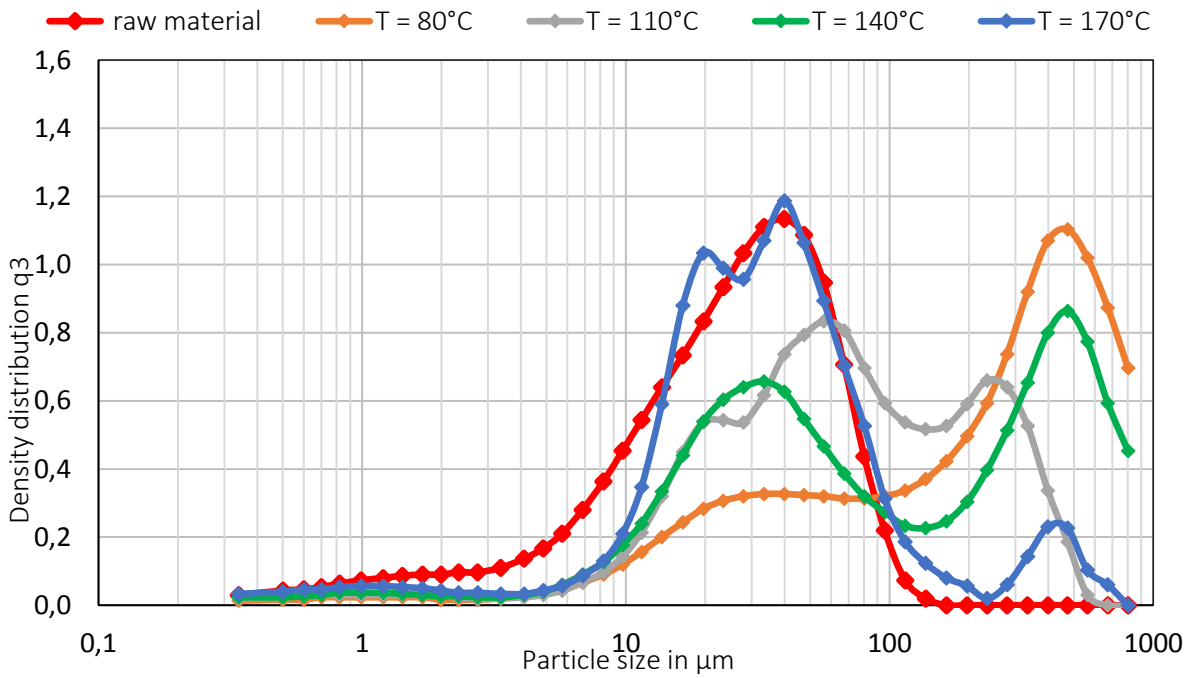

Figure 4-27:q_3 distribution of spray dried lactose at different temperatures with a liquid composition $w_{IPA}=0$

With a liquid content of 100% water, and a spray drying temperature of 80°C the largest particles of all test series were formed. Here the largest agglomerates were built. Looking at the associated DSC curves, this trend is easy to explain. At higher temperatures, more β lactose was formed. The peak

which indicates β lactose was getting bigger. Fast drying produces more amorphous lactose. Amorphous β lactose is not hygroscopic, while amorphous α lactose is hygroscopic. [26] The higher the temperature, the less water-attracting product was created. This also resulted in less agglomeration behavior and consequently smaller particles at higher temperatures. The spray dried sample at 140 °C did not match this trend. Here, due to an experimental error, suspended lactose was dissolved and then spray dried. As a result, this experiment is not comparable with the others in this series of measurements.

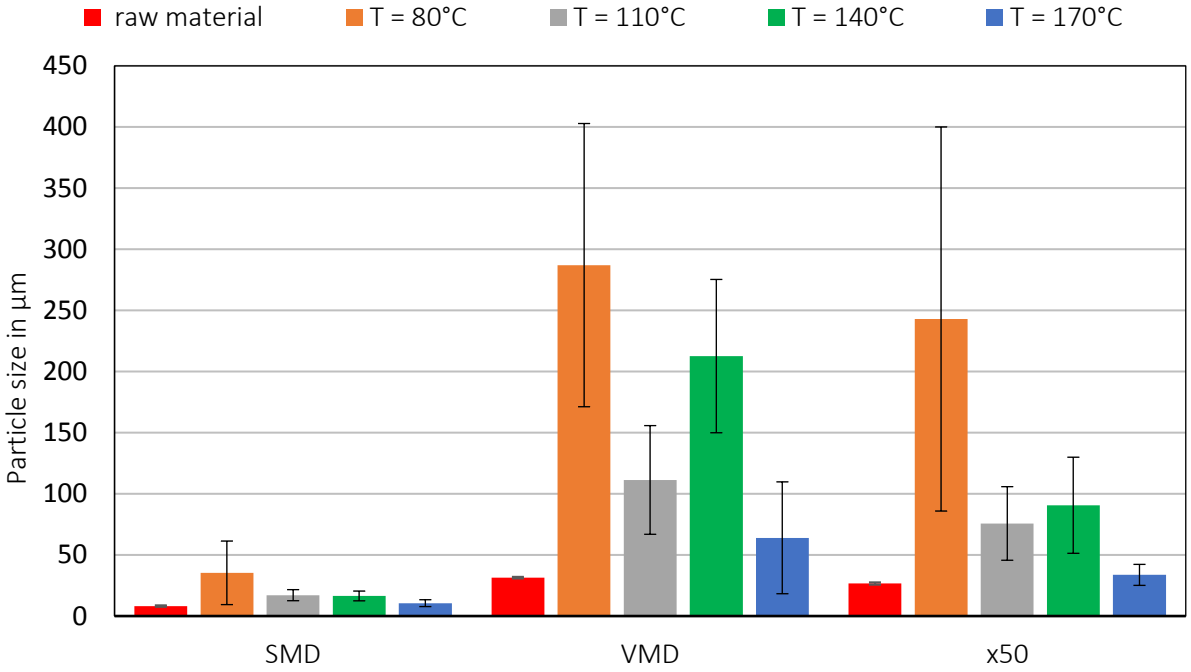

Figure 4-28: SMD, VMD, x_{50} of spray dried lactose at different temperatures with a liquid composition $w_{IPA}=0$

Scanning electron microscopy image (SEM)

In Figure 4-29 spray dried lactose at different temperatures with a saturated solution content of 100 wt% of water is shown. There were almost no particles with the characteristic shape and size of the starting material to recognize. The primary particles were almost completely covered by agglomerates. No significant difference can be detected between the samples with a spray-drying temperature of 80 °C [Figure 4-29 (a)], 110 °C [Figure 4-29 (b)] and 170 °C [Figure 4-29 (d)]. In the sample, which was sprayed at a drying air temperature of 140 ° C, spherical particles can be seen and is shown in Figure 4-29 (c). These spherical particles indicate that the suspended particles must have dissolved in the saturated solution. The saturation came below the saturation state at the time of the spraying process. This case can be traced back to an experimental error. A possible reason for this may be a small temperature change of the suspension to be sprayed in combination with the good solubility of lactose in water. If the temperature of the suspension increased only slightly, the solubility of lactose in water also increased. A necessary heat source could be the spray dryer itself, due to the close position of the delivery hose to the heater, the suspension conveyed therein could have been heated. Another possible heat source could be the heating plate of the magnetic stirrer, which was busted.

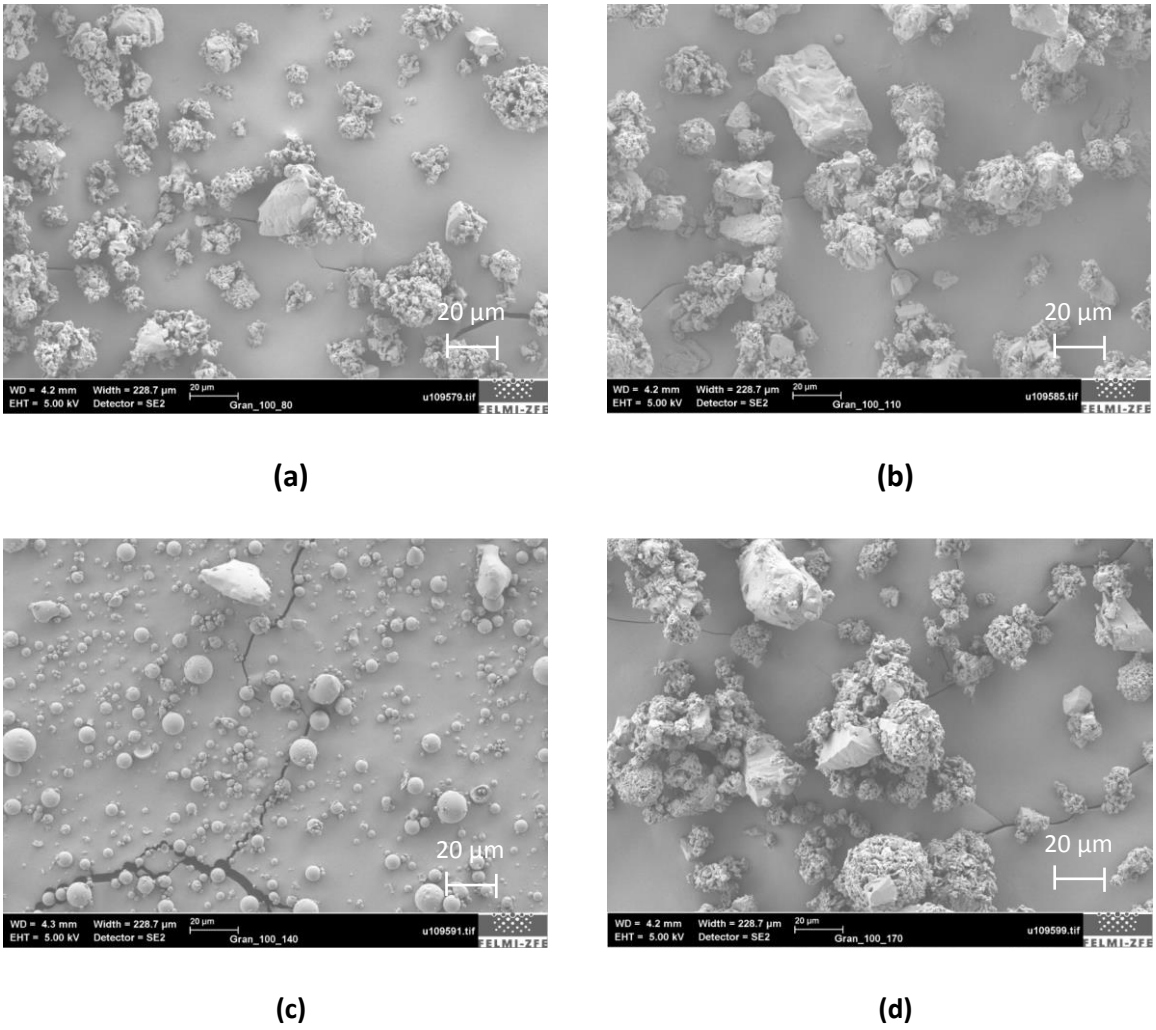

Figure 4-29: SEM Image of spray dried lactose with a liquid composition w_{IPA}= 0; Spray drying temperature (a) 80 °C, (b) 110°C, (c) 140°C, (d) 170°C

Table 4-10 shows the moisture content of each sample in tabular form. The indication of humidity is in percent. The moisture content of the spray dried sample at 80 °C was with 3.537 wt% high compared to the other samples. The energy input at 80 °C was too low to allow all water to evaporate. At a spray drying temperature of 170 °C, the moisture content of 0.597 wt% was in range of those samples which were sprayed with 100 wt% isopropanol in the liquid.

Table 4-10: Residual moisture w_{IPA}=0

			Residual moisture [wt%]			
X_d	***w_{IPA}***	***w_{H2O}***	***80°C***	***110°C***	***140°C***	***170°C***
$7.2*10^{-4}$	*0*	*100*	*3.537*	*2.509*	*1.241*	*0.597*

4.2. Analysis of sprayed suspensions

With the sprayed suspensions, a particle analysis in wet-dispersion form was carried out by Helos equipment.

4.2.1. Schlick nozzle

Figure 4-30 shows the particle size distribution of the starting suspensions with different solids content. The solids content is shown in percent by mass. The Schlick nozzle had also been tested with higher viscous liquids. The largest possible solids content at which no clogging occurred was 35 wt%.

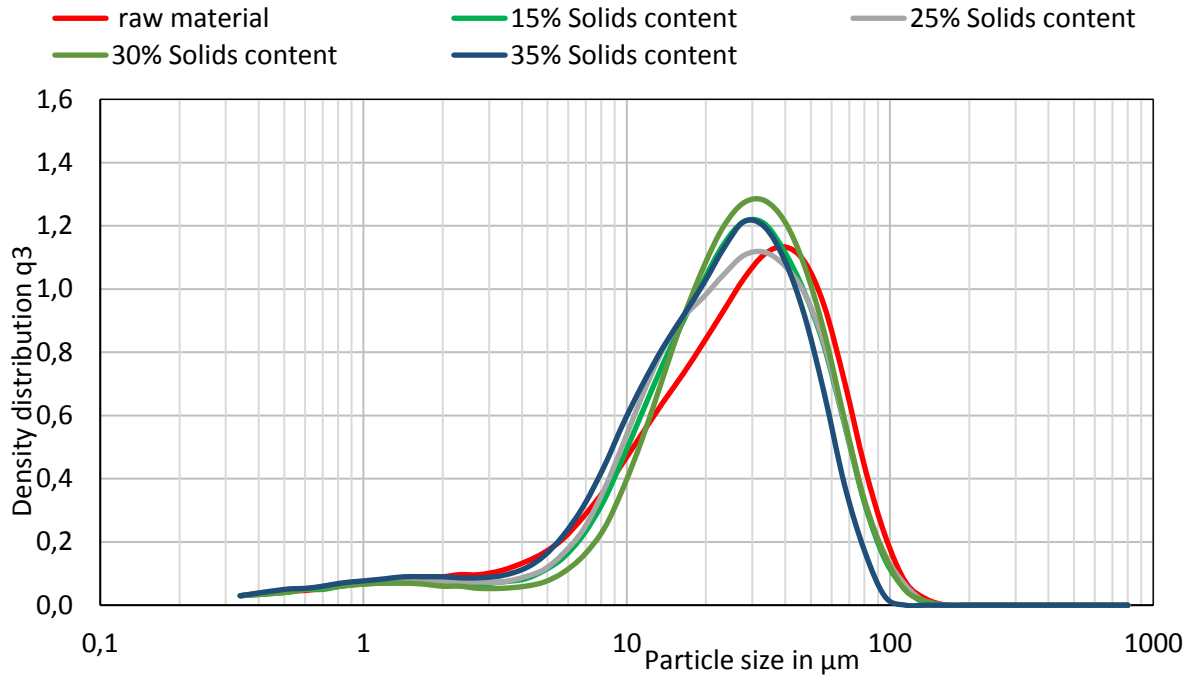

Figure 4-30: Schlick nozzle: Density distribution q_3 of the initial suspension

Figure 4-31 shows the SMD, VMD, and x_{50} of the raw suspension. The measured particle sizes were smaller compared to the original GranuLac® 230. One possible reason for this could be that the particles wear each other during the dispersion process by the stirrer. This would also explain the trend that the smallest particle characteristics were found at the highest solids content.

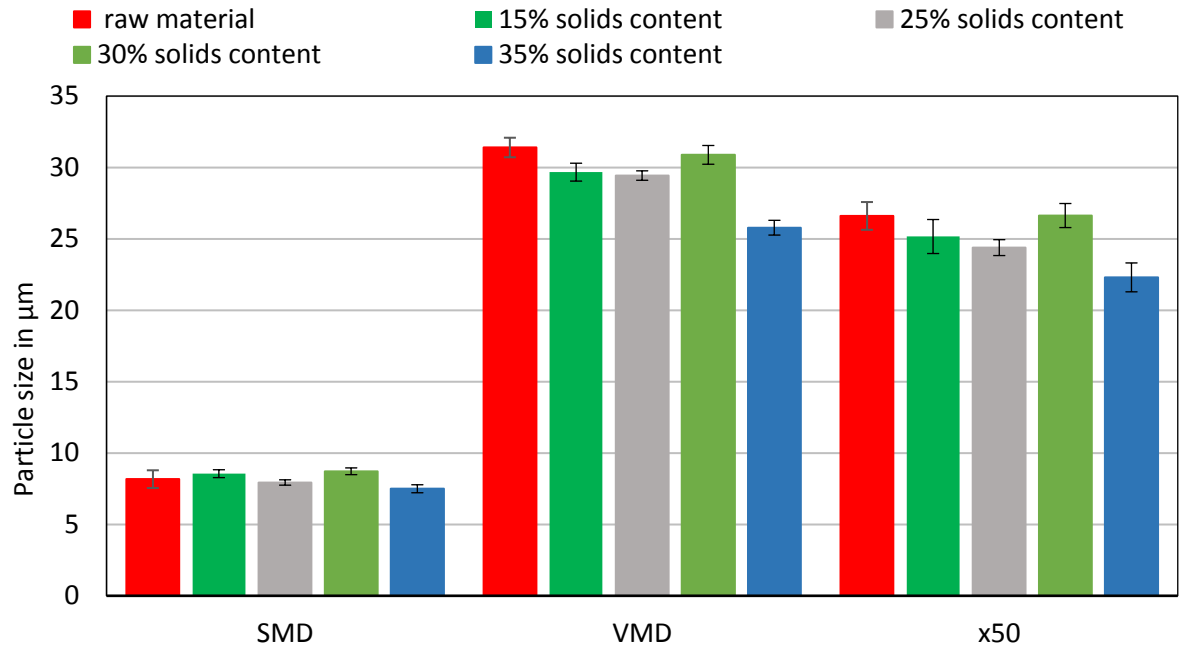

Figure 4-31: Schlick nozzle: SMD, VMD, x_{50} of initial suspension

Figure 4-32 shows the density distribution of the sprayed suspension. Again, the solids content refers to mass percent.

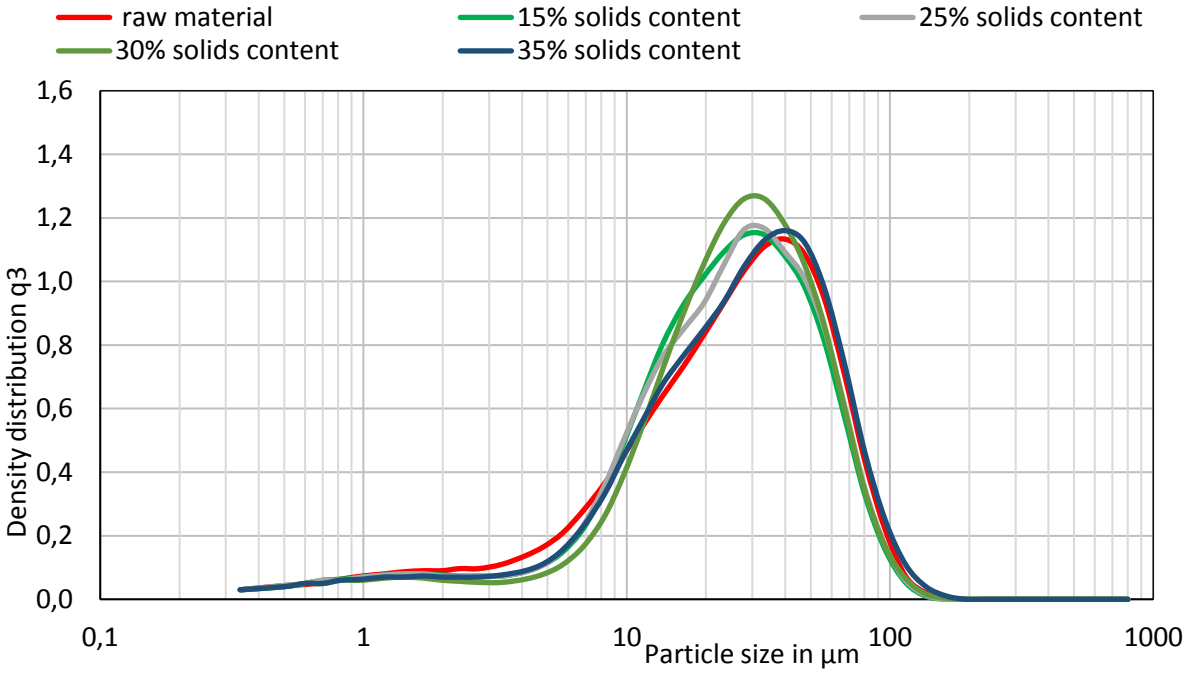

Figure 4-32: Schlick nozzle: Density distribution q_3 of sprayed suspension

The SMD, VMD and x_{50} of the sprayed suspension are shown in Figure 4-33. If the particle sizes SMD, VMD and x_{50} of the initial suspension are compared with those of the sprayed suspension, a significant change in the sizes is seen especially in the sample series with 35 wt% solids content. This cannot be only due to the standard deviation. The reason could be that isopropanol evaporated faster during the spraying process due to the higher vapor pressure than water. As a result, the proportion of water in the sprayed suspension became higher and thereby also the solubility for lactose increased. By

dissolving fine particles, the fines content of the suspension decreased. Furthermore, with increasing solids content, the liquid content of the suspension decreased. If the saturated state of the solution was undershot, less lactose could dissolved because of the smaller amount of isopropanol and water. In addition, the dissolution of suspended lactose probably had less effect on particle size distribution because at higher solids concentrations more particles were present.

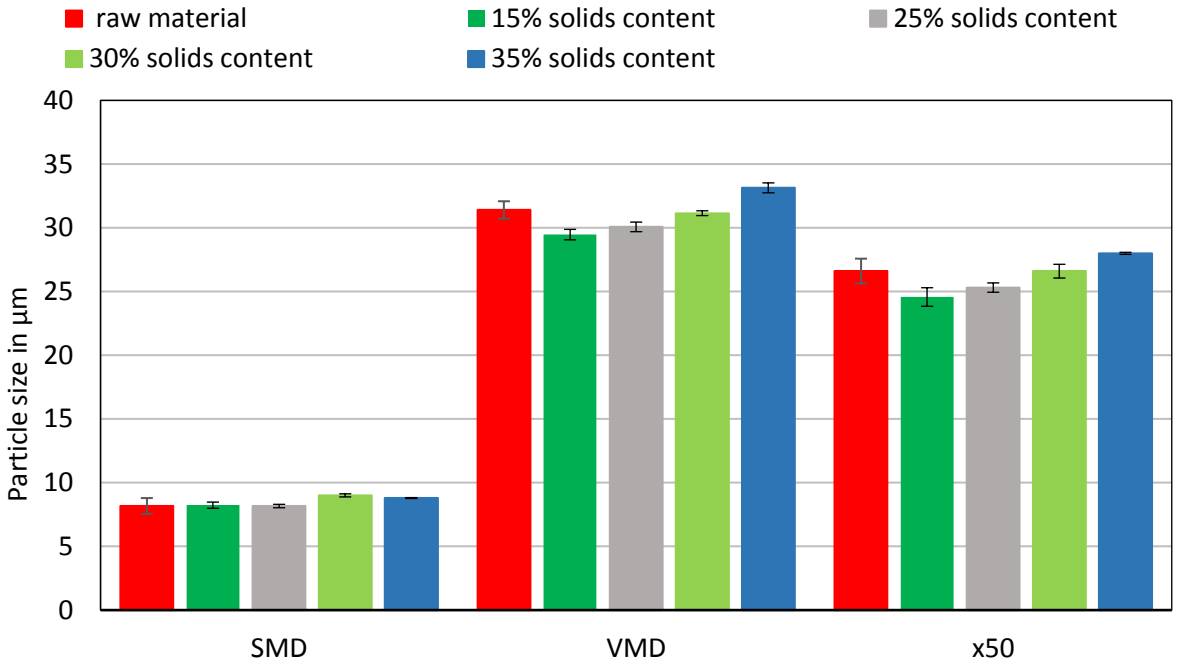

Figure 4-33: Schlick nozzle: SMD, VMD, x_{50} of sprayed suspension

Figure 4-34 shows the SMD, VMD and x_{50} of the suspension with 35 wt% solids from different measurement points when pumping the suspension to the nozzle. It can be seen that the starting suspension had much smaller particle sizes than the GranuLac® 230. The particle size then remained nearly constant during the passage through the pump and also during the delivery through the nozzle without atomizing air. Only when spraying the suspension, an increase in the particle size can be seen. The reason for this could be that agglomeration occurred during the spraying process and therefore the size of the particles increased.

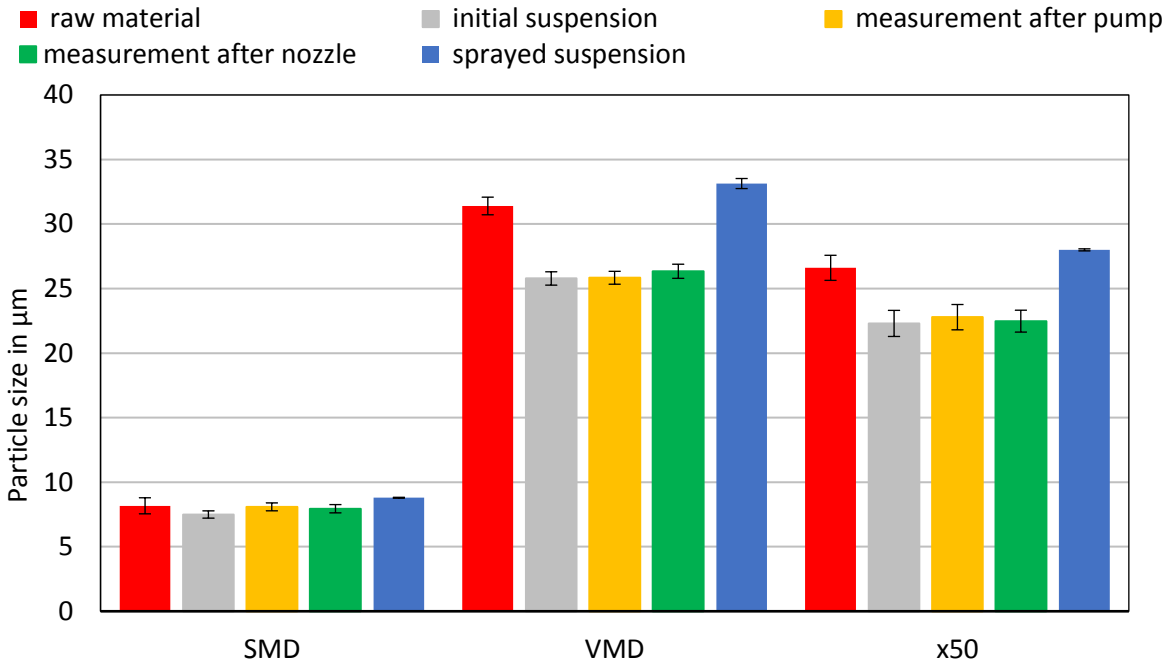

Figure 4-34: Particle measurement 35 wt% solids content

Figure 4-35 shows the change of the VMD at the individual measuring points in relation to the starting material. For all initial suspension, which were then sprayed with the Schlick nozzle, a reduction of the VMD value was found. In order to prevent settling of the suspended particles, they had to be kept in motion by constant stirring. The reduction of the VMD value could be explained by frequent particle collisions. The largest reduction of the VMD occurred in the suspension with the highest solids content. The large difference to the results of the suspension with lower solids content may indicate an additional dissolution of particles. Due to temperature increase of the saturated solution caused by rising room temperature, the solubility of the saturated solution could be increased and suspended particles were dissolved. The VMD of the suspension was further reduced in pump delivery on the 15 wt%, 25 wt% and 30 wt% test series. One explanation could be that the lactose solubility was increased by increasing the temperature. The increase in temperature could be due to friction between eccentric screw and pump housing. At higher solids content, this effect was less significant due to the larger number of particles. This assumption is also confirmed by the constant VMD in the suspension with 35 wt% solids. For the 25 wt% solids suspension, no particle size measurements were made after the pump or after passing through the spray nozzle. As the suspension passed through the nozzle, an increase in VMD was generally observed. This trend could have been caused by particle agglomeration. After spraying, the VMD value again became smaller or larger in the suspension with 35 wt% solids content. One reason for this could be that during spraying, isopropanol was evaporated and the water content of the saturated solution was increased. This also increased the solubility for lactose. Particles were partially dissolved and the VMD became smaller. As the solids content increased, this influence became smaller. Spraying involved particle agglomeration and dissolution of the particles. At high solids concentrations, the particle agglomeration covered the dissolution.

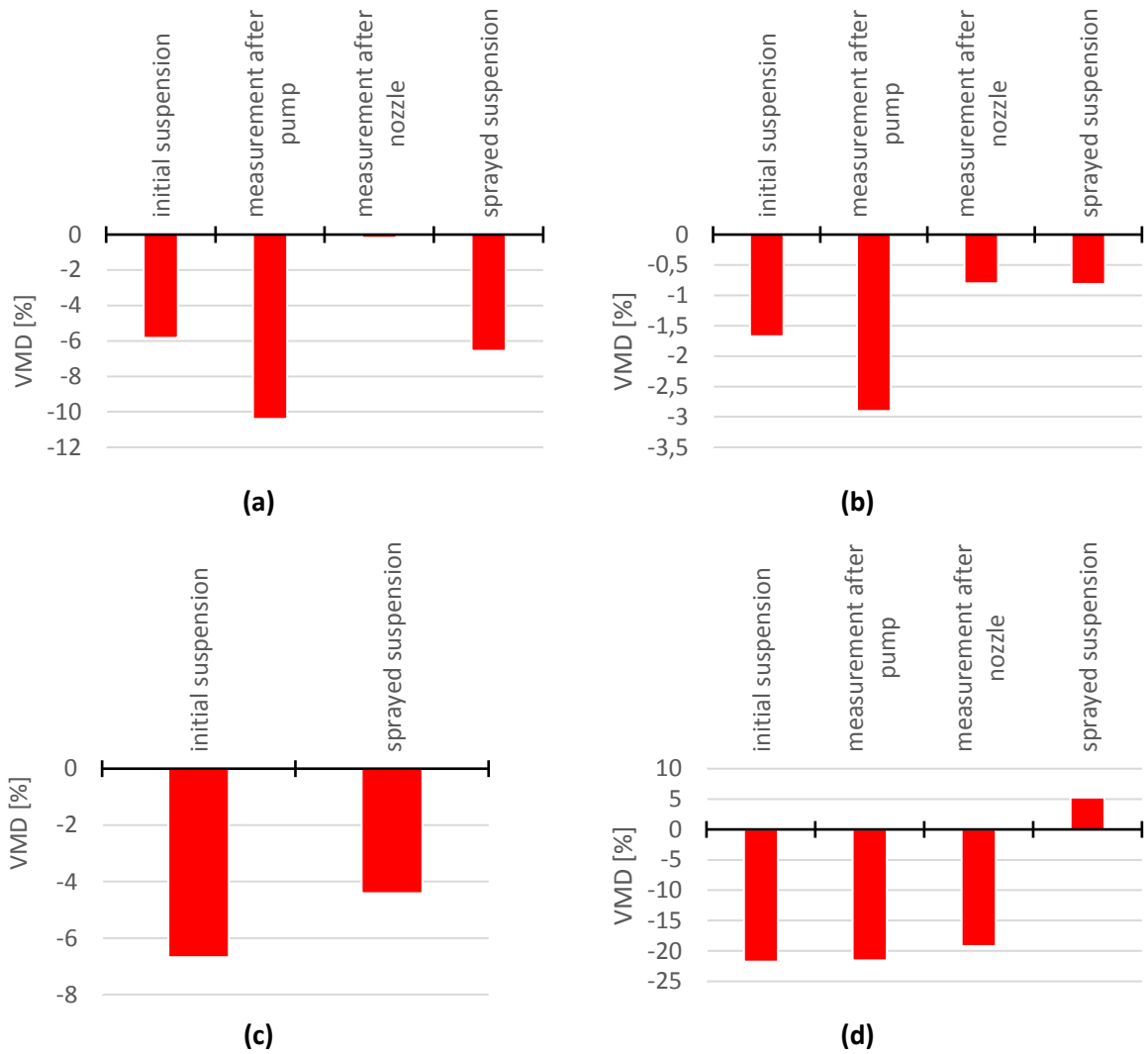

Figure 4-35: Change in VMD compared to raw material; solids content: (a) 15%, (b) 30%, (c) 25%, (d) 35%

4.2.2. Bete nozzle

The Bete nozzle was tested with suspensions with a solids content of 5 and 10 wt%. At 10 wt% solids, the nozzle clogged after 1.5 minutes of operation. Thus, the maximum possible solids content was less than 10 wt%. Figure 4-36 shows the density distributions of the starting suspensions.

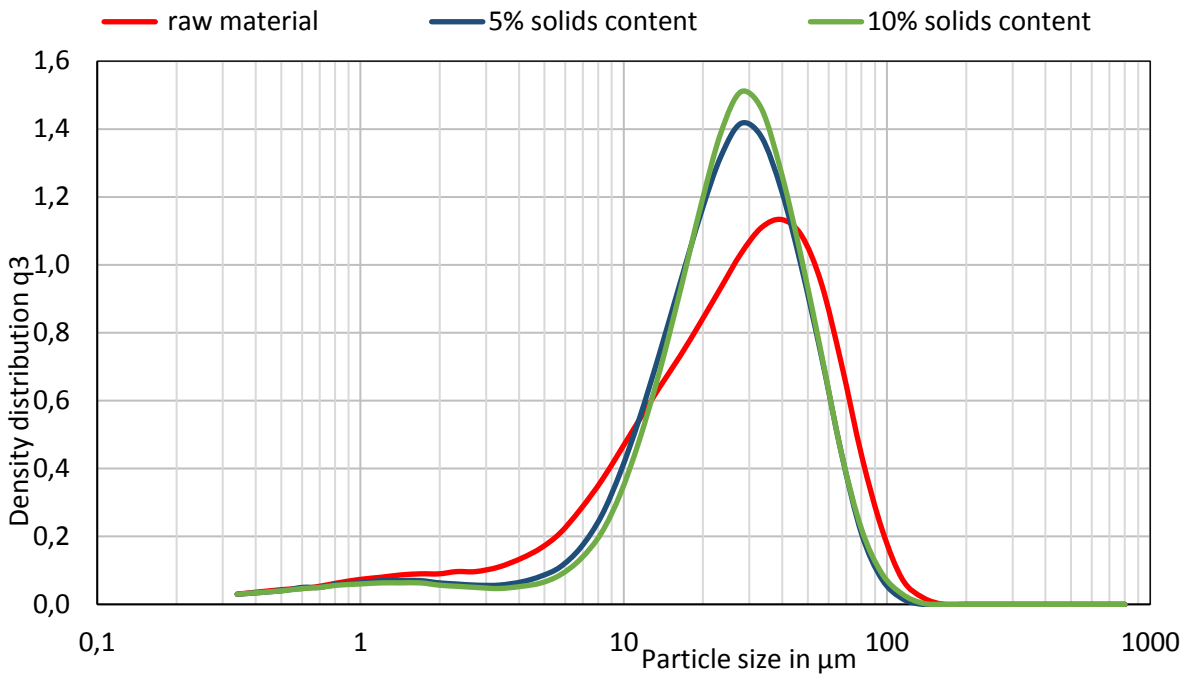

Figure 4-36: Bete nozzle: Density distribution q_3 of initial suspension

The associated SMD, VMD, and x_{50} are shown in Figure 4-37. As with the previous starting suspensions (compare Figure 4-31), a reduction of the individual particle sizes can be seen. A possible explanation would be that the particles in the suspension collided with each other and thereby became smaller. This particle abrasion could be caused by the introduction of shear forces during the stirring process.

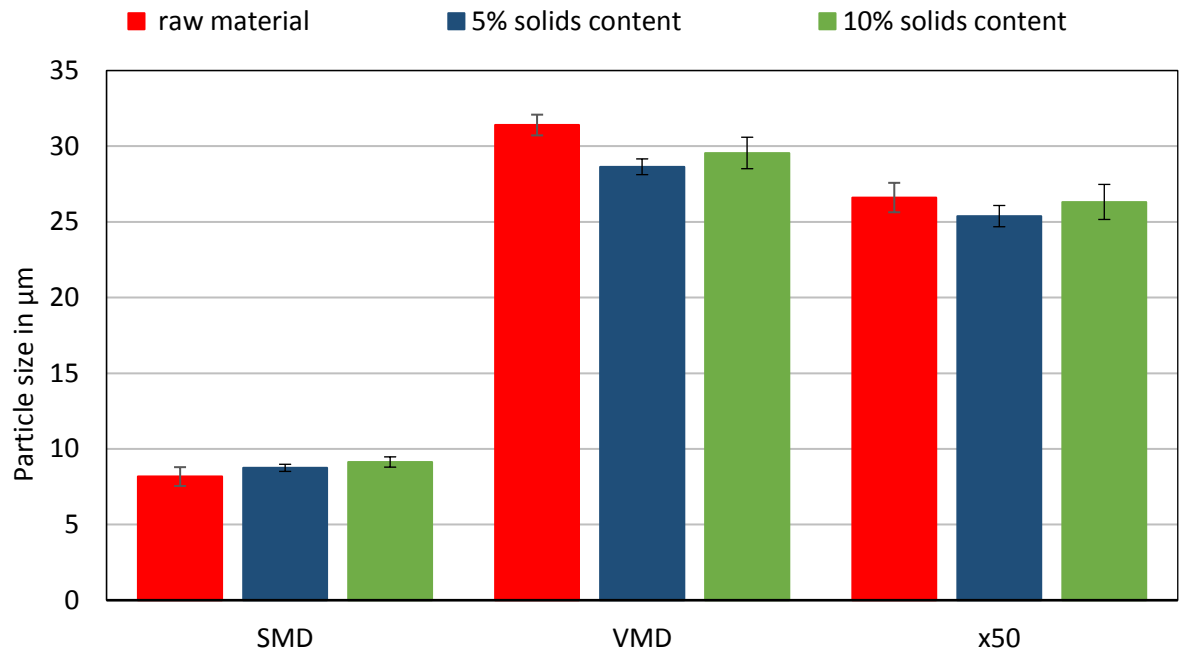

Figure 4-37: Bete nozzle: SMD, VMD, x_{50} of initial suspension

The density distributions of the sprayed suspensions with the Bete nozzle are shown in Figure 4-38 and show the same trend as those sprayed suspensions with the Schlick nozzle. The density curve was getting narrower compared to that of the starting material.

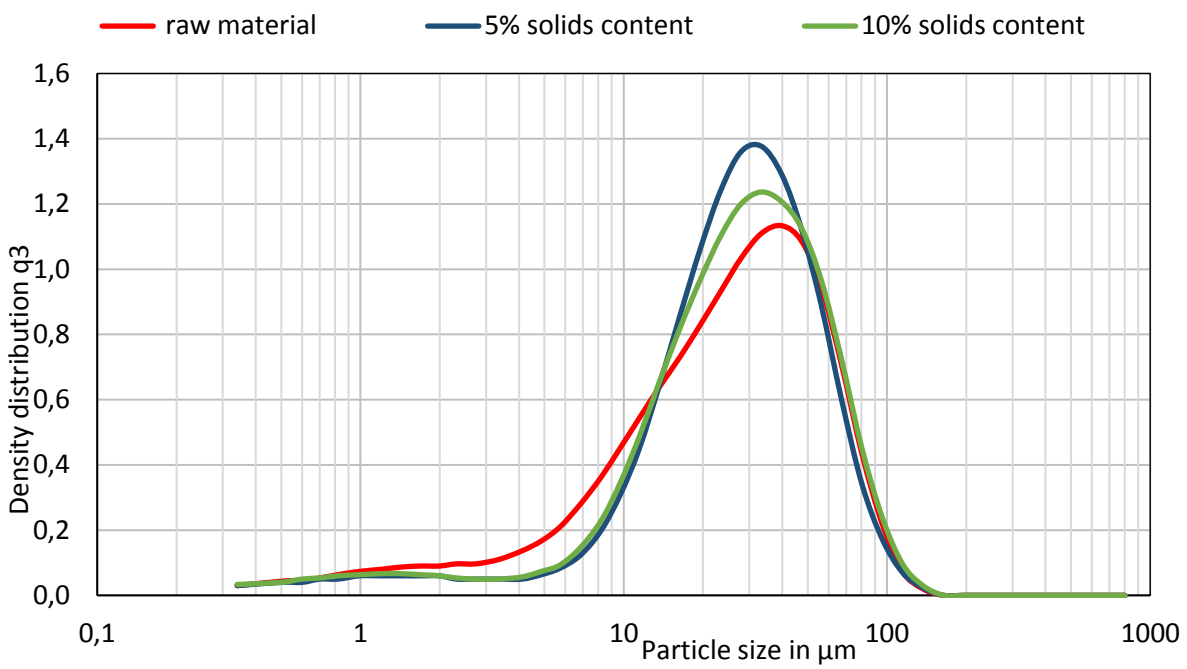

Figure 4-38: Bete nozzle: Density distribution q_3 of sprayed suspension

After spraying, the particle sizes SMD, VMD and x_{50} increased again compared to the starting suspension. The accompanying illustration is Figure 4-39. This can in turn be explained by the easier evaporation of isopropanol and the resulting better solubility of lactose due to the higher water content in the liquid phase of the sprayed suspension. As a result, smaller particles dissolved or agglomerated to larger ones.

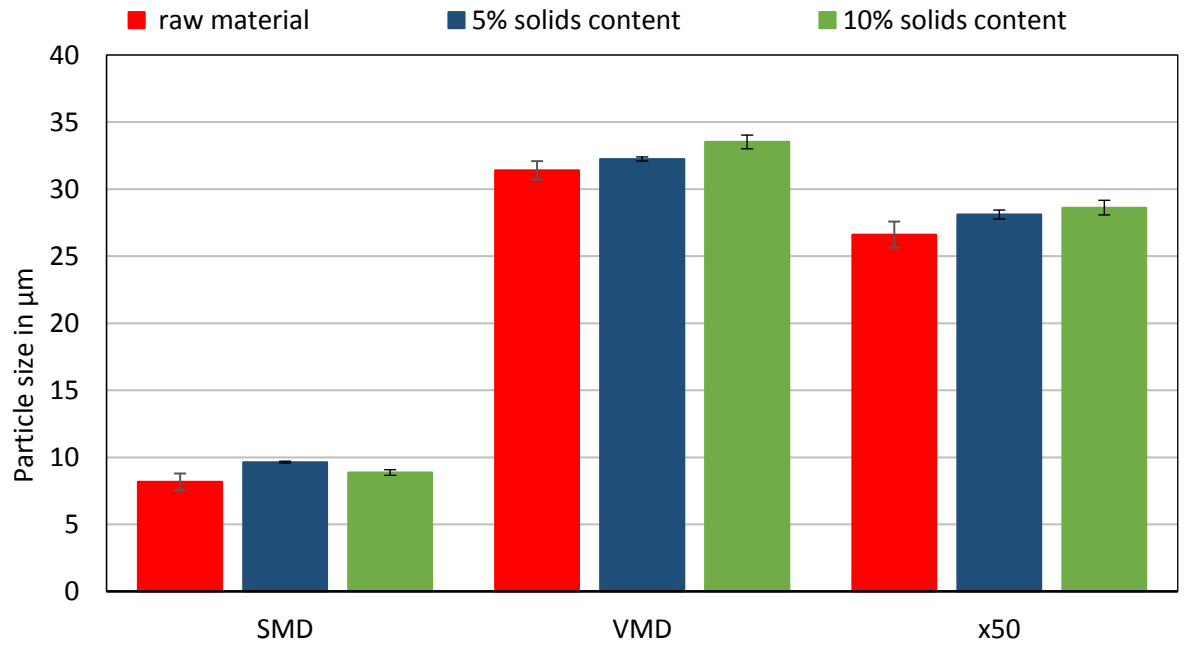

Figure 4-39: Bete nozzle: SMD, VMD, x_{50} of sprayed suspension

In Figure 4-40 the VMD of the suspension at different measuring points is compared to the raw material. The VMD of the starting suspension was smaller in the suspensions with 5% and 10 wt% solids compared to the raw material. This can be explained by an increased abrasion of the particles by the stirring process. Furthermore, this reduction of the particles could have been enhanced by dissolving the dispersed particles in the liquid phase. This could be due to a temperature increase of the saturated solution. Possible reason could be a temperature difference of the room in which the initial suspension was prepared and the room in which the spray test was carried out. The measurement of the suspension after the pump showed an increase in the VMD value at 5 wt% solids. This could have happened through agglomeration in the eccentric screw of the pump. For the 10 wt% solids suspension, the VMD diameter decreased compared to the raw material. In this case a temperature increase and an associated higher solubility of the lactose could have reduced the VMD. The temperature increase could be caused by friction in the pump housing by the eccentric screw. The pump performance was 13% for the suspension with 10 wt% solids content. For the suspension with 5 wt% solids content, the pump power was 30%. As a result, the residence time of the 10% solids suspension in the pump was longer and warmed up more. For the suspension with 5 wt% solids content, the VMD decreased as it passed through the nozzle without atomizing. The reason could be that isopropanol evaporated and thus the water content of the suspension became larger. This increased the solubility for lactose and dispersed particles were partially dissolved. In the case of the suspension with 10 wt% solids, the Bete nozzle clogged after a short period of operation by agglomeration in the nozzle channel. A significant increase in VMD was measured. During the spraying process an increase of the VMD was detected in both cases. The reason might be agglomeration.

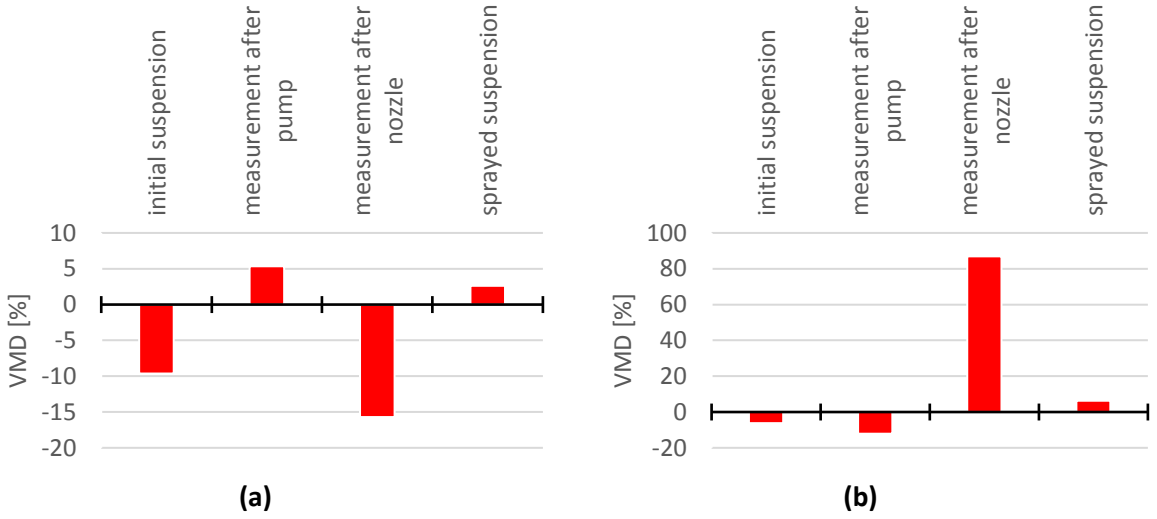

Figure 4-40: Change in VMD compared to raw material; solids content (a) 5%, (b) 10%

5. Conclusion

The spray dryer from ProCept was used to spray lactose suspensions containing 10 wt% of solid and 90 wt% of solution at different drying temperatures. The liquid phase consisted of different water / isopropanol ratios.

The DSC measurement showed that β lactose is produced only at higher water content. In the sprayed sample whose liquid phase consisted of 100% isopropanol, no β lactose was found. In spray drying, amorphous lactose is usually produced due to the rapid drying. Amorphous lactose was not detected in all spray dried samples. There was no trend to predict the formation of amorphous lactose. Due to this arbitrary formation of amorphous lactose, it is suggested that amorphous lactose was converted to crystalline lactose by ambient moisture uptake during sample storage.

Considering the results of the density distribution, the SMD, VMD, and x_{50} of all samples the following statements can be made. The particle size generally increases with rising water content of the liquid fraction. This can be explained by the fact that the agglomeration behavior rises with increasing water content. The water acts as a binder for particle accumulation. The unexpected trend that particle size decreases with increasing drying temperature at lower isopropanol concentration can be explained by the associated DSC curve. Responsible is the hygroscopic effect of amorphous lactose and increased agglomeration of lactose due to water absorption.

In general, analysis of the electron micrographs indicates that agglomeration accelerated by increasing water content of the saturated solution. In a saturated solution containing 100% by weight of isopropanol, no significant changes in particle shape and size can be detected. Lactose is practically insoluble in isopropanol, which means that during spray drying no material bridges between particles can be formed by precipitation of dissolved lactose. With increasing water content, the amount of dissolved lactose also increases, thereby also creating more material bridges and formation of agglomerates.

With the spray nozzle test stand spray nozzles were tested for their usability of spraying viscous suspensions and particle size changes during the spraying process were recorded.

An explosion protection concept was developed for the spray nozzle test stand. The result consists of a suction, the partial inertization with nitrogen and the constant oxygen concentration monitoring in the exhaust stream and a gas scrubber to wash out isopropanol. Two different spray nozzles were tested. With the nozzle from Schlick, a suspension containing 35 wt% of solid was sprayed over the test duration of 30 minutes. The Bete nozzle clogged at a solids content of 10 wt% after 1.5 minutes of operation. The largest change in particle size with respect to the original material was found in dispersing the suspension. The energy input by the stirrer and particle collisions were likely to result in increased abrasion and particle size reduction. At other measuring points, which were to show changes by the pumping process and passage through the nozzle, no significant changes in the particle size could be detected. By spraying the particle size increased or decreased. It can be assumed that the faster evaporation of isopropanol increases the solubility for lactose, thereby completely dissolving smaller particles. Particle size was significantly influenced by 2 effects during spraying. On the one hand, the evaporation of isopropanol during the spraying process increased the solubility for lactose.

Suspended particles could dissolve and the particles became smaller. On the other hand, agglomeration took place. Depending on which effect predominated when spraying the individual suspensions, this led to a reduction or enlargement of the particles.

6.List of references

1. Stieß, M. *Mechanische Verfahrenstechnik - Partikeltechnologie 1*. (2009).
2. Cal, K. & Sollohub, K. Spray drying technique. I: Hardware and process parameters. *J. Pharm. Sci.* **99,** 575–586 (2010).
3. C.Anandharamakrishnan and Padma Ishwarya S. Introduction to spray drying. *Spray Dry. Tech. Food Ingred. Encapsulation* 1–36 (2015). doi:10.1002/9781118863985
4. Trullinger, C. Controlling atomization in your spray dryer. *Powder Bulk Eng.* 1–3
5. VTU Engineering. *Process Safety*. (2013).
6. Steen, H. *Handbuch des Explosionsschutzes Weinheim*. (WILEY VCH, 2000).
7. VTU Engineering. *Sicherheitstechnische Kennzahlen Sicherheitstechnische Kennzahlen*. (2007).
8. BG RCI Berufsgenossenschaft Rohstoffe und chemische Industrie. EX Info. (2018). Available at: https://www.bgrci.de/exinfode/ex-schutz-wissen/expertenwissen/brennbare-staeube/325-wie-wirkt-sich-vakuum-auf-das-staubexplosionsverhalten-aus/. (Accessed: 12th November 2017)
9. Medienerzeugnisse, B. E. T. E. Gefährdungsbeurteilung Explosionsrisiken. (2016). Available at: http://www.bgdp.de/pages/service/download/medien/230-19_DP.pdf. (Accessed: 15th December 2017)
10. Oliver Fuß. Ermittlung und Berechnung der Sauerstoffgrenzkonzentration von brennbaren Gasen. (Universität Duisburg- Essen, 2004).
11. Krause, U. Prof. Dr.-Ing. U. Krause Vertiefung Explosionsschutz 135. 135–145
12. Österreich, R. *BGBl. II Nr. 309/2004*. **2004,** 2–5 (2004).
13. European Union. *Richtlinie 1999/92/EG des Europäischen Parlaments und des Rates*. (1999).
14. European Union. *Directive 2014/34/EU of the European Parliament and of the Council*. **2014,** 309–356 (2014).
15. Österreich. *BGBl I No. 77/2015*. **2015,** 2–5 (2004).
16. Österreich. *BGBl I No. 96/2016*. **2016,** 2–5 (2004).
17. Österreich. *BGBl. II Nr. 52/2016*. **2016,** 2–5 (2004).
18. Wirtschaftskammer Österreich. CE-Kennzeichnung zum Explosionsschutz von Geräten (ATEX-Richtlinie). (2017). Available at: https://www.wko.at/service/innovation-technologie-digitalisierung/ce-kennzeichnung-explosionsschutz-geraete-atex-richtlinie.html. (Accessed: 7th December 2017)
19. Schmitz, S. *Rekristallisation von teilamorpher und amorpher Laktose*. (2011).
20. Belitz, H.-D., Grosch, Werner, Schieberle, P. *Lehrbuch der Lebensmittelchemie*. (Springer Verlag).

21. Heike P. Schuchmann, H. S. *Lebensmittelverfahrenstechnik*. (Wiley, 2005).

22. Carl Roth. ABSCHNITT 1 : Bezeichnung des Stoffs beziehungsweise des Gemischs und des ABSCHNITT 2 : Mögliche Gefahren. *Sicherheitsdatenblatt* **2006,** 1–11 (2015).

23. Kreimer, M. *et al.* Mechanical strength of microspheres produced by drying of acoustically levitated suspension droplets. *Powder Technol.* **325,** 247–260 (2018).

24. Düsen-Schlick GmbH. *SCHLICK Classic-Line*.

25. Bete Deutschland. *Bete Düsen*.

26. Alfred Töpel. *Chemie und Physik der Milch*. (2016).

27. Ibach, A. & Kind, M. Untersuchungen zur Kristallisation von amorphen lactosehaltigen Pulvern. *Chemie-Ingenieur-Technik* **79,** 303–312 (2007).

28. Palzer Stefan. Kinetik unerwünschter Agglomerationsprozesse bei der Lagerung und Verarbeitung amorpher Lebensmittelpulver. (2004).

29. Wittmann, R. Amorphe Laktose. (2014).